Diffusion coefficients in liquid systems : measurement and molecular simulation

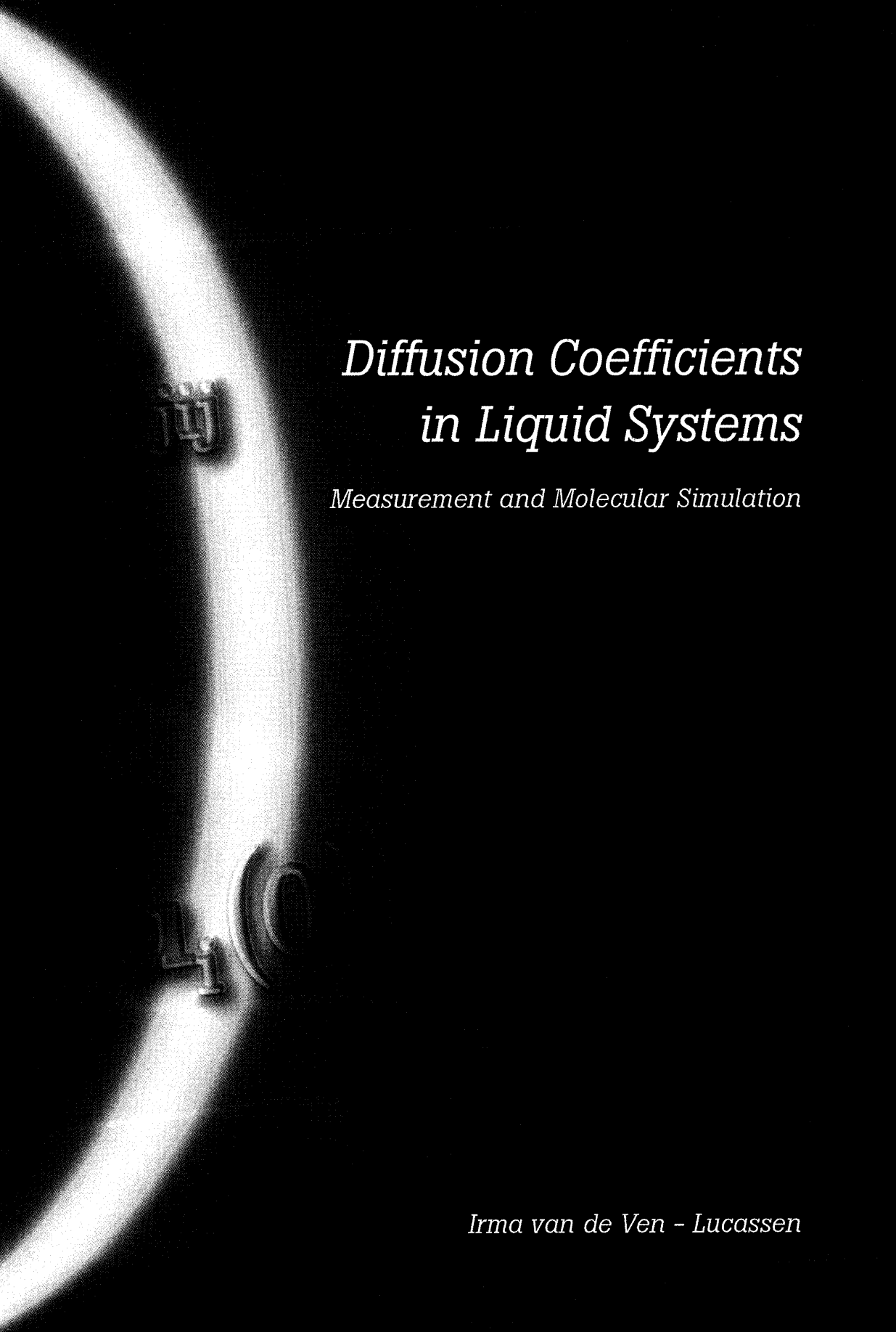

Diffusion Coefficients in Liquid Systems

Measurement and Molecular Simulation

Irma van de Ven - Lucassen

Diffusion Coefficients in Liquid Systems

Measurement and Molecular Simulation

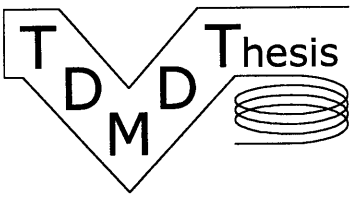

Irma van de Ven - Lucassen

CIP-DATA LIBRARY TECHNISCHE UNIVERSITEIT EINDHOVEN

Ven-Lucassen, Irma M.J.J. van de

Diffusion coefficients in liquid systems : measurement and molecular simulation / by Irma M.J.J. van de Ven-Lucassen. - Eindhoven : Technische Universiteit Eindhoven, 1999
Proefschrift
ISBN 90-3862551-0
NUGI 813
Trefwoorden: moleculaire dynamica / computersimulatie / diffusie ; vloeistoffen
Subject headings: molecular dynamics / computer simulation / diffusion ; liquids

Omslagontwerp: Ben Mobach, TUE
Druk: Universiteitsdrukkerij TUE

DIFFUSION COEFFICIENTS IN LIQUID SYSTEMS

MEASUREMENT AND MOLECULAR SIMULATION

PROEFSCHRIFT

ter verkrijging van de graad van doctor aan de
Technische Universiteit Eindhoven, op gezag van de
Rector Magnificus, prof.dr. M. Rem, voor een
commissie aangewezen door het College voor
Promoties in het openbaar te verdedigen
op woensdag 30 juni 1999 om 16.00 uur

door

Irma Maria Johanna Jacqueline
van de Ven - Lucassen

geboren te Margraten

Dit proefschrift is goedgekeurd door de promotoren:

prof.dr.ir. P.J.A.M. Kerkhof
en
prof.dr.ir. B. Smit

Copromotor:
dr.ir. A.J.J. van der Zanden

Voor Alex,
Stephanie en Annick

Het in dit proefschrift beschreven onderzoek werd financieel
ondersteund door de Stichting scheikundig onderzoek in Nederland.

SUMMARY

Molecular diffusion in liquids plays an important role in many chemical engineering processes. Therefore, knowledge of diffusion coefficients is important for the design of process equipment. Empirical and semi-empirical correlations, which have been developed to predict the liquid diffusion coefficients in terms of solute and solvent properties, often are not accurate enough to solve the nonroutine problems. This thesis describes how diffusion coefficients can be obtained by measurement and by molecular simulation. The study has been focused on diffusion in aqueous non-electrolyte solutions.

The Taylor dispersion method is an experimental technique widely used for the measurement of diffusion coefficients in liquid systems. This work starts with the description of a highly labour-efficient implementation of the method for measuring with binary liquid systems. The experimental set-up consists of standard HPLC components and has been fully automated. Software has been developed for processing the data; diffusion coefficients can easily be calculated from the measured concentration against time curve in various ways. Experiments performed on the methanol + water system and the ethanol + water system at various temperatures have shown that the binary diffusion coefficients can here be obtained with an accuracy of 0.5 - 1.5%.

The experimental set-up and the software for binary systems have been extended to determine the diffusion coefficients in ternary liquid systems. A differential refractometer and an ultraviolet-visible detector record the dispersion of the injected solutes. The diffusion coefficients are calculated directly by fitting the theoretical dispersion equations to about six experimental curves simultaneously. If the ternary diffusion effects in the measured dispersion profiles have not been obscured by the inaccuracy of the experimental method or an unfavourable relative detector sensitivity, the diffusion coefficients are precise (±2% - 10%). Experiments on the system methanol + acetone + water have shown that the Taylor dispersion method is not

always suitable for the determination of all ternary diffusion coefficients.

If one component in the ternary system is very dilute, the equations in the fitting procedure can be simplified. For the determination of the diffusion coefficients of the ternary systems glucose + water + dilute methanol, ethanol, or acetone the simplified fitting procedure has been used. The precision of the diffusion coefficients depends on the relative detector sensitivities for the components. The main-diffusion coefficients are more precise than the cross-diffusion coefficient (±2% vs. ±5 - 10%).

Diffusion coefficients can also be obtained from computer experiments. Molecular Dynamics (MD) is a simulation technique to compute the dynamic properties of many-particle systems by solving the classical equations of motion (Newton's equations) for the particles. Two methods have been compared for the calculation of Maxwell-Stefan diffusion coefficients. The first method is a non-equilibrium molecular dynamics (NEMD) algorithm, in which the system is driven away from equilibrium and the system response is monitored. The second method is the equilibrium molecular dynamics (EMD) calculation of the appropriate Green-Kubo equation. Simulations have been performed for systems of Lennard-Jones particles at various densities and temperatures. The systems have been divided into two or three components by attaching a colour label to the particles. Since a colour label plays no role in the dynamics, the Maxwell-Stefan diffusion coefficients of the binary and ternary systems are equal to the self-diffusion coefficient. In binary systems the Maxwell-Stefan diffusion coefficients, determined by the Green-Kubo (EMD) method, were found to be more accurate than the NEMD coefficients. The Green-Kubo method is also less time consuming and is therefore preferred. In ternary systems only the Green-Kubo method has been used. The Maxwell-Stefan diffusion coefficients agree well with the self-diffusion coefficient. For low mole fractions of the coloured components the diffusion coefficients are less accurate.

Subsequent simulations have been performed on binary and ternary systems of Lennard-Jones particles, in which the components differ by their dynamical behaviour owing to different values of the mass parameters and the Lennard-Jones energy-, and size

parameters. Also in these systems the GK method has determined the diffusion coefficients adequately.

Next, the self-diffusion coefficients and Maxwell-Stefan diffusion coefficients of liquid systems of particles with a more complicated structure have been calculated, i.e. methanol + water mixtures. For the description of the physical behaviour of the methanol and water particles a more complex interaction function than the Lennard-Jones potential is required. Two different force fields for each component have been used, in order to study the influence of the force field on the calculated self-diffusion coefficients of the pure liquids. The better performing force fields have been used for the determination of the diffusion coefficients in the methanol + water mixtures. The self-diffusion coefficients of both components in the mixtures of water and methanol are more accurate at high mole fractions of methanol. This can be explained by the better performance of the methanol force field. The Maxwell-Stefan diffusion coefficients in the mixtures of methanol and water agree fairly well with the experimental values. Since the measurements provide Fick diffusion coefficients, the measured coefficients have been transformed into Maxwell-Stefan coefficients, using thermodynamic correction factors.

The thesis concludes with a discussion of the results of the measurement and molecular simulation. The MD simulations of the methanol + water mixtures have shown the possibility of predicting the diffusion coefficients provided that the force fields and the simulation procedures (system size, simulation time) will be optimised.

SAMENVATTING

Moleculaire diffusie in vloeistoffen speelt een belangrijke rol in veel chemisch-technologische processen. Voor het ontwerpen van de procesapparatuur is het daarom van belang de diffusiecoëfficiënten te kennen. De empirische en semi-empirische relaties, die ontwikkeld zijn om de diffusiecoëfficiënten in vloeistoffen te voorspellen met behulp van de eigenschappen van de opgeloste stof en van het oplosmiddel, zijn niet nauwkeurig genoeg om niet-routinematige problemen op te lossen. Dit proefschrift beschrijft hoe diffusiecoëfficiënten verkregen kunnen worden met behulp van metingen en moleculaire simulaties. Het onderzoek is toegespitst op diffusie in waterige oplossingen van niet-electrolyten.

De Taylor dispersie methode is een meetmethode, die algemeen gebruikt wordt voor het meten van diffusiecoëfficiënten in vloeistoffen. Dit onderzoek begint met de beschrijving van een zeer gebruiksvriendelijke implementatie van de methode voor het meten met binaire vloeistofmengsels. De opstelling bestaat uit standaard HPLC-componenten en is volledig geautomatiseerd. Er is software ontwikkeld om de data te verwerken; de diffusiecoëfficiënten kunnen vrij gemakkelijk berekend worden uit de gemeten concentratie-tijd curve op diverse manieren. Metingen, uitgevoerd aan het methanol + water mengsel en het ethanol + water mengsel bij verschillende temperaturen hebben aangetoond, dat de binaire diffusiecoëfficiënten hier bepaald kunnen worden met een nauwkeurigheid van 0.5 – 1.5%.

De meetopstelling en de software voor binaire mengsels zijn aangepast voor het bepalen van de diffusiecoëfficiënten in ternaire vloeistofmengsels. Een differentiële refractometer en een ultraviolet-detector registreren de dispersie van de geïnjecteerde opgeloste stoffen. De diffusiecoëfficiënten worden rechtstreeks berekend uit de gemeten concentratieprofielen door de theoretische dispersievergelijkingen aan ongeveer zes profielen simultaan te fitten. Als de effecten van de ternaire diffusie in de gemeten dispersieprofielen niet vertroebeld zijn door de onnauwkeurigheid van de meetmethode of door een ongunstige relatieve detectorgevoeligheid, dan zijn de

diffusiecoëfficiënten precies (±2% – 10%). Experimenten aan het systeem methanol + aceton + water hebben aangetoond, dat de Taylor dispersie methode niet altijd geschikt is voor het bepalen van alle ternaire diffusie-coëfficiënten.

Als één component in het ternaire systeem erg verdund is, kunnen de vergelijkingen in de fitprocedure vereenvoudigd worden. Bij de bepaling van de diffusiecoëfficiënten van de ternaire systemen glucose + water + verdund methanol, ethanol of aceton is gebruik gemaakt van deze vereenvoudigde fitprocedure. De precisie van de diffusiecoëfficiënten is afhankelijk van de relatieve gevoeligheid van de detector voor de componenten. De hoofd-diffusiecoëfficiënten zijn preciezer dan de kruis-diffusiecoëfficiënt (±2% vs ±5 – 10%).

Diffusiecoëfficiënten kunnen ook bepaald worden door middel van computerexperimenten. Moleculaire Dynamica (MD) is een simulatiemethode om de dynamische eigenschappen van systemen, die uit meerdere deeltjes bestaan, te berekenen door voor deze deeltjes de klassieke bewegingsvergelijkingen (de vergelijkingen van Newton) op te lossen. Er zijn twee methoden vergeleken voor de berekening van de Maxwell-Stefan diffusiecoëfficiënten. De eerste methode is een niet-evenwichts moleculaire dynamica (NEMD) algoritme, waarin het systeem uit evenwicht gebracht wordt en de respons van het systeem gevolgd wordt. De tweede methode is de evenwichts moleculaire dynamica (EMD) berekening van de geschikte Green-Kubo vergelijking. Er zijn simulaties uitgevoerd voor systemen van Lennard-Jones deeltjes bij verschillende temperaturen en drukken. De systemen zijn verdeeld in twee of drie componenten door aan de deeltjes een kleur te geven. Omdat de kleur geen rol speelt in de dynamica, zijn de Maxwell-Stefan diffusiecoëfficiënten van de binaire en ternaire systemen gelijk aan de zelf-diffusiecoëfficiënt. In binaire systemen blijken de Maxwell-Stefan coëfficiënten, bepaald met behulp van de Green-Kubo (EMD) methode, nauwkeuriger te zijn dan de NEMD coëfficiënten. De Green-Kubo methode is ook minder tijdrovend en geniet daarom de voorkeur. In ternaire systemen is alleen de Green-Kubo methode gebruikt. De Maxwell-Stefan diffusiecoëfficiënten komen goed overeen met de zelf-diffusiecoëfficiënt. Voor lage molfracties van de gekleurde componenten zijn de diffusiecoëfficiënten minder nauwkeurig.

Er zijn vervolgens simulaties uitgevoerd voor binaire en ternaire systemen van Lennard-Jones deeltjes, waarin de componenten verschillen in hun dynamisch gedrag ten gevolge van verschillende waarden van de massa en de Lennard-Jones energie- en grootte-parameters. Ook in deze systemen zijn de diffusiecoëfficiënten met behulp van de Green-Kubo methode goed berekend.

Vervolgens zijn de zelf-diffusiecoëfficiënten en de Maxwell-Stefan diffusiecoëfficiënten berekend voor vloeibare systemen van deeltjes met een gecompliceerdere structuur, met name methanol + water mengsels. Voor de beschrijving van het fysisch gedrag van de methanol- en water-deeltjes is een krachtveld nodig, dat complexer is dan de Lennard-Jones potentiaal. Voor elke component zijn twee verschillende krachtvelden gebruikt, ten einde de invloed van het krachtveld op de berekening van de zelf-diffusiecoëfficiënt in de zuivere vloeistoffen te onderzoeken. De krachtvelden, die het best voldoen, zijn gebruikt voor de berekening van de diffusiecoëfficiënten in de methanol + water mengsels. De zelf-diffusiecoëfficiënten van beide componenten in de mengsels van methanol en water zijn nauwkeuriger bij hoge molfracties methanol. Dit kan verklaard worden door een beter functionerend krachtveld van methanol. De Maxwell-Stefan diffusiecoëfficiënten in de mengsels van methanol en water komen redelijk goed overeen met de gemeten waarden. Omdat bij de metingen Fick diffusiecoëfficiënten bepaald worden, zijn deze eerst omgerekend naar Maxwell-Stefan diffusiecoëfficiënten met behulp van thermodynamische correctiefactoren.

Dit proefschrift besluit met een discussie over de resultaten van de metingen en de moleculaire simulaties. De MD simulaties van de methanol + water mengsels hebben aangetoond dat het mogelijk is de diffusiecoëfficiënten te voorspellen, mits de krachtvelden en de simulatieprocedures (systeemgrootte, simulatietijd) geoptimaliseerd worden.

CONTENTS

1. INTRODUCTION

General introduction

Diffusion can be described as a mixing process on a microscopic scale, caused by the molecular motion of the particles. In liquids it is a slow process, and this slowness is responsible for its importance. It can be the rate-determining step in many mass transfer operations, such as distillation, extraction, and in industrial reactions using porous catalysts. It controls, for instance, the release of flavour from food. Therefore, knowledge of diffusion rates is important for the design of process equipment [1].*

Two common models can describe molecular diffusion in multicomponent liquids [2-4]:

1. A generalisation of Fick's law to multicomponent systems [5]. Fick's law is a phenomenological description of diffusion for binary liquid systems [6].
2. An extension of the Maxwell-Stefan equations to liquids [2, 7]. The Maxwell-Stefan equations were developed for describing multicomponent diffusion in gases [8-11].

The generalised Fick's law as well as the generalised Maxwell-Stefan equations can be derived from irreversible thermodynamics [2]. Both models use diffusion coefficients as parameters. The Fick diffusion coefficients can be transformed into the Maxwell-Stefan diffusion coefficients and vice versa, using the thermodynamic correction factors portraying the non-ideal behaviour [2, 7].

Theories for calculating diffusion coefficients in non-electrolyte liquid mixtures have been based on the hydrodynamic theory, kinetic theory, thermodynamic theory, absolute rate theory, statistical mechanics, and other concepts. Many empirical and semi-empirical correlations have been developed, which attempt to predict the liquid diffusion coefficient in terms of solute and solvent properties [1, 2, 4, 12-28]. None is very accurate. The estimates of the liquid diffusion

* References are given at the end of each chapter.

coefficients using these correlations help to solve only the routine problems. In most nonroutine problems, however, more accurate values of the diffusion coefficients are required. These can be obtained by supplementing the estimates with a good supply of experimental data. Therefore, measurements of the diffusion coefficients are necessary.

Almost all methods for the measurement of the diffusion coefficients in liquids employ Fick's model. Experimental techniques used widely are the diaphragm cell technique, interferometric methods and the Taylor dispersion method [1, 2, 4, 12, 17, 29]. Although the diaphragm cell technique and the interferometric methods permit more accurate measurements, the Taylor dispersion method is often preferred: this method does not need any repeated calibration, is fast, the set-up consists of standard HPLC components, and the measurements can easily be automated. In binary systems, the Taylor dispersion method is also an accurate technique. In multicomponent systems, however, the measurement of diffusion coefficients is still difficult and time-consuming [4].

A third way to obtain diffusion coefficients could be from computer experiments. Computer simulations are not only used to test new theories before applying them to the real world. More commonly, computer simulations are applied to predict the properties of materials, such as the location of the freezing point and the adsorption isotherms. It is often easier and less expensive to perform a computer experiment than to measure the property of the real material, especially at very high temperatures or pressures. Also properties of future materials can be predicted. In a computer experiment it is possible to take a "sample" of the material, and to solve Newton's equations of motion for this sample during a specific duration of time. The desired quantity, expressed as a function of the positions and momenta of the particles in the system, can then be "measured", i.e. calculated. Diffusion depends on molecular motions that take place over molecular distances. Thus, the mechanism of diffusion, and the prediction of the diffusion coefficients, can be studied by performing an abovementioned computer experiment.

Molecular Dynamics (MD) is a simulation technique to compute the dynamic properties of many-particle systems by solving the

classical equations of motion (Newton's equations) for the particles. The transport properties, e.g. the diffusion coefficients, can be calculated by performing an equilibrium molecular dynamics (EMD) simulation or a non-equilibrium molecular dynamics (NEMD) simulation [30-38]. In an EMD simulation, the appropriate equilibrium time-correlation functions are calculated. All possible transport properties can, in principle, be determined from the fluctuating quantities in the equilibrium system from a single EMD run [34]. In an NEMD simulation, the system is driven away from equilibrium by imposing an external field, and the system response is monitored. Diffusion coefficients can be simulated by applying an external force to the individual particles in the system. For different transport properties a completely new simulation is necessary [38].

Because it is still difficult and time-consuming to measure the diffusion coefficients in multicomponent systems, it is interesting to develop a method for calculating the diffusion coefficients from molecular simulations. By comparison of the simulation method with measurements, performed on the real systems, the applicability and reliability of the simulation method can be investigated. This can be the first step to a future application of computer simulations to supplement or even substitute diffusion coefficient measurements.

This work deals with both the measurement and the molecular simulation of diffusion coefficients. The model systems used are chosen for several reasons. For comparison of the results, it is important to use the same model systems in both the simulations and the measurements. These model systems preferably consist of small particles, since the simulations of mixtures of small particles are expected to be easier to accomplish. The detectability of the components is allowed to be difficult, because then the systems are also suitable for the investigation of the applicability and the limitations of the Taylor dispersion method. Finally, for future use of the results in the research of food processing, water has to be one of the components.

For these reasons various binary and ternary liquid mixtures of methanol, ethanol, acetone, and glucose in water have been investigated. The binary system methanol + water consists of small particles and is therefore used in the simulations. The necessary

continuous monitoring of the small concentration differences in solutions of methanol (or ethanol) in water can be performed by the differential refractometer, which is universally usable. The concentration of acetone in the ternary mixture of acetone + methanol + water can be monitored by an ultraviolet-visible detector, which allows the independent simultaneous measurement of the concentrations by two different detectors. This is important for the investigation of the performance of the Taylor dispersion method in ternary diffusion measurements. Another ternary system used, water + glucose + dilute methanol (or ethanol, or acetone), is chosen because of its frequent occurrence in food processing research.

Since almost all methods for the measurement of diffusion coefficients employ Fick's model, the diffusivities found in the literature are usually Fick's diffusion coefficients. In this thesis, therefore, Fick's description of diffusion is used in the computation of the diffusivities from the measurements. However, the Maxwell-Stefan approach is preferred over Fick's law for describing diffusion under influence of external forces, and in multicomponent systems, in which less Maxwell-Stefan diffusion coefficients are necessary [7]. For these reasons, the Maxwell-Stefan approach is chosen for the computation of the diffusivities from the molecular simulations. For comparison, the measured Fick diffusivities can be transformed into Maxwell-Stefan diffusivities and vice versa.

Outline of the thesis

The body of this thesis describes the measurement of diffusion coefficients in binary and ternary liquid systems (chapters 2, 3 and 4), followed by the molecular simulation of diffusion (chapters 5, 6 and 7).

In chapter 2, the development of the instrument for measuring diffusion coefficients in binary liquid systems is described. The experimental technique used is the Taylor dispersion method. The experimental set-up consists of standard HPLC equipment and has been fully automated. Software has been developed for processing the data. Experiments were performed on the binary systems methanol + water and ethanol + water at various temperatures. Chapter 3 describes the extension of the Taylor dispersion method to ternary

liquid systems. Complications in the use of this method for ternary diffusion measurements are illustrated by the measurements on the system methanol + acetone + water. The determination of the diffusion coefficients in the ternary systems glucose + water + dilute methanol, ethanol or acetone is described in chapter 4.

In chapter 5, an EMD method and an NEMD method are compared using simulations of a Lennard-Jones fluid. As a result, the EMD method is preferred. The simulation of the molecular diffusion in ternary Lennard-Jones systems is described in chapter 6. In chapter 7, the developed simulation method is applied to the binary liquid system methanol + water.

Finally, a short discussion of the results is given in chapter 8.

Note

Chapters 2 to 7 are a collection of articles. Therefore, every chapter is self-contained, and it is not necessary to read all chapters preceding the chapter one is interested in.

References

[1] Cussler, E. L., 1984, 1997 (second ed.), *Diffusion. Mass transfer in fluid systems* (Cambridge: University Press).
[2] Cussler, E. L., 1976, *Multicomponent diffusion* (Amsterdam: Elsevier).
[3] Taylor, R., and Krishna, R., 1993, *Multicomponent Mass Transfer* (New York: Wiley).
[4] Rutten, Ph. W. M., 1992, Ph. D. thesis, Delft University of Technology.
[5] Onsager, L., 1945, *Ann. N. Y. Acad. Sci.*, **46**, 241.
[6] Fick, A., 1855, *Ann. der Physik*, **94**, 59.
[7] Krishna, R., and Wesselingh, J. A., 1997, *Chem. Eng. Sci.*, **52**, 861.
[8] Maxwell, J. C., 1866, *Phil. Trans. Roy. Soc.*, **157**, 49.
[9] Maxwell, J. C., 1868, *Phil. Mag.*, **35**, 129.
[10] Maxwell, J. C., 1868, *Phil. Mag.*, **35**, 185.
[11] Stefan, J., 1871, *Sitzungsber. Akad. Wiss. Wien*, **63**, 63.

[12] Johnson, P. A., and Babb, A. L., 1956a, *Chemical Reviews*, **56**, 387.
[13] Bird, R. B., Stewart, W. E., and Lightfoot, E. N., 1960, *Transport phenomena* (New York: Wiley).
[14] Loflin, T, and McLaughlin, E., 1969, *J. Phys. Chem.*, **73**, 186.
[15] Perkins, L. R., and Geankoplis, C. J., 1969, *Chem. Eng. Sci.*, **24**, 1035.
[16] Ghai, R. K., Ertl, H., and Dullien, F. A. L., 1973, *AIChE J.*, **19**, 881.
[17] Ertl, H., Ghai, R. K., and Dullien, F. A. L., 1974, *AIChE J.*, **20**, 1.
[18] Erdey-Gruz, T., 1974, *Transport phenomena in aqueous solutions*, (London: Adam Hilger).
[19] Termonia, Y., and Alexandrowicz, Z., 1980, *Molec. Phys.*, **39**, 725.
[20] Reid, R. C., Prausnitz, J. M., and Poling, B. E., 1987, *The properties of gases and liquids*, 4th Edn. (New York: McGraw-Hill).
[21] Kestin, J., and Wakeham, W. A., 1988, *Transport properties of fluids: thermal conductivity, viscosity, and diffusion coefficient, Cindas Data Series on Material Prop.*, Vol I-1 (New York: Hemisphere Publ. Corp.).
[22] Kooijman, H. A., and Taylor, R., 1991, *Ind. Eng. Chem. Res.*, **30**, 1217.
[23] Castillo, R., Garza, C., and Dominguez, H., 1993, *J. Chem. Phys.*, **99**, 9899.
[24] Castillo, R., Garza, C., and Dominguez, H., 1994, *J. Chem. Phys.*, **100**, 6649.
[25] Mill, R., Malhotra, R., Woolf, L. A., and Miller, D. G., 1994, *J. Phys. Chem.*, **98**, 5565.
[26] Pertler, M., Blass, E., and Stevens, G. W., 1996, *AIChE J.*, **42**, 910.
[27] Wesselingh, J. A., and Bollen, A. M., 1997, *Trans. IchemE. Part A*, **75**, 590.
[28] Fei, W., and Bart, H-J., 1998, *Chem. Ing. Techn.*, **70**, 1309.
[29] Wakeham, W. A., Nagashima, A., and Sengers, J. V., 1991, *Measurement of the Transport Properties of Fluids, Experimental Thermodynamics*, Vol III (Oxford: Blackwell).
[30] Schoen, M., and Hoheisel, C., 1984, *Molec. Phys.*, **52**, 33.
[31] Hansen, J. P., and McDonald, I. R., 1986, *Theory of Simple Liquids*, 2nd Edn. (London: Academic Press).

[32] Allen, M. P., and Tildesley, D. J., 1987, *Computer Simulations of Liquids* (Oxford: Clarendon).
[33] Chandler, D., 1987, *Introduction to Modern Statistical Mechanics* (Oxford University Press).
[34] Evans, D. J., and Morriss, G. P., 1990, *Statistical Mechanics of Non-Equilibrium Fluids* (San Diego: Academic Press).
[35] Van Gunsteren, W. F., and Berendsen, H. J. C., 1990, *Angew. Chem.*, **102**, 1020.
[36] Cummings, P. T., and Evans, D. J., 1992, *Ind. Eng. Chem. Res.*, **31**, 1237.
[37] Frenkel, D., and Smit, B., 1996, *Understanding Molecular Simulation* (San Diego: Academic Press).
[38] Berendsen, H. J. C., 1991, *Computer Simulation in Material Science* (Dordrecht: Kluwer) p. 139.

2. FAST AND CONVENIENT IMPLEMENTATION OF THE TAYLOR DISPERSION METHOD

Abstract*

A highly labour-efficient implementation of the Taylor dispersion method for measuring mutual diffusion coefficients in binary liquid systems is described. The experimental set-up has been fully automated; it is possible to measure the diffusion coefficients over the entire concentration range in a single experiment using standard HPLC equipment. Software has been developed for processing the data; diffusion coefficients can be calculated from the measured concentration against time curve in various ways (e.g. from the first and second moments and by fitting procedures) within a few seconds. Experiments on the methanol + water system (25 °C and 35 °C) and the ethanol + water system (25 °C and 40 °C) have an accuracy of 0.5 - 1.5%.

* The main part of this chapter has been published: Van de Ven - Lucassen, I. M. J. J., Kieviet, F. G., and Kerkhof, P. J. A. M., 1995, *J. Chem. Eng. Data*, **40**, 407.

Introduction

Liquid diffusion plays an important role in chemical engineering, and the design of process equipment requires knowledge of mutual diffusion coefficients. The purpose of this work is to develop an apparatus for measuring diffusion coefficients in liquid systems over a wide range of temperature and pressure in a fast, accurate, and labour-efficient way. The instrument developed here should not need any repeated calibration, and the calculation of the diffusion coefficient from the measured variables is simple and easy to computerise.

Experimental techniques used widely for measuring diffusion coefficients are the diaphragm cell technique, interferometric methods, and the Taylor dispersion method [1-5]. Interferometric methods permit the most accurate measurements near room temperature, but it is not (yet) possible to employ these instruments over a wide range of temperature and pressure. The disadvantages of the diaphragm cell are the necessity for calibration of the cell with a system of known diffusivity. Another disadvantage is the long measuring time. The Taylor dispersion technique provides a good alternative. The method is fast, the set-up consists of standard HPLC components, and the measurements can be readily automated [6]. Therefore we have chosen the Taylor dispersion method.

The Taylor dispersion method (TDM) is based on the following principle [7, 8]: a slow, laminar flow of a liquid mixture is pumped through a long capillary and a narrow pulse of a mixture of a slightly different composition is injected into this capillary. Due to the combined effects of convective flow and molecular diffusion, the pulse ultimately assumes a Gaussian distribution, whose temporal variance is dependent on both the average flow velocity and the molecular diffusivity.

At the end of the diffusion capillary the concentration is measured as a function of time; the diffusion coefficient is calculated from the first and second temporal moments or by fitting the dispersion equation to the experimental curve.

Theory

When a pulse of a different concentration is injected into a fluid flowing slowly through a long capillary, it spreads out due to the laminar velocity profile in the tube and the molecular diffusion. The concentration at the end of the diffusion tube is given by

$$C_i = \frac{V_i c_i}{2\pi R^2} \frac{1}{\sqrt{(\pi k t)}} \exp\left(\frac{-L^2\left(1-\frac{t}{\tau}\right)^2}{4kt} \right). \tag{2.1}$$

In this expression $V_i c_i$ is the number of moles of component i in the injected pulse in excess of those present in the same volume of the carrier stream (solvent), C_i is the radially-averaged concentration of component i at time t relative to the background concentration, R is the internal radius of the diffusion tube, L is the diffusion tube length, and $\tau \equiv L / U$ is the mean residence time with U the linear velocity averaged over the cross section. The dispersion coefficient k is found to be [9]

$$k = \frac{R^2 L^2}{48\tau^2 D_{12}} + D_{12}, \tag{2.2}$$

where D_{12} is the binary molecular diffusion coefficient. In practice, Eq 2.2 simplifies to [7, 8]

$$k = \frac{R^2 L^2}{48\tau^2 D_{12}} \tag{2.3}$$

for diffusion in liquids, since in TDM equipment the second term is several orders of magnitude smaller than the first term.

The assumptions made in the derivation of eq 2.1 impose some constraints on the experimental conditions:

- Axial (molecular) diffusion can be ignored when $U > \alpha_1 \cdot D_{12}/R$. α_1 is a constant: its value ranges from 6.9 [7, 8] to 700 [14] [7, 8, 10-17].

- Radial concentration differences are assumed to be small when $U < \alpha_2 \cdot (L \cdot D_{12})/R^2$. α_2 ranges from 4 to 0.1 [6, 7, 10-15, 18-24].
- If $\alpha_2 = 0.048$ [25], the perturbations due to temperature / pressure reduction occurring in a short length between the capillary and the detector are negligible.
- The development of secondary flow due to the coiling of the capillary can be neglected when $De^2Sc \leq 20$ and $R_c/R \geq 100$, in which the Dean number $De = (2R\rho U/\eta) \cdot (R/R_c)^{1/2}$, the Schmidt number $Sc = (\eta/\rho D_{12})$, η the solvent viscosity, ρ the solvent density, and R_c the radius of the tubing coil [14, 15, 20, 21, 24, 27-33].

Other restrictions on the experimental conditions and corrections on the ideal average residence time and variance are well described by Alizadeh [14] and Baldauf [26].

When the concentration is measured, the relation between the detector signal $s(t)$ and the concentration against time curve (eq 2.1) is assumed to be

$$s(t) = w \cdot C_i + a + b \cdot t + \varepsilon(t), \tag{2.4}$$

in which w is the detector sensitivity, a and b compensate for the detector drift (which is assumed to be linear in time), and $\varepsilon(t)$ is noise. The signal is sampled with a sample interval of $\Delta t_i : y^*_i = s(t_i)$. The sample interval Δt_i must be chosen such that it provides a minimum of N data points within the solute peak (N = 200 [24]).

Diffusion coefficients can be calculated from the measured concentration against time curves in two different ways: calculation from the first and second moments; fitting of the theoretical eq 2.4 to the experimental curve.

Calculation from the first and second moments

For the calculation of the first and second moments the discrete signal without the drift is required: $y_i = y^*_i - (a + b\ t_i)$. For the calculation of a and b, regions of this signal are visually marked in our software as baseline, i.e. the concentration negligibly small. Through these regions of the signal the drift is fitted and subtracted from the signal.

The first moment $\bar{t}$ and the second moment σ^2 are defined as follows:

$$\bar{t} = \frac{\sum_{i=0}^{N} t_i y_i \Delta t_i}{\sum_{i=0}^{N} y_i \Delta t_i}, \text{ and } \sigma^2 = \frac{\sum_{i=0}^{N} (t_i - \bar{t})^2 y_i \Delta t_i}{\sum_{i=0}^{N} y_i \Delta t_i}. \tag{2.5}$$

The mean residence time can be calculated for either a closed or an open system: For a closed system (no diffusion through the cross-section at both ends of the tube, finite tube) $\tau \equiv \bar{t}$. For this system Taylor derived the explicit relation [7, 8]

$$D_{12} = \frac{R^2 \bar{t}}{24\sigma^2}. \tag{2.6}$$

For an open system (infinite tube) the expression can be derived

$$\tau = \bar{t} - \frac{R^2}{24 D_{12}}, \tag{2.7}$$

which results in an implicit relation for the diffusion coefficient (eq 2.3 combined with Van der Laan [25]):

$$D_{12} = \frac{R^2}{48\sigma^2}\left\{\bar{t} - \frac{R^2}{24 D_{12}} + \left[\left(\bar{t} - \frac{R^2}{24 D_{12}}\right)^2 + 8\sigma^2\right]^{1/2}\right\}. \tag{2.8}$$

Other relations have been derived by Alizadeh [14] and Matthews [34, 35].

Fitting of the theoretical equation 2.4 to the experimental curve

This can be done in several different ways:

- The drift parameters a and b are calculated as indicated above. The term $V_i c_i w$ is calculated by integration of the signal. D_{12} is fitted, τ is calculated using eq 2.7 during the iterative process (one-parameter fit).

- a, b, and $V_i c_i w$ are calculated as in 1. D_{12} and τ are fitted (two-parameter fit).
- a, b, and $V_i c_i w$ and D_{12} are fitted; τ is calculated during the fitting process using eq 2.7 (four-parameter fit).
- a, b, and $V_i c_i w$, D_{12} and τ are fitted [4, 36] (five-parameter fit).

Other fitting procedures are possible (e.g. three-parameter fits).

Calculation methods were compared by processing a concentration against time curve calculated by means of eq 2.1 with a superposition of randomly generated noise or superposition of an experimentally measured baseline.

Calculation of moments is extremely simple and fast. The Van der Laan method (eq 2.8) yields the best fit to the shape of the experimental curve (visualisation), the smallest sum of squares $\sum_{i=1}^{N}(y_i - wC_i)^2$, and minimal deviations in D_{12} and τ. Fitting is more accurate though. The one- and two-parameter fits are, of course, faster than the four- and five-parameter fits, and they yield consistent diffusion coefficients and are therefore preferred.

Equipment and experimental procedure

The apparatus used is shown schematically in figure 2.1. The pump must deliver a constant laminar flow. Several pumps of different types were tested. The amplitude and frequency of the fluctuations in the pressure were measured at various backpressures (figure 2.2). We selected an HPLC pump (type LKB2150) combining a low pulsation and constant flow with the capability of continuous operation. Implementation of computer control in our software was relatively easy. The selection valve allows the solvents to be changed during one experiment. To prevent bubbles from disturbing the flow, an in-line degasser (Separations DG1300) was installed. Moreover, the solvent flask was purged once with helium for 10 - 15 min. The pump was connected to an autosampler (Spark Marathon) with a fixed volume sample loop (20 µl); the sample tray can hold 96 vials.

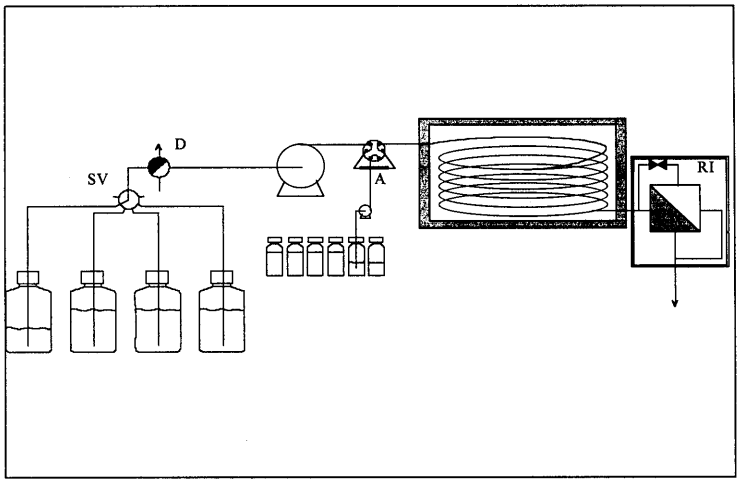

Figure 2.1. *Experimental set-up:* SV, *selection valve;* D, *degasser;* A, *autosampler;* RI, *refractive index detector*

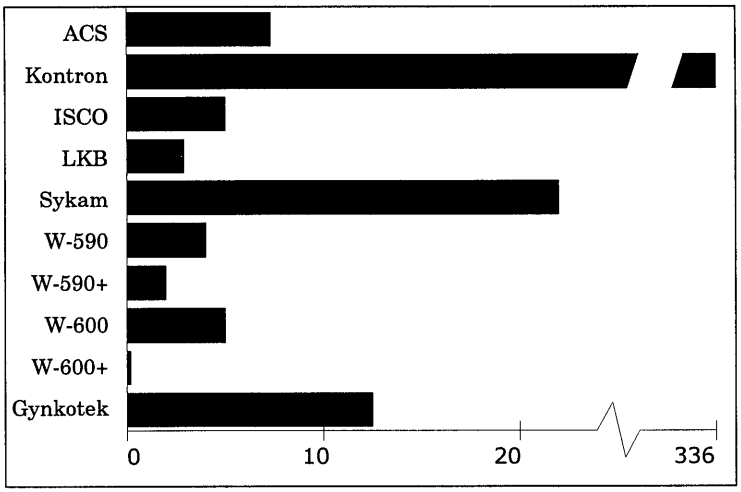

Figure 2.2. *Pulsations of the pump (pulsations in* 10^{-5} *bar, back pressure 2 bar):* ACS, *ACS 351 isocratic HPLC pump;* ISCO, *ISCO LC-5000 syringe pump;* Kontron, *Kontron HPLC*; LKB, *LKB2150 HPLC pump;* Sykam, *Sykam S-1000 HPLC pump;* W-590, *Waters 590 Programmable Solvent Delivery Module;* W-590+, *W-590 + pulsation dampeners;* W-600, *Waters 600/625 MS PowerLine multi-solvent delivery system;* W-600+, *W-600 + pulsation dampeners;* Gynkotek, *Gynkotek HPLC pump Model 300.*

Zero dead volume fittings were used to connect the diffusion tube with the autosampler and the detector. For installation of the capillary tube in a water bath of circular cross section (d_b = 0.50 m), which could be kept at the desired temperature within ±0.025 °C with a Lauda CSG 2.0 kW thermostat, it was necessary to coil the tube horizontally (d_c = 0.40 m). To measure the diffusion coefficient in liquid systems with a wide range of viscosities (and diffusion coefficients), stainless steel tubes (*i.d.* = 1.041 mm) of various lengths (10, 15, 25, 50 m) were installed. The differential refractometer (Shodex SE61) measured the difference in refractive index between the sample stream and the reference liquid (solvent). The analogous output signal of the refractometer was converted by a Multilab system, which consists of an A/D-D/A conversion system developed at Eindhoven University of Technology (sample interval 0.98 s yielding 3000 - 4000 data points per peak, including parts of the baseline in front of and behind the peak). The Multilab was used to interface between detector and PC and between selection valve and PC. The pump and autosampler were controlled directly by a personal computer.

Software has been developed for data acquisition and controlling the equipment (called Linus) which makes it possible to measure diffusion coefficients in 16 different solvents in a single experiment. All aspects of the experiment except the preparation of the solvents and sample solutions have been automated. An optional manual control was included. To process the data, a module was added to an MS Windows signal processing software package that provides extensive visualisation and data-manipulating capabilities. This module provides various methods for the calculation of the diffusion coefficient from the first and second moments (eq 2.5), using the equations of Taylor (eq 2.6, Van der Laan correction eq 2.7 optional), Van der Laan (eq 2.8), Alizadeh [14] and Matthews [34, 35], and by means of fitting procedures, based on the least-squares approximation between the experimental data points and the points calculated according to eqs 2.1 and 2.3. The method of Levenberg and Marquardt [37] is used for two-parameter fitting and the Golden section search algorithm [38] for the one-parameter fitting. Initial guesses for the diffusion coefficient are obtained by means of the equation of Matthews [34, 35]. The amount in the injected pulse, $V_i c_i$, is calculated by equalising the integral of the measured concentration against time curve to the integral of eq 2.1, assuming the detector response to be

linear with the concentration. Visual confirmation of the calculated values of τ and D_{12} is possible by overlaying the experimental peak with the fitted peak.

In a typical diffusion experiment, the solutions are prepared by mass and mixing and degassed by sparging with helium. Injection solutions are made by volumetrical mixing of the degassed solvents. The flow velocity is set in accordance with the conditions of the previous section. In Linus a new program is created (or an already existing method is edited), and after an emulation, the program is run.

Preparation of the solvents and injection solutions (sufficient for three experiments) takes one day's work, and creating the new program takes a few minutes. The data gathered in a week's run can be processed within a few hours. Calculation of the diffusion coefficient from one concentration against time curve takes only a few seconds.

Experimental results and discussion

Diffusion coefficients were measured for methanol + water and ethanol + water. Deionized water filtered through a Milli-Q Water Purification System (Millipore, resistivity 18 MΩ.cm) was used. Analytical-grade methanol (purity ≥ 99.8%, water < 0.05%) and ethanol (purity ≥ 99.8%, water < 0.2%) were obtained from Merck and used without further purification.

Experiments were performed to show that the detector response was linear with concentration and to test the effect of the concentration of the injected sample on the measurement of the diffusion coefficient. Samples of increasing methanol concentration were injected into pure water, and the peak area and the diffusion coefficient were calculated. Between injection and detection of a sample, subsequent samples were injected for enhanced time efficiency. Simultaneous dispersion of two or more δ-pulses in the tube did not disturb the diffusion process provided the time between two subsequent injections was large enough to prevent overlapping of the solute peaks. Degassing of the injection solutions after preparation appeared to be unnecessary.

The diffusion coefficient as a function of the methanol concentration of the sample injected into pure water is shown in figure

2.3. Below a concentration difference of 5 vol% no influence was observed. A minimum difference of 0.5 vol% was necessary to obtain an accurate concentration against time curve (as a result of detector noise). Measurements at other solvent compositions confirmed this result. Experiments for the system ethanol + water also showed a linear detector response and an independence of the concentration difference up to 4 vol%.

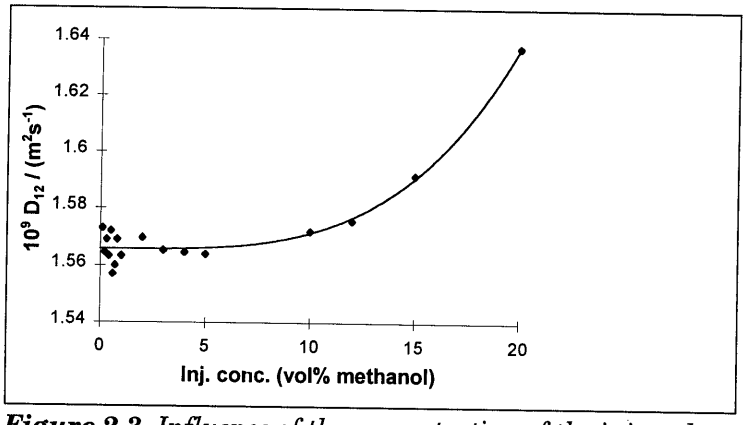

Figure 2.3. *Influence of the concentration of the injected sample (methanol in water, 25 °C):* ♦, D_{12}; —, *fit (powerlog).*

To examine whether short time pulsations produced by the pump influence dispersion, experiments were carried out using a "pulsation-free" ISCO syringe pump (500 cm^3) as well as our LKB pump; solvents were pure water and a water + methanol mixture (83 vol% methanol). The noise in the concentration against time curves of the ISCO experiments appeared to decrease a little and was of a slightly different shape. The calculated diffusion coefficients and the inaccuracy in the results were not significantly different. Therefore, we preferred the LKB pump.

To investigate the influence of the mean residence time (and the flow velocity), experiments were carried out at various flow velocities in the 15 m tube as well as in the 25 m tube for both the methanol + water and the ethanol + water system. The results as shown in figure 2.4 demonstrate the validity of the experimental conditions described previously.

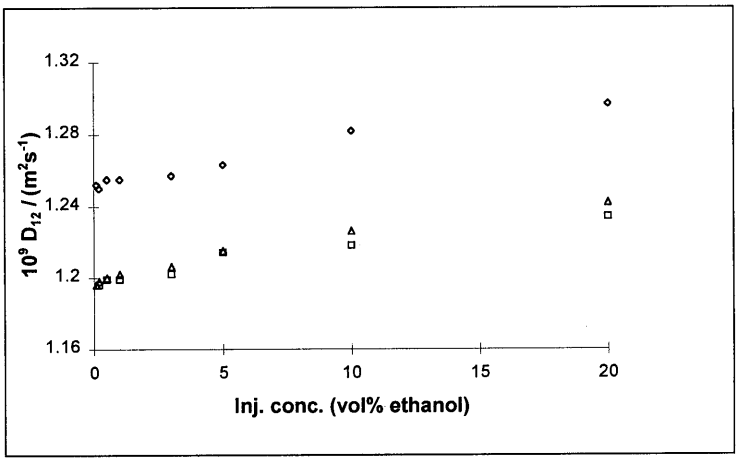

Figure 2.4. *Influence of the flow and the injection concentration (ethanol in water, 25 °C): □, 0.1 $cm^3.min^{-1}$; Δ, 0.2 $cm^3.min^{-1}$; ◊, 0.4 $cm^3.min^{-1}$.*

Table 1. *Mutual diffusion coefficients for methanol(1) + water(2) at 25 °C and 35 °C*

	25 °C				35 °C
x_1	$10^9 D_{12}$ / ($m^2.s^{-1}$)	inacc,%	$10^9 D_{12}$ / ($m^2.s^{-1}$)	inacc,%	$10^9 D_{12}$ / ($m^2.s^{-1}$)
0	1.560	0.49	1.560	0.49	1.94
0.048	1.350	1.88			
0.058			1.330	0.77	1.66
0.100	1.210	0.70			
0.123			1.170	1.67	1.45
0.160	1.070	0.92			
0.194			1.030	1.40	1.29
0.236	0.989	1.35			
0.272			0.956	1.82	1.21
0.307	0.940	3.91			
0.366			0.948	2.85	1.22
0.400	0.957	3.63			
0.458			0.978	2.88	1.25
0.510	1.030	3.88			
0.568			1.119	3.15	1.41
0.640	1.200	1.80			
0.691			1.266	0.30	1.71
0.801	1.630	4.91			
0.835			1.845	7.56	2.12
0.996	2.130	2.34	2.145	4.33	2.61

Table 2. *Mutual diffusion coefficients for ethanol(1) + water(2) at 25 °C and 40 °C*

	25 °C		40 °C	
x_1	$10^9 D_{12}$ / ($m^2.s^{-1}$)	inacc,%	$10^9 D_{12}$ / ($m^2.s^{-1}$)	inacc,%
0	1.200	0.5	1.745	0.3
0.09			1.020	4.7
0.10	0.695	1.1		
0.20	0.393	2.8	0.642	4.7
0.23			0.595	2.9
0.24	0.374	1.6		
0.27			0.573	6.3
0.28	0.367	0.9		
0.36			0.629	4.1
0.37	0.392	2.8		
0.42	0.444	5.9	0.677	7.0
0.48			0.821	2.4
0.49	0.504	5.0		
0.56	0.692	58.4		
0.73			1.318	5.3
0.74	0.834	5.3		
0.94	1.100	3.0		

Finally, the binary diffusion coefficients of the methanol + water system and the ethanol + water system at various temperatures were measured as a function of composition. After the eluents were switched, the system was flushed for 30 min at a high flow rate (1.5 $cm^3.min^{-1}$) and for 6 h at the flow rate of the diffusion experiment (e.g. 0.15 $cm^3.min^{-1}$) to attain a stable, linear baseline.

Results are listed in tables 1 and 2; each value is the average of the calculated diffusion coefficients of several injections (various sample concentrations in the range 0.5 - 5 vol%). The values at mole fraction 0 are extrapolated (sample concentration 0%). The confidence limits ("inaccuracy") of the data (calculated according to the Student's t distribution, probability level 95%, two-tail test [39]) increase close to the maximum in the refractive index-concentration curve of the system, as expected.

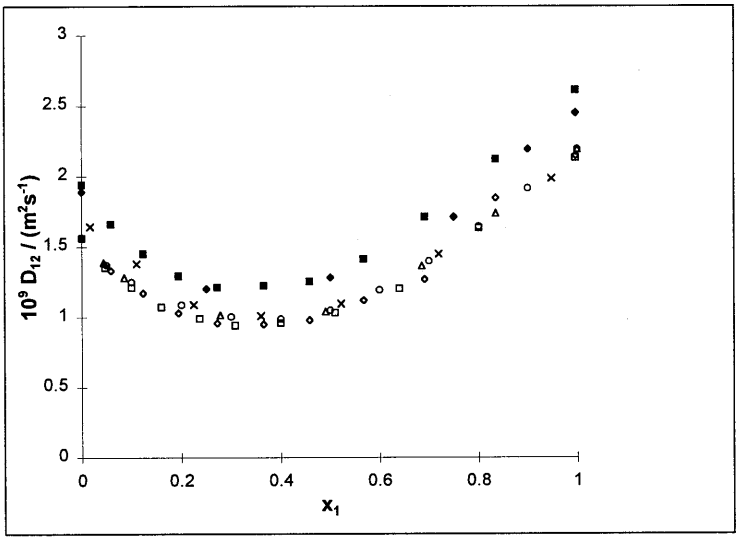

Figure 2.5. *Diffusion coefficient methanol(1) + water(2).*
25 °C: □, expt 1; ◊, expt 2; ×, ref 5 (dual bellows diaphragm cell, 3%);
○, ref 41 (diaphragm cell); Δ, ref 42 (diaphragm cell).
35 °C: ■, expt; ♦, ref 40 (Taylor dispersion, 1%).
The points at mole fractions 0 and 1 are extrapolated values.

Comparison with literature values in figures 2.5 and 2.6 shows a good agreement. The high deviation in the points of Pratt [24] at mole fraction 0.44 and ours at mole fraction 0.56 for the ethanol + water system is believed to be caused by using the refractive index detector close to the maximum in the refractive index-concentration curve. For the methanol + water system fewer literature values are available. The higher experimental values of Kircher [5] are believed to be caused by the method used (dual bellows diaphragm cell). As Woolf [41, 42] did not mention the accuracy of the measurements, it is not possible to decide whether the deviation is significant. Taylor dispersion data at 25 °C were not available. At 35 °C and high mole fractions the diffusion coefficients of Lee and Li [40] are lower than the diffusion coefficients obtained in our measurements, with a deviation of 5 - 8%.

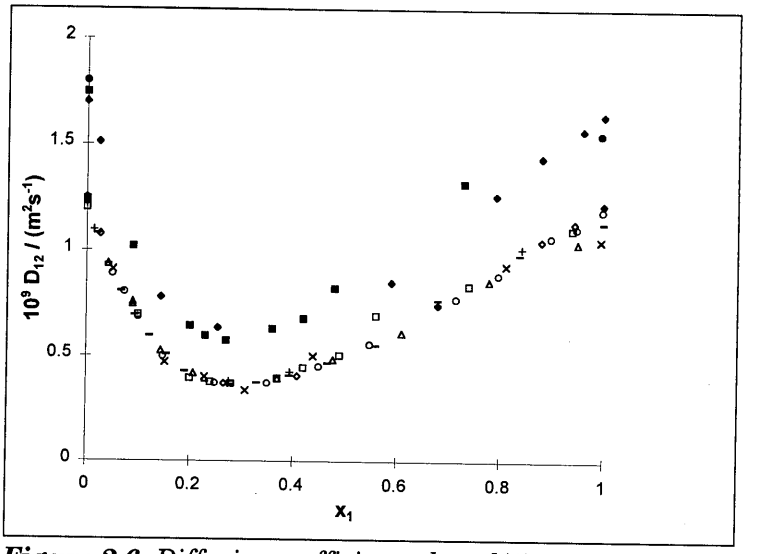

Figure 2.6. *Diffusion coefficient ethanol(1) + water(2).*
25 °C: □, expt; Δ, ref 5 (dual bellows diaphragm cell, 3%); ×, ref 24 (Taylor dispersion, 2.5%); ○, ref 43 (Taylor dispersion, 2%); ◊, ref 44 (diaphragm cell, 2.6%); —, ref 45 (diaphragm cell, 1%); +, ref 46 (diaphragm cell, 2%).
40 °C: ■, expt; •, ref 24 (Taylor dispersion, 2.5%); ♦, ref 44 (diaphragm cell, 2.6%).
The points at mole fractions 0 and 1 are extrapolated values.

Conclusions

The Taylor dispersion method for measuring diffusion coefficients is an accurate technique. In this paper we have shown that the technique can be fast as well if the experimental set-up is extensively automated.

Various calculation methods have been discussed. A simple one-parameter fit or even the Van der Laan equation newly presented in this paper yields sufficiently accurate results.

In easily determinable systems diffusion coefficients can be measured with an inaccuracy of ±0.5 - 1.5%, e.g. our measurements on methanol and ethanol in pure water. Concentration differences in methanol + water and ethanol + water mixtures with a composition close to the maximum in the refractive index-concentration curve are

more difficult to measure; in this case the inaccuracy in the obtained diffusion coefficients is less then ±4 - 5%.

References

[1] Johnson, P. A. and Babb, A. L., 1956a, *Chem. Rev.*, **56**, 387.

[2] Cussler, E. L., 1976, *Multicomponent diffusion* (Amsterdam: Elsevier).

[3] Kestin, J. and Wakeham, W. A., 1988, *Transport properties of fluids: Thermal conductivity, Viscosity, and Diffusion Coefficient, Cindas Data Series on Material Properties* (New York: Hemisphere) Vol I-1.

[4] Erkey, C. and Akgerman, A., 1991, In *Measurement of the transport properties of fluids*, Wakeham, W. A., Nagashima, A., and Sengers, J. V., Eds., Experimental Thermodynamics, Vol. III, IUPAC, Physical Chemistry Division, Commission on Thermodynamics (Oxford, U.K.: Blackwell Scientific Publications) Chapter 9, p. 251.

[5] Kircher, K., 1983, Diss. Universitat und Gesamthochschule Siegen.

[6] Ouano, A. C., 1972, *Ind. Eng. Chem. Fundam.*, **11**, 268.

[7] Taylor, G., 1953, *Proc. Roy. Soc. London,* **A219**, 186.

[8] Taylor, G., 1954, *Proc. Roy. Soc. London,* **A225**, 473.

[9] Aris, R., 1956, *Proc. Roy. Soc. London,* **A235**, 67.

[10] Ananthakrishnan, V., Gill, W. N., and Barduhn, A. J., 1965, *AIChE J.,* **11**, 1063.

[11] Gill, W. N. and Ananthakrishnan, V., 1966, *AIChE J.,* **12**, 906.

[12] Gill, W. N., 1967, *Proc. Roy. Soc. London,* **A298**, 335.

[13] Gill, W. N. and Sankarasubramanian, R., 1970, *Proc. Roy. Soc. London,* **A316**, 341.

[14] Alizadeh, A., Nieto de Castro, C. A., and Wakeham, W. A., 1980, *Int. J. Thermophysics,* **1**, 243.

[15] Alizadeh, A. A.; Wakeham, W. A., 1982, *Int. J. Thermophysics,* **3**, 307-323.

[16] Danckwerts, P. V., 1953, *Chem. Eng. Sci.,* **2**, 1.

[17] Kalugin, P. A., Sokol, A. V., and Tatarinova, E. B., 1990, *Europhys. Lett.,* **13**, 417.

[18] Levenspiel, O.; Smith, W. K., 1957, *Chem. Eng. Sci.,* **6**, 227.

[19] Bailey, H. R. and Gogarty, W. B., 1962, *Proc. Roy. Soc. London,* **A269**, 352.
[20] Van Andel, E., Kramers, H., and de Voogd, A., 1964, *Chem. Eng. Sci.,* **19**, 77.
[21] Andersson, B. and Bergglin, T., 1981, *Proc. Roy. Soc. London,* **A377**, 251.
[22] Koltunova, L. N., 1992, *Chem. Eng. Commun.,* **114**, 1.
[23] Sun, C. K. J. and Chen, S. H., 1985, *AIChE J.,* **31**, 1904.
[24] Pratt, K. C. and Wakeham, W. A., 1975, *Proc. Roy. Soc. London,* **A336**, 393.
[25] Van der Laan, E. Th., 1958, *Chem. Eng. Sci.,* **7**, 187.
[26] Baldauf, W., 1981, Diss. Techn. Univ. Berlin.
[27] Erdogan, M. E. and Chatwin, P. C., 1967, *J. Fluid Mech.,* **29**, 465.
[28] Nunge, R. J., Lin, T. S., and Gill, W. N., 1972, *J. Fluid Mech.,* **51**, 363.
[29] Nigam, K. D. P. and Vasudeva, K., 1976, *Chem. Eng. Sci.,* **31**, 835.
[30] Pratt, K. C. and Wakeham, W. A., 1975, *Proc. Roy. Soc. London,* **A342**, 401.
[31] Janssen, L. A. M., 1976, *Chem. Eng. Sci.,* **31**, 215.
[32] Van den Berg, J. H. M. and Deelder, R. S., 1979, *Chem. Eng. Sci.,* **34**, 1345.
[33] Tominaga, T. and Matsumoto, S., 1986, *J. Phys. Chem.,* **90**, 139.
[34] Matthews, M. A., Rodden, J. B., and Akgerman, A., 1987, *J. Chem. Eng. Data,* **32**, 317.
[35] Matthews, M. A., Rodden, J. B., and Akgerman, A., 1987, *J. Chem. Eng. Data,* **32**, 319.
[36] Rutten, Ph. W. M., 1992, Ph. D. thesis, Delft University of Technology.
[37] Press, W. H., Flannery, B. P., Teukolsky, S. A., and Vetterling, W. T., 1990, *Numerical Recipes in Pascal* (Cambridge, U.K.: Cambridge University Press).
[38] Hultquist, P. F., 1988, *Numerical methods for engineers and computer scientists* (Menlo Park, CA: The Benjamin/Cummings Publishing).
[39] Perry, R. H. and Chilton, C. H., 1969, *Chemical Engineers' Handbook,* 5th ed. (McGraw-Hill Book: New York).
[40] Lee, Y. E. and Li, S. F. Y., 1991, *J. Chem. Eng. Data,* **36**, 240.
[41] Woolf, L. A., 1985, *Pure Appl. Chem.,* **57**, 1083.

[42] Derlacki, Z. J., Easteal, A. J., Edge, A. V. J., Woolf, L. A., and Roksandic, Z., 1985, *J. Phys. Chem.*, **89**, 5318.

[43] Harris, K. R., Goscinska, T., and Lam, H. N., 1993, *J. Chem. Soc., Faraday Trans.*, **89**, 1969.

[44] Tyn, M. T. and Calus, W. F., 1975, *J. Chem. Eng. Data,* **20**, 310.

[45] Hammond, B. R. and Stokes, R. H., 1953, *Trans. Faraday Soc.*, **49**, 890.

[46] Dullien, F. A. L. and Shemilt, L. W., 1961, *Can. J. Chem. Eng.*, **39**, 242.

3. COMPLICATIONS IN THE USE OF THE TAYLOR DISPERSION METHOD FOR TERNARY DIFFUSION MEASUREMENTS: METHANOL + ACETONE + WATER MIXTURES

Abstract*

The Taylor dispersion technique is used to measure the ternary mutual diffusion coefficients of aqueous non-electrolyte solutions at 25 °C. The dispersion of the injected solutes is recorded by a differential refractometer and an ultraviolet-visible detector. The diffusion coefficients are calculated directly by fitting the theoretical dispersion equations to about six experimental curves simultaneously. If the ternary diffusion effects in the measured dispersion profiles are not obscured by the inaccuracy of the experimental method or an unfavourable relative detector sensitivity, the diffusion coefficients are precise. For the system methanol + acetone + water, it is shown that the Taylor dispersion method is unsuitable for the determination of all diffusion coefficients if the methanol mole fraction is smaller than 0.45 or the acetone mole fraction is larger than 0.001.

* The main part of this chapter has been published: Van de Ven - Lucassen, I. M. J. J., Kemmere, M. F., and Kerkhof, P. J. A. M., 1997, *J. Solution Chem.*, **26**, 1145.

Introduction

Diffusion coefficients in liquid systems can be measured by the Taylor Dispersion Method (TDM) [1-5]. For binary systems this method is fast and convenient. The measured binary diffusion coefficients have an accuracy of 0.5 - 1.5% [6]. The diffusion behaviour in ternary or multicomponent systems, however, is more complicated. In a ternary system, e.g., four Fick diffusion coefficients have to be determined from the dispersion curves of two components. Ternary mutual diffusion coefficients were determined from Taylor dispersion profiles by Leaist et al. The three-component systems consisted of water + salt 1 + salt 2 or water + salt + organic solute. The diffusion coefficients were calculated from the temporal moments of the detector signal [7, 8] or by fitting the theoretical equation of the dispersion profile to the experimental curve [8-14]. The main-diffusion coefficients were more accurate than the cross-diffusion coefficients. The experimental curve was measured by a differential refractometer (RI detector). Since changes in concentration of both solutes influence the detector signal, the concentrations of the two solutes were not measured independently. Therefore, the precision of the determination of the diffusion coefficients was dependent on the ratio w_1/w_2 of the refractive index increments per mole of solute 1 and solute 2. Independent measurement of the concentration profiles of the two solutes may increase the precision of the diffusion coefficients. One of the first attempts to obtain two independent concentration measurements from one dispersion experiment was accomplished by Rutten [15]. For the determination of the ternary diffusion coefficients in the aqueous region of the system glycerol + acetone + water he used one ultraviolet-visible (UV) detector at two different wavelengths or a UV detector combined with an RI detector.

In this work the determination of ternary diffusion coefficients by the Taylor dispersion method is discussed for aqueous solutions of non-electrolytes using an RI detector as well as a UV detector. Special attention is paid to the development of the fitting procedures and the limitations of the method.

Theory of the Taylor dispersion method

Diffusion in a three-component system is described by the coupled Fick equations

$$\mathbf{J}_1 = -D_{11}\nabla C_1 - D_{12}\nabla C_2 \tag{3.1a}$$

$$\mathbf{J}_2 = -D_{21}\nabla C_1 - D_{22}\nabla C_2\,, \tag{3.1b}$$

where $\mathbf{J}_i$ is the molar flux of component i, ∇C_i the gradient of concentration of component i, D_{ii} is a main-diffusion coefficient and $D_{ij,i\neq j}$ a cross-diffusion coefficient. The ternary diffusion coefficients can be measured by the Taylor dispersion technique: A pulse of different concentrations C_1 and C_2 is injected into the ternary mixture (solvent) flowing slowly through a long capillary. The pulse spreads out due to the laminar velocity profile and molecular diffusion. The concentrations C_1, C_2 at the end of the diffusion tube are given by the fundamental working equations of Price [16]

$$C_1 = \frac{A_1}{2\pi R^2}\frac{1}{\sqrt{\pi\sigma_1 t}}\exp\left\{-\frac{(t-\tau)^2U^2}{4\sigma_1 t}\right\} + \frac{A_2}{2\pi R^2}\frac{1}{\sqrt{\pi\sigma_2 t}}\exp\left\{-\frac{(t-\tau)^2U^2}{4\sigma_2 t}\right\}, \tag{3.2a}$$

$$C_2 = \frac{A_3}{2\pi R^2}\frac{1}{\sqrt{\pi\sigma_1 t}}\exp\left\{-\frac{(t-\tau)^2U^2}{4\sigma_1 t}\right\} + \frac{A_4}{2\pi R^2}\frac{1}{\sqrt{\pi\sigma_2 t}}\exp\left\{-\frac{(t-\tau)^2U^2}{4\sigma_2 t}\right\}, \tag{3.2b}$$

with

$$A_1 = \frac{\left\{D_{22} - \frac{1}{2}\left(D_{11} + D_{22} - \sqrt{(D_{11}-D_{22})^2 + 4D_{12}D_{21}}\right)\right\}M_1 - D_{12}M_2}{\sqrt{(D_{11}-D_{22})^2 + 4D_{12}D_{21}}}, \tag{3.2c}$$

$$A_2 = \frac{\left\{D_{22} - \frac{1}{2}\left(D_{11} + D_{22} + \sqrt{(D_{11}-D_{22})^2 + 4D_{12}D_{21}}\right)\right\}M_1 - D_{12}M_2}{-\sqrt{(D_{11}-D_{22})^2 + 4D_{12}D_{21}}}, \tag{3.2d}$$

$$A_3 = \frac{\left\{D_{11} - \frac{1}{2}\left(D_{11} + D_{22} - \sqrt{(D_{11} - D_{22})^2 + 4D_{12}D_{21}}\right)\right\}M_2 - D_{21}M_1}{\sqrt{(D_{11} - D_{22})^2 + 4D_{12}D_{21}}},$$

(3.2e)

$$A_4 = \frac{\left\{D_{11} - \frac{1}{2}\left(D_{11} + D_{22} + \sqrt{(D_{11} - D_{22})^2 + 4D_{12}D_{21}}\right)\right\}M_2 - D_{21}M_1}{-\sqrt{(D_{11} - D_{22})^2 + 4D_{12}D_{21}}},$$

(3.2f)

$$\sigma_1 = \frac{1}{2}\frac{R^2U^2}{48}\frac{D_{11} + D_{22} + \sqrt{(D_{11} - D_{22})^2 + 4D_{12}D_{21}}}{D_{11}D_{22} - D_{12}D_{21}}, \quad (3.2g)$$

$$\sigma_2 = \frac{1}{2}\frac{R^2U^2}{48}\frac{D_{11} + D_{22} - \sqrt{(D_{11} - D_{22})^2 + 4D_{12}D_{21}}}{D_{11}D_{22} - D_{12}D_{21}}, \quad (3.2h)$$

in which M_i represents the number of moles of component i in the injected pulse in excess of those in the same volume of the carrier stream: $M_1 = A_1 + A_2$ and $M_2 = A_3 + A_4$. C_i is the radially averaged concentration at time t relative to the background concentration, τ is the mean residence time, R the internal radius of the diffusion tube and U the linear velocity averaged over the cross section.

The sum of the main-diffusion coefficients is positive: $D_{11} + D_{22} > 0$. Further conditions for the diffusion coefficients are $D_{11}D_{22} - D_{12}D_{21} > 0$ and $(D_{11} - D_{22})^2 + 4D_{12}D_{21} > 0$ [17-19].

The assumptions made in the derivation of the working equations are similar to those of the binary dispersion technique [6] with an effective diffusion coefficient D_{eff} [16]. By comparing Toor's method [18], used in the derivation of Price's equations, with Taylor's derivation of the binary equation [2, 3], D_{eff} can be described with the eigenvalues of the D_{ij} matrix

$$D_{eff} = \frac{2(D_{11}D_{22} - D_{12}D_{21})}{D_{11} + D_{22} \pm \sqrt{(D_{11} - D_{22})^2 + 4D_{12}D_{21}}}. \quad (3.3)$$

The effective diffusion coefficient is of the same order of magnitude as the main-diffusion coefficients and is used in the equations that provide the criteria for the operating conditions (e.g., calculation of the flow rate) [6, 16].

The calculation of the Fick diffusion coefficients may be complicated due to their mutual dependence. In a solvent-fixed situation, in which diffusion causes no bulk motion of the liquid, the following relation can be derived [20]

$$(D_{12})_s \mu_{11} - (D_{11})_s \mu_{12} = (D_{21})_s \mu_{22} - (D_{22})_s \mu_{21}, \tag{3.4a}$$

where $\mu_{ij} = \left(\frac{\partial \mu_i}{\partial C_j}\right)_{T,p,C_{k\neq 0,j}}$, μ_i is the molar chemical potential and $(D_{ij})_s$ the solvent-fixed diffusion coefficient. For volume-fixed diffusion coefficients a similar relation has been derived by Dunlop [21]. Transformation of the volume-fixed diffusion coefficients D_{ij}, measured by the Taylor dispersion method, to the solvent-fixed diffusion coefficients is possible by [22]

$$(D_{ij})_s = D_{ij} + \frac{C_i}{C_0 \bar{V}_0} \sum_{k=1}^{n-1} \bar{V}_k D_{kj} \quad (i, j = 1, \ldots n\text{-}1), \tag{3.4b}$$

where C_i is the molar concentration and $\bar{V}_i$ the partial molar volume of component i. The subscript 0 refers to the solvent.

Near infinite dilution $(D_{ij})_s$ is equal to D_{ij}. For low concentrations of the solute components, and even in relatively concentrated solutions, the solvent-fixed- and the volume-fixed diffusion coefficients may differ only by 1 - 5% [22]. Furthermore, the thermodynamic, molar concentration-based matrix $(\Gamma_c)_{ij}$ can be simplified to [23]

$$(\Gamma_c)_{ij} = \delta_{ij} + C_i \frac{\partial \ln \gamma_i}{\partial C_j} = \delta_{ij} + x_i \frac{\partial \ln \gamma_i}{\partial x_j} = \Gamma_{ij} = \frac{x_i}{RT} \mu_{ij}, \tag{3.5}$$

in which δ_{ij} is the Kronecker delta, γ_i the activity coefficient of component i defined by convention I [24], and Γ_{ij} the thermodynamic

mole fraction-based matrix. Combination of equations 3.4 and 3.5 leads to

$$D_{21} = \left(\frac{x_2}{x_1} D_{12}\Gamma_{11} - \frac{x_2}{x_1} D_{11}\Gamma_{12} + D_{22}\Gamma_{21} \right) \Big/ \Gamma_{22} . \tag{3.6}$$

Eq 3.6 is valid at low concentrations of the solute components and provides good estimates at higher concentrations.

The working equations of Price, eq 3.2 simplify for very low concentrations of the solute components. If the concentration of component 2 tends to zero (tracer), $D_{21} \approx 0$ [25], and eqs 3.2a, 3.2b become, respectively

$$C_1 = \frac{-\dfrac{D_{12}}{D_{11}-D_{22}} M_2}{2\pi R^2} \frac{1}{\sqrt{\pi \dfrac{R^2U^2}{48D_{22}} t}} \exp\left\{ - \frac{(t-\tau)^2}{4\dfrac{R^2}{48D_{22}} t} \right\} + \frac{M_1 + \dfrac{D_{12}}{D_{11}-D_{22}} M_2}{2\pi R^2} \frac{1}{\sqrt{\pi \dfrac{R^2U^2}{48D_{11}} t}} \exp\left\{ - \frac{(t-\tau)^2}{4\dfrac{R^2}{48D_{11}} t} \right\}, \tag{3.7a}$$

$$C_2 = \frac{M_2}{2\pi R^2} \frac{1}{\sqrt{\pi \dfrac{R^2U^2}{48D_{22}} t}} \exp\left\{ - \frac{(t-\tau)^2}{4\dfrac{R^2}{48D_{22}} t} \right\}. \tag{3.7b}$$

The concentration curve of component 2 resembles a single Gaussian and is independent of the injected amount of component 1. Similar equations can be derived if component 1 tends to zero (component 1 is tracer), i.e., $D_{12} \approx 0$. If both components tend to zero, C_1 and C_2 are both single Gaussians: The concentration curve of component 1 is not influenced by the injection amount of component 2 and vice versa.

When the concentration is measured, the relation between the detector signal $s(t)$ and the concentration vs. time curves, eq 3.2, is assumed to be

$$s(t) = w_1C_1 + w_2C_2 + a + bt + \varepsilon(t)\,, \tag{3.8}$$

in which w_i is the detector sensitivity for component i, a and b compensate for the detector drift (which is assumed to be linear in time), and $\varepsilon(t)$ is noise. The signal is sampled with a sample interval of $\Delta t_i = 0.98$ s: $y^*_i = s(t_i)$.

Diffusion coefficients can be calculated from the measured dispersion peaks in two different ways: Calculation from the temporal moments [7, 8]; fitting of the theoretical eq 3.2, combined with eq 3.8, to the experimental curve [8-14]. In this work only fitting procedures with the diffusion coefficients as fitting parameters will be used. In these fitting procedures a discrete signal without drift is required: $y_i = y^*_i - (a + b\ t_i)$. For the calculation of a and b, regions of the detected signal, where the concentration is negligible, are visually marked in our software as baseline. Through these regions of the signal the drift is fitted and subtracted from the signal.

Fitting procedures

Fitting of the theoretical equations to the experimental curves can be done in several different ways:

- fitting to a single curve
- simultaneously fitting of two or more curves (with different injection concentrations) from one detector
- simultaneously fitting of two or more curves from two different detectors (different detector sensitivities).

Furthermore, all these procedures are able to fit

- D_{11}, D_{22}, D_{12}, D_{21} (4-parameter fit); residence time τ calculated [6], detector sensitivities calculated from the peak areas.
- D_{11}, D_{22}, D_{12} (3-parameter fit); D_{21} is calculated during the iterative process using eq 3.6, residence time τ and detector sensitivities calculated as above.
- 4- or 3-parameter fit + residence time τ
- 4- or 3-parameter fit + residence time τ + detector sensitivities w_1 and w_2.

Combinations of these procedures and other fitting procedures are possible [7, 8].

The fitting procedures were developed in two test series. First, an ideal detector signal was calculated by means of eq 3.2. The values of the parameters used are listed in table 3.1. This ideal signal was processed by fitting procedures based on the least-squares approximation between the experimental data points (= ideal signal) and the points calculated. These fitting procedures were written in the SAS for Windows-package (version 6.08/6.10, SAS Institute Inc.), using the method of Gauss-Newton method as well as the Marquardt method. D_{11}, D_{22}, D_{12} (τ, w_1 and w_2) were fitting parameters; D_{21} was always calculated using eq 3.6. The detector sensitivities and the mole fraction ratio x_2/x_1 were varied. Two curves with different values of the detector sensitivities were simultaneously fitted, simulating different detectors. The influence of noise was tested by a superposition of randomly generated noise on the signal (0.5%, 1%, 5%, 20%). The Marquardt method yields the best results. In some cases it is difficult to achieve convergence depending on the ratio of the detector sensitivities and the mole fraction ratio. The accuracy of the diffusion coefficients is good. The cross coefficients are of poorer precision than the main coefficients. The values of the residence time and the detector sensitivities (if fitted) are very accurate. Noise of less than 1% causes no problems in the calculation of the diffusion coefficients.

Table 3.1. *Parameters of ideal signal series I*

D_{11} (10^{-9} $m^2.s^{-1}$)	1.30	M_1 (10^{-3} mol)	0.14
D_{22} (10^{-9} $m^2.s^{-1}$)	0.80	M_2 (10^{-3} mol)	-0.14
D_{12} (10^{-9} $m^2.s^{-1}$)	-0.02	τ (s)	12000
D_{21} (10^{-9} $m^2.s^{-1}$)	-0.01 [a]	U (10^{-3} $m.s^{-1}$)	0.002
(calc. acc. eq 3.6)	-0.0045 [b]	$w_{1,RI}$ ($RIU.m^3.mol^{-1}$)	1; 300; 600
Γ_{11}	0.9	$w_{1,UV}$ ($AU.m^3.mol^{-1}$)	0.015
Γ_{22}	0.9	$w_{2,RI}$ ($RIU.m^3.mol^{-1}$)	1; 200; 400
Γ_{12}	-0.01	$w_{2,UV}$ ($AU.m^3.mol^{-1}$)	-
Γ_{21}	-0.005	noise (%)	0.5; 1; 5; 20

[a] $x_2 / x_1 = 1$
[b] $x_2 / x_1 = 0.015$

The developed fitting procedures were tested on experimental curves of the systems acetone + ethyl benzene + water and glucose +

acetone + water. Simultaneously fitting of two or more curves with different injection concentrations showed an increase of precision and a decrease of convergence difficulties. Disadvantages of the procedures were the long calculation times. Another problem was the determination of accurate activity coefficients, needed in calculating D_{21} according to eq 3.6. Reduction of the calculation times was achieved by dividing the ternary systems into three types, resulting in a reduction of the necessary fitting parameters and a simplification of the working equations for two types:

1. solvent(0) + tracer(1) + tracer(2): fitting parameters D_{11} and D_{22}; $D_{12} = 0$, $D_{21} = 0$.
2. solvent(0) + solute(1) + tracer(2): fitting parameters D_{11}, D_{22}, and D_{12}; $D_{21} = 0$.
3. solvent(0) + solute(1) + solute(2): fitting parameters D_{11}, D_{22}, D_{12} and D_{21}.

Use of the thermodynamical eq 3.6, i.e., knowledge of the activity coefficients, is only necessary for type 3. For each type a fitting procedure was developed, using Marquardt's method.

Ideal signals were calculated for each type of ternary system. Parameters were chosen to simulate a real ternary system like water(0) + methanol(1) + acetone(2) (table 3.2a). The UV detector measured the concentration of component 2 by absorbance changes; the RI detector measured changes in concentration (by refractive index) of component 1 as well as component 2. Results of the testing of the fitting procedures are listed in table 3.2b.

From the UV signals of type 1 and type 2, D_{22} can be calculated by means of eq 3.7b. This calculation is fast and very accurate. At least two RI signals of type 1 have to be simultaneously fitted to calculate the diffusion coefficients D_{11} and D_{22} (eq. 7b and the analogous for C_1). The accuracy is high. The RI signals of type 2 were used to calculate the diffusion coefficients D_{11}, D_{22} and D_{12} (eqs 3.7a, 3.7b). The accuracy of D_{12} is less than that of D_{11} and D_{22}. D_{12} is strongly correlated with D_{22}. The determination of the diffusion coefficients of type 3 was more difficult (eq 3.2). In series IIa the UV signals achieved convergence with accurate values of the diffusion coefficient. The RI signals, however, did not show convergence. In series IIb convergence was achieved by simultaneously fitting of 6 RI signals, provided that the starting values of the fitting parameters were close to the real values. The accuracy was dependent on the combinations of signals used.

Table 3.2a. *Parameters of ideal signals, series IIa, IIb*[a]

Common parameters

	w_1	w_2		
$w_{i,RI\ det.}$	1000	5000	$\tau_{RI\ det.}$	10100
$w_{i,UV\ det.}$	0	0.015	$\tau_{UV\ det.}$	9750
U	2.354			
R (10^{-3} m)	0.520			

Series IIa

signal code	2a	2b	2c	2d	2e	2f
M_1	5.7	5.2	4.9	4.5	4.0	3.5
M_2	3.6	4.7	1.2	2.4	3.6	4.8

	type 1	**type 2** ($x_2/x_1 = 2.43.10^{-11}$)	**type 3** ($x_2/x_1 = 0.27$)
D_{11}	1.560	1.498	1.494
D_{22}	1.300	1.372	1.331
D_{12}	0	-0.214	-0.387
D_{21}	0	0	-0.108
Γ_{11}	1	0.9453	0.9067
Γ_{22}	1	1	0.8750
Γ_{12}	0	-0.1158	-0.1956
Γ_{21}	0	0	-0.0588

Series IIb type 3

($x_2/x_1 = 1.0$)

signalcode	2g	2h	2i	2j	2k	2l	2m	2n
M_1	-5.7	-5.7	0.010	0.010	5.7	5.7	5.7	5.7
M_2	5.7	0.010	-5.7	5.7	5.7	-5.7	-1.0	-0.010

D_{11}	1.668	Γ_{11}	0.9478
D_{22}	1.136	Γ_{22}	0.6628
D_{12}	-0.298	Γ_{12}	-0.1348
D_{21}	-0.372	Γ_{21}	-0.1664

[a]units as in table 3.1.

In general, the accuracy was improved by the use of τ, w_1 and w_2 as fitting parameters. The thermodynamic eq 3.6 was only used to obtain a starting value of D_{21}. The determination of the diffusion

Table 3.2b. *Results of testing fitting procedures. Inaccuracy (%) of the diffusion coefficients, residence time, and detector sensitivities, dependent on the number of signals simultaneously fitted*

Series IIa

	type 1					**type 2**				**type 3**	
	1 RI	2 RI	6 RI	1 UV	6 UV	1 RI	6 RI	1 UV	6 UV	6 RI	6 UV
D_{11}	-	<0.1	<0.03	-	-	-	<0.1	-	-	no conv.	<0.06
D_{22}	-	<0.03	<0.009	<0.004	<0.002	-	<0.1	<5	<0.002		<0.5
D_{12}						-	<4	-	-		<1
D_{21}											<0.8
τ							0.00005				
w_1							0.02				
w_2							0.004				
N.B.	eq 3.6 not needed					eq 3.6 not applicable (zero values)				$w_1 = 0$ and eq 3.6 used	

Series IIb type 3 (two different combinations of 6 RI signals)

	6 RI (comb. 1)	6 RI (comb. 2)
D_{11}	0.04	0.08
D_{22}	0.1	0.2
D_{12}	0.4	0.7
D_{21}	2	3
w_1	1	3

N.B. Strong correlation between D_{12} and w_1, w_2.
Accuracy of the results calculated with use of eq 3.6 poorer than without eq 3.6

coefficients from the concentration vs. time curves of the Taylor dispersion method is only possible under certain conditions, dependent on the ratios M_1/M_2 and w_1/w_2, the values of the diffusion coefficients and the noise level.

The fitting procedure, in which RI signals and UV signals of the same injections were simultaneously fitted, was compared with the procedure, in which the result of the UV fittings (D_{22}) was used as a

fixed value in the RI fittings. The first method was rather complicated due to the different values of the residence time τ and the accuracy was poorer. Moreover, in many real systems it is not possible to get two independent detector signals from one injection. Very often only RI signals are available.

Therefore, the simultaneous fitting of the UV and RI signals (or two other independent detector signals) will not be discussed further in this work.

Experimental

The apparatus used differs slightly from that discussed earlier for binary systems [6]. A UV detector and two extra diffusion tubes were added to the original binary set-up. The equipment for the measurement of diffusion coefficients in ternary liquid systems is shown schematically in figure 3.1.

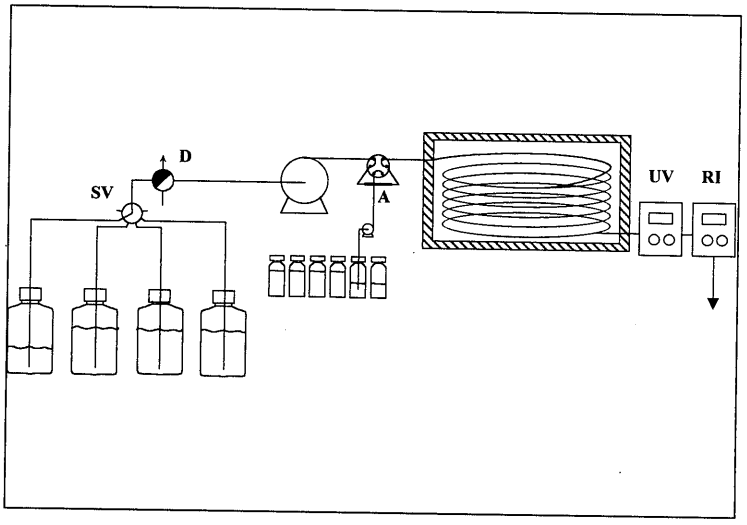

Figure 3.1. *Experimental set-up for measurement of diffusion coefficients in ternary liquid systems:* SV, *selection valve;* D, *degasser;* A, *autosampler;* UV, *ultraviolet-visible detector;* RI, *refractive index detector.*

Deionized water filtered through a Milli-Q water purification system (Millipore, resistivity 18 MΩ·cm) was used. Analytical-grade methanol (purity ≥ 99.8%, water < 0.05%), ethanol (purity ≥ 99.8%, water < 0.2%), acetone (purity ≥ 99.5%, water < 0.2%), D(+)-glucose anhydrous (purity ≥ 99.0%, water < 0.2%) and ethyl benzene (purity ≥ 99%) were obtained from Merck and used without further purification. All experiments were performed at 25 °C. The determination of the mean residence time was very accurate both in the binary experiments and the ternary experiments (inaccuracy << 0.01%).

Solutions were prepared by mass and degassed by sparging with helium. Injection solutions were made by volumetrical mixing of the degassed solvents. To prevent bubbles from disturbing the flow, an in-line degasser (Separations DG1300) was installed. The HPLC pump (type LKB2150), which maintained a steady flow, was connected to an autosampler (Spark Marathon) with a fixed volume sample loop of 20 μL. Zero dead volume fittings were used to connect the diffusion tube with the autosampler and the UV detector and a short capillary tube between the UV and RI detectors. Several diffusion tubes were installed: stainless steel tubes (*i.d.* = 1.041 mm) of various lengths (10, 15, 25, 50 m) and PEEK (Poly Ether Ether Ketone) tubes (*i.d.* = 1.04 mm) of two lengths (15, 25 m). The internal radii of the tubes were determined in several ways: by gravimetry and residence time measurements as well as by calibration with diffusion measurements of the systems methanol + water (whole concentration range), ethanol + water, acetone + water.

The eluted peaks were detected with a UV detector (Applied Biosystems 785A) and subsequently by a differential refractometer (Shodex SE61). The UV detector was installed between the capillary tube and the RI detector of the original binary set-up. For the conversion of the analogous output signal of the UV detector a hardware interface device (Strawberry-Tree Mini16 ADC) was installed in the personal computer. The software for data acquisition and controlling the equipment as well as the data processing software package were adequately extended.

The procedure for the measurement of diffusion coefficients in binary systems is described in detail by Van de Ven-Lucassen et al [6]. Before starting an experiment the system was flushed for at least six h at the flow rate of the diffusion experiment to attain a stable, linear baseline in each detector. The flow velocity was set in accordance with

the conditions described in the section theory (typically 0.12 cm^3min^{-1}). Diffusion samples were injected every 1.5 – 2 h. The extended original software package was used to apply a baseline correction to each experimental curve. Binary fits were done for dispersion peaks obtained from $M_2 = 0$ or $M_1 = 0$ injections: the mean residence time τ, the binary diffusion coefficient (D_{11} or D_{22}) and the peak area were calculated. The detector sensitivity (w_1 or w_2) was determined from the peak area and the injected amount. These values could be used as starting values for the fitting parameters in the ternary procedures.

Results and discussion

Diffusion coefficients were measured for the ternary systems acetone + ethyl benzene + water, glucose + acetone + water, and methanol + acetone + water. Preliminary measurements were done for the binary systems methanol + water, ethanol + water, acetone + water, glucose + water, and ethyl benzene + water.

Binary systems

Experiments with the binary systems methanol + water, ethanol + water, acetone + water, and glucose + water, were performed to show that the detector response was linear with concentration and to study the influence of the concentration of the injected sample on the measurement of the diffusion coefficients. In these experiments the stainless steel tubes as well as the PEEK tubes were used. For each binary system a minimum difference in concentration between injection solution and solvent was necessary to obtain an accurate experimental curve as a result of detector noise. This minimum difference was dependent on the binary system and the detector used. Above a certain concentration difference the calculated diffusion coefficients started to increase, probably due to secondary flow effects. This maximum concentration difference was independent of the detector used. For both detectors the response was linear over a much wider range of concentration differences. The maximum concentration difference was 5 vol% for methanol + water, 4 vol% for ethanol + water, 6 vol% for acetone + water (UV and RI detectors), and 3 wt% for glucose + water. For the RI and UV detectors and for both types of capillary tubes, the calculated diffusion coefficients were not

significantly different. Moreover, the values of the binary diffusion coefficients, measured with the ternary set-up, were within the uncertainty of the measurements with the original binary set-up [6]. Injections of solutions that were denser or less dense than the solvent did not influence the measured diffusion coefficients. The inaccuracy of the results was lower for the PEEK tubes (PEEK: 0.5%; stainless steel: 1.5%). For the system acetone + water the UV detector was more accurate (uncertainty UV: 0.3%; RI: 0.5%).

Injections of dilute ethyl benzene (0.01 – 5.5 vol%) into pure water showed tailing in the measured concentration against time curves due to adsorption at the wall of the PEEK tube. If ethyl benzene was present in the solvent (0.01 vol% ethyl benzene in water) no tailing was observed. Although it is possible to calculate a diffusion coefficient from an asymmetric peak [26], tailing was avoided in the subsequent experiments. The dispersion profiles of high injection concentrations of ethyl benzene (5 vol%) were non-Gaussian and irreproducible, because of demixing in the injection vials, due to the very low solubility of ethyl benzene in water [27]. Therefore, only injection concentrations < 2 vol% could be used.

The binary experiments led to the selection of the PEEK capillary for the ternary experiments. For all experiments the concentration difference between injection solution and solvent applied was chosen well below the maxima of the binary systems, which appeared to agree with a value of the Grashof number less than 100 as mentioned by Ananthakrishnan et al [28]. ($Gr = d^3 \cdot g \cdot (\Delta\rho/\rho)/\nu^2$ in which d is the tube diameter, g the gravity constant, $\Delta\rho$ the density difference between injection solution and solvent, ρ the density and ν the kinematic viscosity of the solvent.).

Ternary systems

Acetone(1) + Ethyl benzene(2) + Water(0)

Ethyl benzene was used at infinite dilution: $D_{21} = 0$. The value of D_{12}, estimated with eq 3.6, was -7.10^{-12} $m^2.s^{-1}$ with $D_{11} = 1.3.10^{-9}$ $m^2.s^{-1}$ (acetone in water[29]) and $D_{22} = 7.9.10^{-10}$ $m^2.s^{-1}$ (ethyl benzene in water) and a thermodynamic matrix Γ_{ij} estimated from the UNIQUAC model [17, 30, 31] with parameters from Rutten [15] and Macedo and Rasmussen [32]. The flow rate was 0.10 – 0.11 $cm^3.min^{-1}$. Acetone was detected at a wavelength of 266 nm, ethyl benzene at 215 nm. The RI detector response was the summation of the acetone and ethyl

benzene refractive index differences between peak and solvent. For each solvent, three to six experiments with at least ten different injections were performed, in each experiment 3 to 9 RI peaks of different injection concentrations were simultaneously fitted and at least three different combinations of peaks. Results are shown in table 3.3.

Table 3.3. *Diffusion coefficients at 25 °C for the acetone(1) + ethyl benzene(2) + water(0) system*[a]

		Ethyl benzene	
	Acetone	0 (vol%)	0.01 (vol%)
	0 (vol%)		
D_{11}		1.297 ± 0.004	1.30 ± 0.01
D_{22}		0.775[b,c] / 0.673[b,c]	0.83 / 0.78
		± 0.01 / 0.006	± 0.01 / 0.01
D_{12}		-	-
		D_{11} = 1.30 (ref 29)	
	0.2 (vol%)		
D_{11}			1.30 ± 0.01
D_{22}		0.787 ± 0.004	
D_{12}		0.002[c] ± 0.004	
	0.4 (vol%)		
D_{11}			1.296 ± 0.005
			D_{11} fixed value 1.300:
D_{22}			0.758 ± 0.046
D_{12}			0.005 ± 0.003

[a]units as in table 3.1
[b]tailing
[c]unreliable

The cross-diffusion coefficient D_{12} is very imprecise owing to the strong correlation between D_{12} and D_{22}: 0.4% deviation in the value of D_{22} causes 40% deviation in D_{12}, D_{11} fixed (deviation D_{11} = 0.8%: deviation D_{12} = 0.4%, D_{22} fixed). Another cause of the inaccuracy of D_{12} was the relative RI detector sensitivity w_1/w_2 of 4500/600. At this ratio of w_1/w_2 the ternary effects were best detected if $M_1 << M_2$ (eqs 3.7, 3.8). If the ternary peak was compared with a summation of two

binary peaks (i.e., D_{12} = 0), the maximum difference between these two curves was ±2% for a cross-diffusion coefficient D_{12} of $\pm 5.10^{-12} m^2.s^{-1}$ (fig 3.2, curves 1 and 2). The same difference could be caused by an inaccuracy of 2% in the determination of the injected amounts M_1 and M_2 (fig 3.2, curves 3 and 4). Noise can mask these differences.

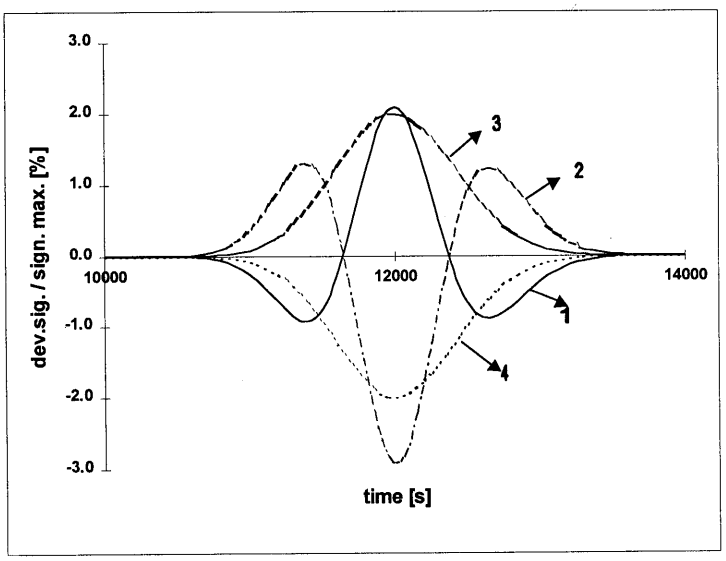

Figure 3.2. *Acetone(1) + ethylbenzene(2) + water(0) at 25 °C. Influence of the cross-diffusion coefficient and injection amount on the deviation of the detected "ternary" signal compared to the "binary-sum" signal. Dev. sign./sign. max. = (ternary signal (t_i) – binary-sum signal (t_i)) / binary-sum signal ($t_{max} = \tau$). Parameters of the binary-sum signal:* $D_{11} = 1.30.10^{-9}\ m^2.s^{-1}$; $D_{22} = 7.9.10^{-10}\ m^2.s^{-1}$; $D_{12} = 0$; $D_{21} = 0$; $w_1/w_2 = 4500/600$; $M_1 = 1.00.10^{-10}$ *mol;* $M_2 = 7.00.10^{-6}$ *mol.*
Curve 1: $D_{12} = 5.0.10^{-12}\ m^2.s^{-1}$; *Curve 2:* $D_{12} = -7.0.10^{-12}\ m^2.s^{-1}$; *Curve 3:* $M_2 = 7.14.10^{-6}$ *mol; Curve 4:* $M_2 = 6.86.10^{-6}$ *mol.*

Glucose(1) + Acetone(2) + Water(0)

Glucose (5 wt%, x_1 = 0.0052) and acetone (0.2 vol%, x_2 = 0.0005) were dissolved in pure water. The flow rate was 0.09 $cm^3.min^{-1}$. In this mixture the cross-diffusion coefficient D_{21} was zero (acetone tracer component). The estimated value of D_{12} is 3.10^{-11} $m^2.s^{-1}$ with D_{11} = $6.7.10^{-10}$ $m^2.s^{-1}$ (glucose in water) and D_{22} = $1.3.10^{-9}$ $m^2.s^{-1}$ (acetone in water) and a thermodynamic matrix Γ_{ij} estimated from the UNIQUAC model [17, 30, 31] with parameters from Rutten [15] and Reid et al [33]. The dispersion of acetone was measured by the UV detector at 266 nm. The RI detector response was the summation of the glucose and acetone refractive index differences between eluted peak and solvent. Four experiments were performed with 9 to 12 different injections, in each experiment six RI peaks were simultaneously fitted in at least three different combinations of peaks.

Table 3.4. *Deviation (%) in the dispersion peak for the glucose(1) + acetone(2) + water(0) system*[a]

injected amount		as a result of an inaccuracy of				compared with D_{12} = 0, if	
M_1	M_2	1% in M_1	2% in M_1	1% in M_2	2% in M_2	D_{12} = 0.05	D_{12} = 0.1
-0.140	0.020	2.8	5.7	3.8	7.7	1.3	2.7
-0.140	0.010	3.1	6.2	2.1	4.2	0.73	1.5
-0.140	-0.0005	1	1.9	0.03	0.07	0.011	0.023
-0.050	0.010	1.1	2.2	2.1	4.4	0.75	1.5

[a]units as in table 3.1.

Within the experimental precision all experiments gave identical results for the main-diffusion coefficients: D_{11} = 0.652 (± 0.004) $.10^{-9}$ $m^2.s^{-1}$ and D_{22} = 1.167 (± 0.003) $.10^{-9}$ $m^2.s^{-1}$. The accuracy of D_{11} is good compared with the literature: D_{11} = $0.673.10^{-9}$ $m^2.s^{-1}$ (0.39 wt% glucose) [27]. The calculation of the cross-diffusion coefficient was very imprecise: D_{12} = 1.0 (± 0.2) $.10^{-9}$ $m^2.s^{-1}$. D_{12} was strongly correlated with D_{22}. In these experiments the ratio w_2/w_1 was 850/6000. From the RI curves the D_{12} could not be calculated accurately. The maximum difference between the ternary peak and the sum of two binary peaks (i.e., D_{12} = 0), caused by an inaccuracy of 1% in the injected amounts

M_1 and M_2 was much larger than that caused by a cross coefficient of 5.10^{-11} $m^2.s^{-1}$, independent of the injected amounts M_1 and M_2 (table 3.4). Noise masks these differences.

Methanol(1) + Acetone(2) + Water(0)

This ternary system was extensively tested. For the calculation of the density of solutions, prepared by mass, equations of the form

$$\rho_{ij} = \sum_m A_m \cdot x_{i,b}^m , \tag{3.9}$$

and

$$\rho_{ijk} = (\rho_{ij})^{x_{ij}} \cdot (\rho_{jk})^{x_{jk}} \cdot (\rho_{ik})^{x_{ik}} \tag{3.10}$$

were used, in which $x_{i,b}$ is the mole fraction of component i in the binary system of components i and j, x_i the mole fraction of component i in the ternary system of components i, j and k: $x_{i,b} = x_i / (x_i + x_j)$ and $x_{ij} = (x_i + x_j)/2$. ρ_{ij} is the density of the binary system of components i and j at composition $x_{i,b}$, and ρ_{ijk} the density of the ternary system. Similar equations were used for the viscosity of the solutions. These equations were fitted to the experimental values of Noda et al [34]. The values of the constants A_m are given in tables 3.5a and 3.5b. The mean relative deviation of the calculated value vs. the experimental value was 0.006 for the density and 0.05 for the viscosity of the ternary system. The injected amounts of components 1 and 2, M_1 and M_2, were calculated from the sample volume and the density equations with an inaccuracy of ± 2%. The elements of the thermodynamic matrix Γ_{ij} were estimated from the multicomponent form of the UNIQUAC model [17, 30, 31]; parameters used are listed in table 3.5c [35].

Preliminary type 1 experiments (see fitting procedures) were performed with pure water and very dilute solutions of methanol (x_1 = 0.002) and acetone (x_2 = 0.001) as solvents, and injection solutions of 20 different concentrations (Gr < 100). The flow rate was 0.12 $cm^3.min^{-1}$. Methanol was not detected by the UV detector at 266 nm. Both detectors were linear with concentration according to eq 3.8. No adsorption at the wall was observed. The calculated diffusion

Table 3.5a. *Constants of eq 3.9 for calculation of the density of the methanol(1) + acetone(2) + water(0) system*[a]

comp.i	comp.j	A_0	A_1	A_2	A_3	A_4
methanol	water	996.887	-275.817	152.202	-162.454	75.793
acetone	water	996.880	-399.668	260.633	-73.227	
methanol	acetone	784.713	13.886	-12.194	19.387	-19.070

[a]units $kg.cm^{-3}$

Table 3.5b. *Constants of eq 3.9 for calculation of the viscosity of the methanol(1) + acetone(2) + water(0) system*[a]

Comp.i	comp.j	A_0	A_1	A_2	A_3	A_4	A_5
Methanol	water	0.8803	5.8337	-11.7715	1.4854	10.1519	-5.8959
Acetone	water	0.8901	8.3422	-41.1046	72.4864	-57.5002	17.2709
Methanol	acetone	0.3850	0.3530	-1.5645	3.5076	-3.2706	1.2790

[a]units mPa.s

Table 3.5c. *UNIQUAC-parameters of the methanol(1) + acetone(2) + water(0) system*

i	comp.	r	q	q'	A_{i0}	A_{i1}	A_{i2}
0	water	0.92	1.4	1	0	-259.596	-155.31
1	methanol	1.43	1.43	0.96	402.77	0	-119.144
2	acetone	2.5735	2.336	2.336	733.82	429.104	0

coefficients D_{11} and D_{22} were independent of the injected amounts. Neither simultaneous injection of both components nor separate injection did affect the calculated values of the diffusion coefficients. Results are listed in tables 3.6a and 3.6b, type 1.

Next, experiments were performed for the ternary system of type 2: methanol(1) + acetone(2) + water(0). Binary mixtures of methanol + water were used as solvents. The flow rate was 0.12 $cm^3.min^{-1}$. Injection solutions were prepared in vials to give four different values of M_1 with M_2 = 0, 4 different values of M_2 with M_1 = 0, and 6 to 12 different combinations of M_1 and M_2; the methanol-solely and acetone-

Table 3.6a. *Diffusion coefficients and detector sensitivity ratio at 25 °C for the system methanol(1) + acetone(2) + water(0)*[a]

		separate fit				simultaneous fit					
x_1	x_2	w_1/w_2	$D_{11\text{-RI}}$	$D_{22\text{-RI}}$	$D_{22\text{-UV}}$	w_1/w_2	D_{11}	D_{22}	D_{12}	$D_{12,f}$*	D_{21}
						type 1					
0.000	0.000	0.17	1.566	1.299	1.295	0.15	1.649	1.301			
0.000	0.001		1.575	1.292	1.288	0.19	1.658	1.301			
0.002	0.000	0.19	1.568	1.291	1.287	0.22	1.579	1.293			
						type 2					
0.000	0.000		1.566		1.295	0.15					
0.041	0.000		1.405		1.158	0.18	1.404	1.174	-0.013	0.080	
0.086	0.000		1.276		1.051	0.17	1.320	1.139	-0.486	0.089	
0.207	0.000		1.047		0.950	0.21	1.168	0.940	-0.169	-0.259	
0.299	0.000		0.941		1.000	0.03				0.012	
0.411	0.000		0.964		1.119	-0.20	0.971	1.117	-0.485	-0.471	
0.478	0.000		1.018		1.205	-0.46	1.020	1.263	-0.300	-0.413	
0.553	0.000		1.144		1.362	-1.59	1.145	1.360	-0.436	-0.439	
0.641	0.000		1.294		1.565	-34.52	1.296	1.563	-0.475	-0.475	
0.747	0.000		1.576		1.875	1.77	1.557	1.879	-0.548	-0.524	
0.878	0.000		1.805		2.344	0.96	1.788	2.299	-0.892	-0.909	
1.000	0.000		2.172		3.014	-5.13[b]	2.36[b]	2.56[b]			
						type 3					
0.092	0.025					0.14	1.093	0.914	-0.149		-0.119
0.196	0.020					0.07	0.867	0.930	-0.085		-0.028
0.198	0.010					0.09	0.868	0.913	-0.086		-0.039
						[c]	0.887	0.882	-0.073		-0.031
0.624	0.229					0.89	2.230	2.000	-0.229		-0.189

* f = fixed values of D_{11} and D_{22}

[a] units as in table 3.1

[b] inaccurate

[c] $w_{2,\,UV}$ = 0.00032 (AU.m^3.mol^{-1})

solely injections were made twice. To minimise the inaccuracy, only one injection was made from each vial. From the methanol injections the binary diffusion coefficient D_{11} was calculated. The binary diffusion coefficient D_{22} was calculated from the UV signals and was independent of the injected amounts of methanol and acetone. Comparison of the binary diffusion coefficients with the literature [6, 36] showed good agreement (fig 3.3). The ternary diffusion coefficients D_{11}, D_{22} and D_{12} were calculated by simultaneously fitting 6 RI peaks, each with a different value of M_1 and M_2. Starting values were the

Table 3.6b. *Imprecision (%) of diffusion coefficients and detector sensitivity ratio at 25 °C for the methanol(1) + acetone(2) + water(0) system*

		separate fit				simultaneous fit					
x_1	x_2	w_1/w_2	$D_{11\text{-RI}}$	$D_{22\text{-RI}}$	$D_{22\text{-UV}}$	w_1/w_2	D_{11}	D_{22}	D_{12}	$D_{12,f}$*	D_{21}
						type 1					
0.000	0.000	6.9	0.5	0.3	0.1	0.7	1.3	0.4			
0.000	0.001			1.0	0.4	1.6	2.7	0.9			
0.002	0.000	26	0.03	0.1	0.2	1.0	1.6	0.7			
						type 2					
0.000	0.000		0.5		0.1	0.7					
0.041	0.000		0.1		0.2	0.2	0.4	1.1	145	7.7	
0.086	0.000		0.6		0.3	0.2	0.5	0.7	23	6.7	
0.207	0.000		2.5		0.2	3.1	6.2	7.9	542	24	
0.299	0.000		2.9		0.2	0.2				9.2	
0.411	0.000		0.5		0.1	0.3	0.6	0.9	22	1.0	
0.478	0.000		0.1		0.2	0.3	0.4	0.9	17	0.8	
0.553	0.000		1.1		0.2	0.2	0.2	0.6	8.8	0.3	
0.641	0.000		0.8		0.2	2.2	0.1	0.3	3.4	0.1	
0.747	0.000		0.7		0.5	0.1	0.1	0.5	5.2	0.2	
0.878	0.000		0.9		0.2	0.7	0.6	2.0	12	0.4	
1.000	0.000		1.2		0.1	-81[a]	11[a]	176[a]			
						type 3					
0.092	0.025					92	0.4	5.4	15		8.5
0.196	0.020					65	0.6	11	120		17
0.198	0.010					254	0.6	8.5	95		17
						0.2[b]	0.3	8.5	129		9.2
0.624	0.229					14	5.4	3.8	55		39

* f = fixed values of D_{11} and D_{22}

[a] inaccurate

[b] $w_{2,\,UV}$ = 0.00032 (AU.m^3.mol^{-1})

results of the binary fits and D_{12} = 0 or D_{12} estimated using eq 3.6. The values of the main-diffusion coefficients, obtained from six different groups of six peaks, agreed well within the precision of the fitting procedure, except for the cross-diffusion coefficient at low methanol mole fractions. The precision of the ratio of the detector sensitivities w_1/w_2 was more dependent on the chosen combination of dispersion peaks. For systems at low mole fractions of methanol (x_1 below 0.4 to 0.5) D_{12} was very imprecise. The fitting procedures for the experiment at methanol mole fraction 0.3 did not converge. At this mole fraction the main-diffusion coefficients, and the eigenvalues of the diffusion

coefficient matrix, are nearly identical, and it is difficult to determine the ternary diffusion coefficient by any method [37]. The cross-diffusion coefficient D_{12} was also calculated with fixed values of D_{11}, the binary RI diffusion coefficient, and D_{22}, the binary UV diffusion coefficient. However, in this case the value of D_{12} was more dependent on the chosen combination of fitted peaks and the fixed value of D_{22}, caused by the strong correlation between D_{12} and D_{22}. Results are shown in tables 3.6a and 3.6b, type 2 and fig 3.3.

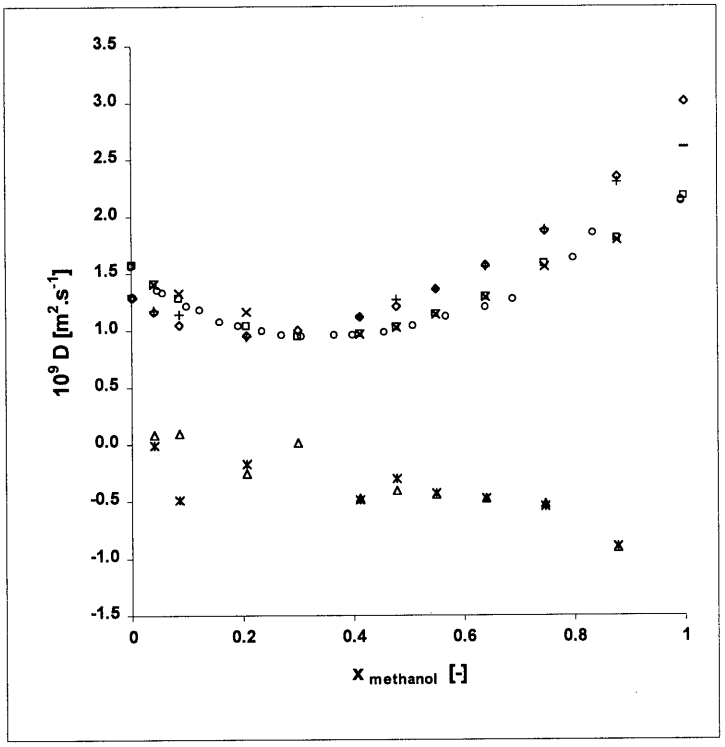

Figure 3.3. *Ternary diffusion coefficients of the system methanol(1) + acetone(2) + water(0) at 25 °C and x_2 = 0:* □, $D_{11\text{-RI}}$; ◊, $D_{22\text{-UV}}$; Δ, $D_{12\text{-fixed}}$; x, $D_{11\text{-tern}}$; +, $D_{22\text{-tern.}}$; ∗, $D_{12\text{-tern.}}$; o, D_{11} *(ref 6);* –, D_{22} *(ref 36).*

It was impossible to calculate the cross-diffusion coefficient D_{12} with even moderate imprecision from the measured dispersion peaks for a

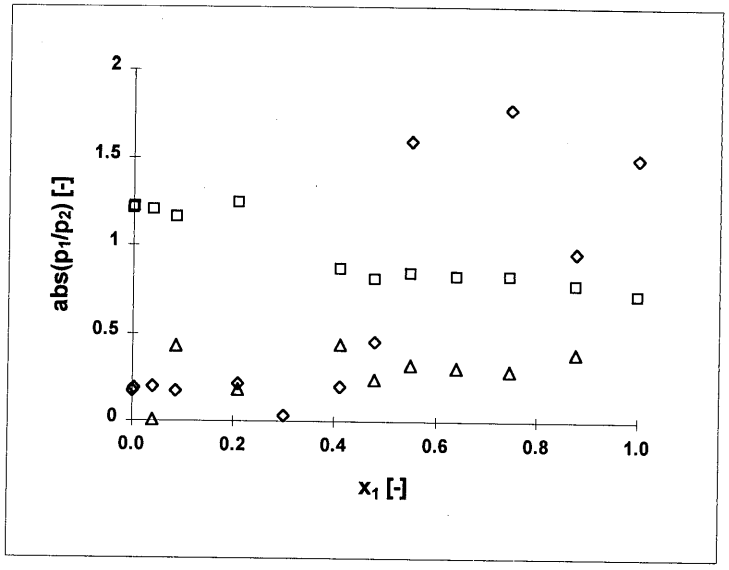

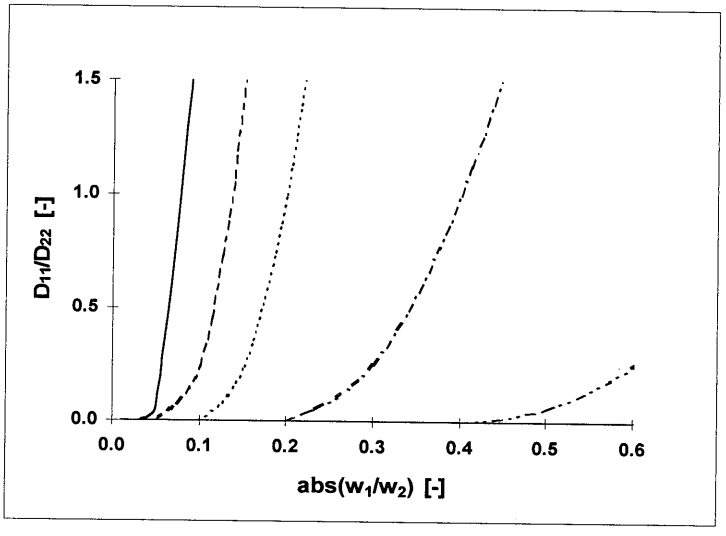

Figure 3.4. *(a) Relative detector sensitivity and diffusion coefficients of the system methanol(1) + acetone(2) + water(0) at 25 °C and x_2 = 0: ◊, $abs(w_1/w_2)$; □, $abs(D_{11}/D_{22})$; Δ, $abs(D_{12}/D_{22})$.*
(b) Minimum measurable value of D_{12}/D_{22} for the system methanol(1) + acetone(2) + water(0) at 25°C and x_2 = 0: ——, $abs(D_{12}/D_{22}) = 0.5$; – – – –, $abs(D_{12}/D_{22}) = 0.3$; ·····, $abs(D_{12}/D_{22}) = 0.2$; – · – · – · –, $abs(D_{12}/D_{22}) = 0.1$; – ·· – ·· – ·· –, $abs(D_{12}/D_{22}) = 0.05$.

mole fraction of methanol less than about 0.5. This was caused by an unfavourable combination of the relative detector sensitivity and the values of the diffusion coefficients as can be seen in figs 3.4a and 3.4b. For $x_1 < 0.45$ the ternary effects were masked by the experimental inaccuracy.

From the ternary experiments of type 3 with high acetone concentrations only RI signals were available, except for the experiment with $x_2 = 0.01$; in this case the UV signals measured at a wavelength of 208 nm (a minimum in the UV spectrum of acetone) appeared to be linear with concentration. The experimental procedure was similar to the type 2 procedure. Starting values for the fitting

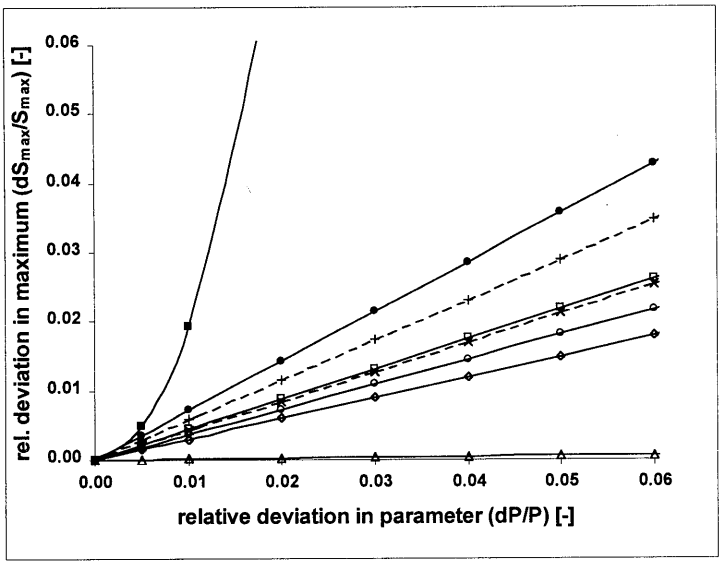

Figure 3.5. *Influence of the inaccuracy of the diffusion coefficients, injection amount, detector sensitivity and residence time on the deviation in the peak maximum ($t = \tau$) of the detected ternary signal compared to the ideal ternary signal, calculated by eq 3.2.*
Parameters of the ideal ternary signal: $D_{11} = 1.10.10^{-9}\ m^2.s^{-1}$; $D_{22} = 9.1.10^{-10}\ m^2.s^{-1}$; $D_{12} = -1.5.10^{-10}$; $D_{21} = -1.2.10^{-10}$; $w_1/w_2 = 0.14$; $M_1 = 8.00.10^{-6}\ mol$; $M_2 = 1.00.10^{-6}\ mol$; $\tau = 10110\ s$.
—△—, D_{12}; —◇—, D_{21}; —□—, D_{11}; —○—, D_{22}; – – x – –, M_1; – – + – –, M_2; —●—, w_1/w_2; —■—, τ.

procedure were values close to the "binary" D_{11} and the "binary" D_{22} calculated from the methanol-solely and acetone-solely injections, or calculated from a type 1 fitting procedure of two or more peaks simultaneously. The cross-diffusion coefficients were estimated using eq 3.6. Results are shown in tables 3.6a and 3.6b, type 3. The precision of the calculated diffusion coefficients, especially of the cross coefficients, was low and dependent on the chosen combination of peaks as well as the starting values of the fitting parameters. Moreover, there were severe convergence problems, caused by the strong correlation between the diffusion coefficients. The influence of the imprecision of the experimental procedure (determination of the injected amounts and the relative detector sensitivity) on the measured dispersion profiles was much stronger than the ternary diffusion effects (fig 3.5). Therefore, the RI detector was not suited for the measurement of this ternary system.

Because only a refractive index detector could be used for the in-line detection of the component concentrations of the system methanol(1) + acetone(2) + water(0) (for acetone concentrations above 1 vol%), the type 3 ternary diffusion measurements of this system could not be performed by the Taylor dispersion method.

Conclusions

The Taylor dispersion method is an accurate and convenient technique for measuring diffusion coefficients in binary systems. In ternary systems the calculation of the main- and cross-diffusion coefficients from the measured dispersion profiles is only possible under certain conditions depending on the ratio of the injected amounts M_1/M_2, the relative detector sensitivity w_1/w_2, the values of the diffusion coefficients, and the noise level. The measurement of accurate dispersion profiles of the components is often hindered by an unfavourable relative sensitivity of the in-line detector used. For moderate cross-diffusion coefficients the imprecision of the experimental procedure can mask the ternary diffusion effects in the dispersion profiles and the diffusion coefficients may not be calculated correctly. This is shown for the system methanol + acetone + water. If the methanol mole fraction is less than 0.45 or the acetone mole fraction is more than 0.001, the only usable refractive index detector

is unsuitable for measuring the dispersion profiles accurately enough to determine the main-diffusion coefficients as well as the cross-diffusion coefficients. Another experimental technique, such as the diaphragm cell method, has to be used.

References

[1] Erkey, C. and Akgerman, A., 1991, in *Measurement of the transport properties fluids*, Wakeham, W. A., Nagashima, A., and Sengers, J. V., eds., (Oxford, U.K.: Blackwell Scientific Publications) chap. 9, p 251.

[2] Taylor, G., 1953, *Proc. Roy. Soc. Lond., A* **219,** 186.

[3] Taylor, G., 1954, *Proc. Roy. Soc. Lond., A* **225,** 473.

[4] Aris, R., 1956, *Proc. Roy. Soc. Lond., A* **235,** 67.

[5] Alizadeh, A., Nieto de Castro, C. A., and Wakeham, W. A., 1980, *Int. J. Thermophysics,* **1,** 243.

[6] Van de Ven - Lucassen, I. M. J. J., Kieviet, F. G., and Kerkhof, P. J. A. M., 1995, *J. Chem. Eng. Data,* **40,** 407. Chapter 2 in this thesis.

[7] Leaist, D. G., 1990, *J. Phys. Chem.,* **94,** 5180.

[8] Leaist, D. G., Hao, L., and Ibrahimov, R., 1993, *J. Chem. Soc. Faraday Trans.,* **89,** 515.

[9] Leaist, D. G., 1991, *J. Solution Chem.,* **20,** 175.

[10] Leaist, D. G., 1991, *J. Chem. Soc., Faraday Trans.I,* **87,** 597.

[11] Deng, Z. and Leaist, D. G., 1991, *Can. J. Chem.,* **69,** 1548.

[12] Deng, Z. and Leaist, D. G., 1992, *J. Solution Chem.,* **21,** 15.

[13] Leaist, D. G. and Hao, L., 1993, *J. Phys. Chem.,* **97,** 1464.

[14] Leaist, D. G. and Hao, L., 1994, *J. Phys. Chem.,* **98,** 4702.

[15] Rutten, Ph. W. M., 1992, Ph. D. thesis, Delft University of Technology.

[16] Price, W. E., 1988, *J. Chem. Soc., Faraday Trans. I,* **84,** 2431.

[17] Taylor R. and Krishna, R., 1993, *Multicomponent Mass Transfer* (New York: Wiley).

[18] Toor, H. L., 1964, *AIChE J.,* **10,** 448.

[19] Miller, D. G., Vitagliano, V., and Sartorio, R., 1986, *J. Phys. Chem.,* **90**, 1509.

[20] Onsager, L., 1945, *Ann. N. Y. Acad. Sci.,* **46**, 241.

[21] Dunlop, P. J., 1964, *J. Phys. Chem.,* **68,** 26.

[22] Wendt, R. P., 1965, *J. Phys. Chem.*, **69**, 1227.
[23] Kerkhof, P. J. A. M., 1996, *Chem. Eng. J.*, **64**, 319, app. D.
[24] Levine, I. N., 1995, *Physical Chemistry*, 4th ed. (New York: McGraw-Hill) chap. 10.
[25] Dunlop, P. J., 1965, *J. Phys. Chem.*, **69**, 4276.
[26] Loh, W., Tonegutti, C. A., and Volpe, P. L. O., 1993, *J. Chem. Soc. Faraday Trans.*, **89**, 113.
[27] Weast, R. C., 1971-1972, *Handbook of Chemistry and Physics*, 52nd ed. (Cleveland, Ohio: CRC Press).
[28] Ananthakrishnan, V., Gill, W. N., and Barduhn, A. J., 1965, *AIChE J.*, **11**, 1063.
[29] Tyn, M. T. and Calus, W. F., 1975, *J. Chem. Eng. Data*, **20**, 310.
[30] Abrams, D. S. and Prausnitz, J. M., 1975, *AIChE J.*, **21**, 116.
[31] Anderson, T. F. and Prausnitz, J. M., 1978, *Ind. Eng. Chem. Process Des. Dev.*, **17** , 552.
[32] Macedo, E. A. and Rasmussen, P., 1979, *Liquid-Liquid Equilibrium Data Collection. Suppl. Chemistry Data Series* **V**, (Frankfurt am Main: Dechema) part 3, p 402.
[33] Reid, R. C., Prausnitz, J. M., and Poling, B., 1987, *The Properties of Gases and Liquids* 4th ed. (New York: McGraw-Hill).
[34] Noda, K., Ohashi, M., and Ishida, K., 1982, *J. Chem. Eng. Data*, **27**, 326.
[35] Gmehling, J., Onken, U., and Arlt, W., 1981, *Vapor-Liquid Equilibrium Data Collection. Aqueous-Organic Systems. Suppl.1, Chemistry Data Series* **I**, (Frankfurt am Main: Dechema) part 1a.
[36] Alimadadian, A. and Colver, C. Ph., 1976, *Can. J. Chem. Eng.*, **54**, 208.
[37] Miller, D. G., Albright, J. G., Mathew, R., Lee, C. M., Rard, J. A., and Eppstein, L. B., 1993, *J. Phys. Chem.*, **97**, 3885.

4. DIFFUSION COEFFICIENTS OF TERNARY MIXTURES OF WATER, GLUCOSE AND DILUTE ETHANOL, METHANOL, OR ACETONE BY THE TAYLOR DISPERSION METHOD

Abstract*

The Taylor dispersion technique is used to determine the diffusion coefficients of the ternary systems glucose + water + dilute methanol, ethanol, or acetone at 25 °C and up to a glucose mole fraction of 0.065. The dispersion of the injected solutes is recorded by a differential refractometer and an ultraviolet-visible detector. The diffusion coefficients are calculated directly by fitting the theoretical dispersion equations to about six experimental curves simultaneously. The precision of the diffusion coefficients is dependent on the relative detector sensitivities of the components. The determination of the main-diffusion coefficients is more precise than of the cross-diffusion coefficient (±2% vs ±5 - 10%).

* The main part of this chapter has been published: Van de Ven – Lucassen, I. M. J. J. and Kerkhof, P. J. A. M., 1999, *J. Chem. Eng. Data*, **44**, 93.

Introduction

Multicomponent diffusion in liquids plays an important role in many chemical engineering processes such as distillation and extraction. For the analysis of the mechanism of volatile loss during the drying of food liquids, ternary diffusion data are required [1]. An experimental technique to measure multicomponent diffusion is the Taylor dispersion method [e.g., 2, 3, 4 and references therein]. In a dispersion experiment, a slow, laminar flow of a liquid mixture is pumped through a long capillary tube and a narrow pulse of a mixture of a slightly different composition is injected into this tube. The injected solutes spread out owing to the combined effects of convective flow and molecular diffusion. At the end of the diffusion tube the dispersion is monitored by a flow-through detector (differential refractometer, ultraviolet-visible detector). The interdiffusion coefficients (called "diffusion coefficients" in this paper) are calculated by fitting the dispersion equations to the experimental curves. In this work the ternary diffusion coefficients are determined for ternary mixtures of α-D-glucose, water, and dilute ethanol, methanol, or acetone.

Theory

Diffusion in a three-component system solvent(0) + solute(1) + solute(2) is described by the coupled Fick equations

$$\mathbf{J}_1 = -D_{11}\nabla C_1 - D_{12}\nabla C_2 , \tag{4.1}$$

and

$$\mathbf{J}_2 = -D_{21}\nabla C_1 - D_{22}\nabla C_2 , \tag{4.2}$$

where $\mathbf{J}_i$ is the molar flux of component i and ∇C_i the gradient in the concentration of component i. The diffusion coefficient D_{ij} gives the flux of component i driven by the gradient in the concentration of component j; D_{ii} is called a main-diffusion coefficient and $D_{ij,i\neq j}$ a cross-diffusion coefficient.

To measure the ternary diffusion coefficients by the Taylor dispersion technique, a pulse of solution of composition $C_{1,b}+\Delta C_1$, $C_{2,b}+\Delta C_2$ is injected into the ternary mixture of composition $C_{1,b}$, $C_{2,b}$ flowing slowly through a long capillary tube. The pulse spreads out owing to the laminar velocity profile and molecular diffusion. The concentrations of the eluted solutes at the end of the diffusion tube are given by the fundamental working equations of Price [5]. If the concentration of component 2 tends to zero (component 2 is a tracer), it is impossible to produce a coupled flow of component 2 and $D_{21} \approx 0$; Price's equations simplify to [e.g. 3, 4]

$$C_1 = \frac{-\dfrac{D_{12}}{D_{11}-D_{22}}M_2}{2\pi R^2}\frac{1}{\sqrt{\pi\dfrac{R^2U^2}{48D_{22}}t}}\exp\left\{-\frac{(t-\tau)^2}{4\dfrac{R^2}{48D_{22}}t}\right\}+$$

$$\frac{M_1+\dfrac{D_{12}}{D_{11}-D_{22}}M_2}{2\pi R^2}\frac{1}{\sqrt{\pi\dfrac{R^2U^2}{48D_{11}}t}}\exp\left\{-\frac{(t-\tau)^2}{4\dfrac{R^2}{48D_{11}}t}\right\}, \tag{4.3}$$

$$C_2 = \frac{M_2}{2\pi R^2} \frac{1}{\sqrt{\pi \frac{R^2 U^2}{48 D_{22}} t}} \exp\left\{ - \frac{(t-\tau)^2}{4 \frac{R^2}{48 D_{22}} t} \right\}, \tag{4.4}$$

in which M_i represents the number of moles of component i in the injected pulse in excess of those in the same volume of the carrier stream. C_i is the radially averaged concentration of component i at time t relative to the background concentration $C_{i,b}$, τ is the mean residence time, R the internal radius of the diffusion tube, and U is the linear velocity averaged over the cross section. The assumptions made in the derivation of the working equations are similar to those of the binary dispersion technique with an effective diffusion coefficient D_{11} or D_{22} [6].

When the dispersion is monitored, the relation between the detector signal $s(t)$ and the concentration against time curves (eqs 4.3, 4.4) is assumed to be

$$s(t) = w_1 C_1 + w_2 C_2 + a + bt + \varepsilon(t), \tag{4.5}$$

in which w_i is the detector sensitivity for component i, a and b compensate for the detector drift (which is assumed to be linear in time), and $\varepsilon(t)$ is noise. The signal is sampled with a sample interval of Δt = 0.98 s. The concentration against time curve of component 1 is dependent on the injected amount of components 1 and 2 and on the main-diffusion coefficients as well as the cross-diffusion coefficient (eq 4.3). The concentration against time curve of component 2 resembles a single Gaussian, only dependent on one main-diffusion coefficient and independent of the injected amount of component 1 (eq 4.4). Determination of the cross-diffusion coefficient D_{12} is only possible under certain conditions depending on the ratio of w_1/w_2, the ratio of the injected amounts M_1/M_2, the values of the diffusion coefficients and the noise level [4].

Diffusion coefficients can be calculated from the measured dispersion profiles in two different ways: calculation from the temporal moments [7] or fitting of the theoretical eqs 4.3 and 4.4 to the experimental curve [e.g., 8]. In this work only fitting procedures will be used with the diffusion coefficients, the mean residence time τ

and the detector sensitivities w_1 and w_2 as fitting parameters. In these fitting procedures the discrete signal y without the drift is required: $y = y^* - (a + b\,t)$, in which y^* is the discrete output signal of the detector. For the calculation of a and b, regions of the detected signal before and after the eluted solute peak, where the concentration is negligible, are visually marked in our software as baseline. Through these regions of the signal the drift is fitted (using a least-squares method) and subtracted from the signal [9].

Equipment and experimental procedure

An extensive description of the equipment for the measurement of diffusion coefficients in binary and ternary liquid systems is given by Van de Ven – Lucassen et al [4, 9]. Solutions were prepared by mass and mixing, and degassed by sparging with helium. Injection solutions were made by volumetrical mixing of the degassed materials. To prevent bubbles from disturbing the flow, an in-line degasser (Separations DG1300) was installed. The HPLC pump (type LKB2150), which maintained a steady flow, was connected to an autosampler (Spark Marathon) with a fixed volume sample loop of 20 μL. Zero dead volume fittings were used to connect the diffusion tube with the autosampler and the ultraviolet-visible detector (UV detector) and a short capillary tube between the UV detector and the differential refractometer (RI detector). The diffusion tube was a 25 m length of PEEK (Poly Ether Ether Ketone) tubing wrapped in a 0.40 m diameter coil. The internal radius of the tube (0.52 ± 0.01 mm) was determined by gravimetry and residence time measurements. From diffusion measurements of the systems methanol + water (whole concentration range), ethanol + water, and acetone + water the internal radius was also calculated (data used were given in [9] and references therein); this radius was not significantly different (0.521 ± 0.003 mm).

The eluted peaks were detected with the UV detector (Applied Biosystems 785A) and subsequently by the differential refractometer (Shodex SE61). The analogous output signal of the refractometer was converted by a Multilab system (A/D-D/A conversion system developed at the Eindhoven University of Technology). For the conversion of the analogous output signal of the UV detector, a hardware interface

device (Strawberry-Tree Mini16 ADC) was built in the personal computer (PC). The multilab was used to interface between PC and RI detector and between PC and selection valve. The pump and the autosampler were controlled directly by the PC. Software has been developed for data acquisition and controlling the equipment as well as for processing of the data.

The procedure for the measurement of diffusion coefficients in binary systems is described in detail by Van de Ven - Lucassen et al [9]. Before a ternary experiment was started, the system was flushed for at least 6 h at the flow rate of the diffusion experiment to attain a stable, linear baseline in each detector. The flow velocity was set in accordance with the conditions, under which Price's equations 4.3 and 4.4 are valid (typically 0.12 $cm^3.min^{-1}$). Diffusion samples were injected every $1^1/_2$ – 2 h. After application of a baseline correction to each experimental curve, binary fits were done for dispersion peaks obtained from $M_2 = 0$ or $M_1 = 0$ injections: the mean residence time τ, the binary diffusion coefficient (D_{11} or D_{22}) and the peak area were calculated. The detector sensitivity (w_1 or w_2) was determined from the peak area and the injected amount. These values could be used as starting values for the fitting parameters in the ternary procedures.

The fitting procedures have been based on the nonlinear least-squares approximation between the experimental data points and the points calculated according to eqs 4.3 and 4.4 [4]. These ternary fitting procedures have been written in the SAS for Windows-package (version 6.10, SAS Institute Inc.), using the method of Marquardt. They are able to fit several experimental curves simultaneously with the following fitting parameters:

- $D_{11}, D_{22}, D_{12}, \tau, w_1$ and w_2
- D_{12}, τ, w_1 and w_2; D_{11} calculated from the binary diffusion experiments; D_{22} calculated from the UV signals (only for acetone as a tracer).

Other combinations of fitting parameters and calculated parameters are possible.

Experimental results and discussion

Diffusion coefficients were measured for the binary systems methanol + water, ethanol + water, acetone + water, and glucose + water and for the ternary systems glucose + ethanol + water, glucose + methanol + water, and glucose + acetone + water.

Water deionized and filtered through a Milli-Q water purification system (Millipore, resistivity 18 MΩ·cm) was used. Analytical-grade methanol (purity ≥ 99.8%, water < 0.05%), ethanol (purity ≥ 99.8%, water < 0.2%), acetone (purity ≥ 99.5%, water < 0.2%), and D(+)-glucose anhydrous (purity ≥ 99.0%, water < 0.2%) were obtained from Merck and used without further purification. All experiments were performed at 25 °C.

Binary systems

Experiments were performed to show that the detector response was linear with concentration and to study the influence of the concentration of the injected sample on the measurement of the diffusion coefficients. Samples of increasing or decreasing glucose concentration were injected into binary mixtures of glucose and water, and the peak area and the diffusion coefficient were calculated. For all values of the injected excess amount of glucose, the detector response was linear. Below an absolute value of the injected excess of 1.10^{-5} mol, the diffusion coefficient was independent of the injected amount; at higher values the diffusion coefficient increased, probably owing to secondary flow effects. Therefore, these high injection concentrations were not used for the determination of the binary and ternary diffusion coefficients. Injections of solutions of increasing methanol, ethanol or acetone concentrations into pure water showed also a linear detector response and an independence of the concentration difference up to 4 - 6 vol% between injection sample and solvent. Injections of solutions of acetone in glucose-water mixtures were detected also by the UV detector at a wavelength of 266 nm. At this wavelength only acetone was detected; i.e., $w_1 = 0$ in eq 4.5. From the UV signal the diffusion coefficient D_{22} ($D_{22,UV}$) and the peak area were calculated. The detector response was linear with the injected amount of acetone, and the diffusion coefficient was independent of the injected amount of acetone.

Table 4.1. *Diffusion coefficients and detector sensitivities at 25 °C of the systems water(0) + glucose(1) + tracer(2)*

	Binary system water + glucose	**Ternary system water(0) + glucose(1) + acetone(2)**
mole fraction x_1	$D_{11,\,bin.}$ / 10^{-10} m^2.s^{-1}	$D_{22,\,UV}$/ 10^{-10} m^2.s^{-1}
0	6.9	12.7
0.015	5.79	9.6
0.025	5.2	
0.035	4.58	6.56
0.05	3.80	4.92
0.065	3.14	3.62

Ternary systems water(0) + glucose(1) + tracer(2)

x_1	D_{11} / 10^{-10} m^2.s^{-1}	D_{22} / 10^{-10} m^2.s^{-1}	D_{12} / 10^{-10} m^2.s^{-1}	w_1 / 10^4RIU.mol^{-1}	w_2 / 10^4RIU.mol^{-1}
			tracer acetone(2)		
0.000	*(7.05)**	*(12.7)**	-0.004	3.474	0.479
0.015	5.75	9.95	0.18	3.380	0.550
0.025	5.36	8.31	0.29	3.105	0.599
0.035	*(4.50)**	*(6.56)**	0.51	3.237	0.588
0.050	3.78	5.02	0.54	3.110	0.362
0.065	3.11	3.84	0.57	2.990	0.633
			tracer ethanol(2)		
0.000	*(7.05)**	*(12.2)**	-0.016	3.449	0.360
0.015	5.75	9.34	0.31	3.389	0.425
0.025	5.11	7.98	0.59	3.209	0.376
0.035	4.44	6.55	0.60	3.201	0.435
0.050	3.77	4.91	0.69	3.111	0.282
0.065	3.11	3.69	0.64	2.990	0.492
			tracer methanol(2)		
0.000	*(7.05)**	*(15.3)**	-0.015	3.435	0.079
0.015	5.77	12.1	0.071	3.409	0.158
0.025	5.27	10.3	0.07	3.075	0.181
0.035	4.56	8.5	0.21	3.259	*(0.180)**
0.050	3.77	6.43	0.49	3.111	0.002
0.065	3.11	4.77	0.29	2.990	0.265

*(...)**, not fitted; fixed values used in the fitting procedures and obtained from the binary experiments

Table 4.2. *Imprecision of the diffusion coefficients and detector sensitivities at 25 °C of the systems water(0) + glucose(1) + tracer(2)*

	Binary system water+glucose	**Ternary system water(0) + glucose(1) + acetone(2)**
mole fraction x_1	$D_{11,\,\mathrm{bin.}}$ / %	$D_{22,\,\mathrm{UV}}$ / %
0	1.6	0.5
0.015	1.0	1.3
0.025	2.5	
0.035	1.7	0.8
0.05	1.2	1.2
0.065	1.0	1.3

Ternary systems water(0) + glucose(1) + tracer(2)

x_1	D_{11} / %	D_{22} / %	D_{12} / %	w_1 / %	w_2 / %
		tracer acetone(2)			
0.000			49	0.02	0.06
0.015	0.08	0.5	6.5	0.04	0.08
0.025	0.19	1.0	11	0.08	0.15
0.035			0.1	0.02	0.03
0.050	0.21	1.0	9.3	0.09	0.32
0.065	0.08	0.2	2.9	0.04	0.06
		tracer ethanol(2)			
0.000			6.0	0.01	0.04
0.015	0.04	0.2	2.1	0.02	0.04
0.025	0.31	1.2	7.8	0.14	0.32
0.035	0.05	0.1	0.8	0.02	0.03
0.050	0.21	0.8	7.5	0.09	0.37
0.065	0.15	0.4	5.8	0.06	0.13
		tracer methanol(2)			
0.000			6.5	0.01	0.16
0.015	0.03	0.5	4.8	0.01	0.09
0.025	0.16	1.3	15	0.07	0.25
0.035	0.28	1.8	10	0.12	
0.050	0.20	1.3	6.0	0.09	54
0.065	0.16	0.8	5.4	0.07	0.23

The diffusion coefficients of the binary system glucose + water (D_{11}) and of the tracer acetone in the glucose + water mixtures ($D_{22,\mathrm{UV}}$) are listed in table 4.1; the precision of the results is given in table 4.2.

The values of the binary D_{11} are the mean of seven injections and the values of the $D_{22,UV}$ are the mean of six injections, each with a different concentration. The confidence limits of the binary D_{11} and $D_{22,UV}$ ("precision") were calculated according to the Student's t distribution, probability level 95%, two-tail test [10].

Ternary systems

The ternary diffusion coefficients of the systems glucose + acetone + water, glucose + ethanol + water, and glucose + methanol + water were determined by injecting ternary mixtures into the binary glucose + water mixture. Injection samples were prepared in vials to give seven different values of M_1 with M_2 = 0, and for each tracer component three different values of M_2 with M_1 = 0 and three different combinations of M_1 and M_2. The ternary diffusion coefficients D_{11}, D_{22} and D_{12}, the mean residence time τ, and the detector sensitivities w_1 and w_2 were calculated by simultaneously fitting of six RI peaks, each with a different value of M_1 and M_2 (mostly two peaks with M_1 = 0, two peaks with M_2 = 0, and two combination peaks). An estimation of the standard errors of all parameters was given by the nonlinear SAS fitting procedures used, and a 95% confidence interval was calculated ("precision"). For all mixtures, the main-diffusion coefficients were more precise than the cross-diffusion coefficient. The inaccuracy of the residence time τ was less than 0.005%. There was a strong correlation between the cross-diffusion coefficient D_{12} and the main-diffusion coefficient of the tracer D_{22}. The values of the diffusion coefficients obtained from a different group of six peaks agreed within 1 - 2% for the main-diffusion coefficients and within the precision of the fitting procedure for the cross-diffusion coefficients. No significant difference was observed between the calculated diffusion coefficients if the starting values were changed, provided convergence was achieved. In general, experiments with tracer component methanol were less accurate. The dispersion curves had a poorer signal-to-noise ratio, and convergence of the fitting procedures was harder to achieve (e.g., at x_1 = 0.035, x_1 = 0.050). This was caused by the lower RI sensitivity for methanol. The strong correlation between D_{12} and D_{22} was studied by fitting six RI peaks (at x_1 = 0.065) simultaneously with D_{11} and D_{22} fixed at a value with a deviation of ±5% of the D_{11} and D_{22}, calculated in a previous fitting procedure. The value of the cross-diffusion coefficient D_{12}, calculated with the fixed D_{11} and D_{22}, was within the

confidence interval of the value of the D_{12}, calculated in the fitting procedure of D_{11}, D_{22}, and D_{12} simultaneously. Results of the ternary diffusion measurements are listed in tables 4.1 and 4.2 and shown in figures 4.1 – 4.4. The binary D_{11} and the $D_{22,UV}$ of acetone agreed well with the values calculated by the ternary fitting procedures.

Comparison of the values at infinite dilution (x_1 = 0) and of the binary D_{11} with literature values in figures 4.1 – 4.3 showed a good agreement. Chandrasekaran and King [1] determined the ternary diffusion coefficients for the system ethanol(1, tracer) + water(2) + glucose(0). As the four diffusion coefficients are dependent on the choice of the solvent, the values of Chandrasekaran and King [1] had to be converted to the system glucose(1) + ethanol(2,tracer) + water(0). Equations used for this conversion were [11]

$$D_{21} \approx 0\,,\ D^*_{12} \approx 0\,,\ D_{11} \approx D^*_{22}\,,\ D_{22} \approx D^*_{11}\,, \text{ and}$$

$$D_{12} = \frac{\overline{V}_2}{\overline{V}_1} D^*_{22} - \frac{\overline{V}_0}{\overline{V}_1} D^*_{21} - \frac{\overline{V}_2}{\overline{V}_1} D^*_{11}\,, \tag{4.5}$$

in which $\overline{V}_i$ is the partial molar volume of component i and D^*_{ij} the original diffusion coefficients, determined by Chandrasekaran and King [1]. The partial molar volumes were calculated using equations describing the partial molar volumes as a function of the mole fractions, the molar mass, and the (mole fraction derivatives of the) density of the mixtures. Density values were obtained from Cerdeirina et al [15] and from Taylor and Rowlinson [16]. Comparison of the converted values with the measured values in figure 4.5 shows a good agreement for the main-diffusion coefficient D_{11}. The values of the measured main-diffusion coefficient D_{22} and of the measured cross-diffusion coefficient D_{12} are higher than the converted literature values. The accuracy of the converted cross-diffusion coefficient was low owing to the procedure followed. The estimation of D^*_{21} and D^*_{11} from a logarithmic graph occurred with only a moderate precision (imprecision > 5%). Chandrasekaran and King [1] showed the results in logarithmic graphs of the diffusion coefficients versus the concentration of water (and the weight percent sugar in solution) and did not mention the accuracy of the measurements explicitly. The calculation using the partial molar volumes and the estimated

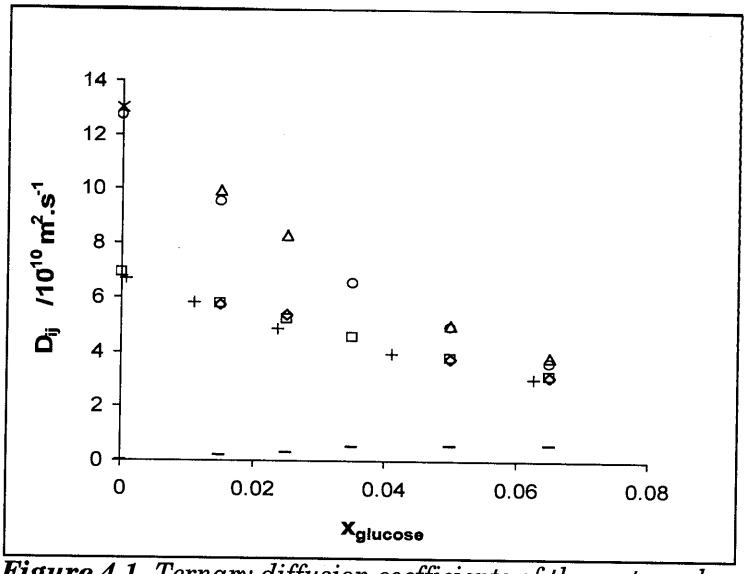

Figure 4.1. *Ternary diffusion coefficients of the system glucose(1) + acetone(2) + water(0) at 25 °C and x_2 = 0: □, binary D_{11} ; ◊, ternary D_{11} ; Δ, ternary D_{22} ; -, ternary D_{12} ; and ○, $D_{22,UV}$, this work; +, binary D_{11} , ref 12, ref 13; and ×, binary D_{22} , ref 14.*

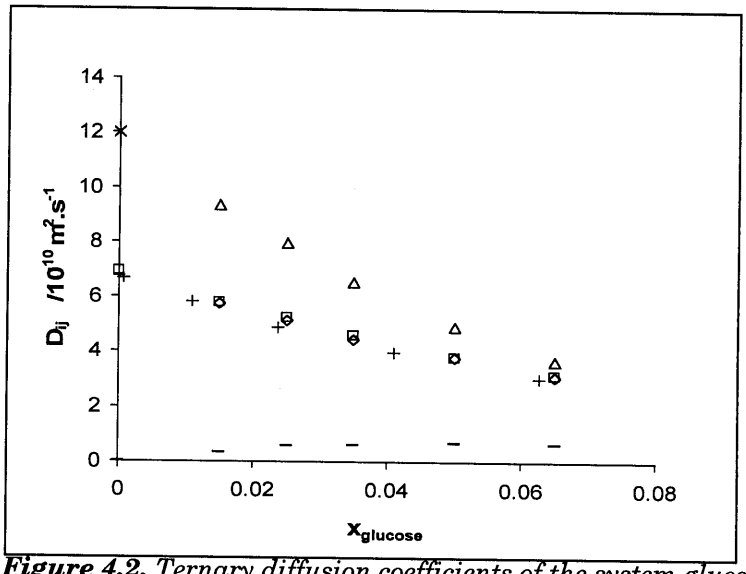

Figure 4.2. *Ternary diffusion coefficients of the system glucose(1) + ethanol(2) + water(0) at 25 °C and x_2 = 0: □, binary D_{11} ; ◊, ternary D_{11} ; Δ, ternary D_{22} ; and -, ternary D_{12} , this work; and +, binary D_{11} , ref 12, ref 13; ×, binary D_{22} , ref 9.*

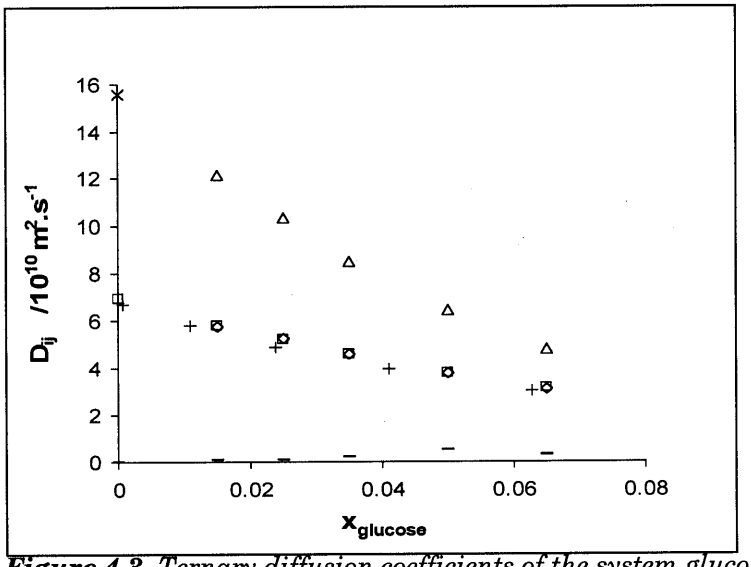

Figure 4.3. *Ternary diffusion coefficients of the system glucose(1) + methanol(2) + water(0) at 25 °C and x_2 = 0: □, binary D_{11} ; ◊, ternary D_{11} ; (Δ) ternary D_{22} ; and -, ternary D_{12} , this work; +, binary D_{11} , ref 12, ref 13; and ×, binary D_{22} , ref 9.*

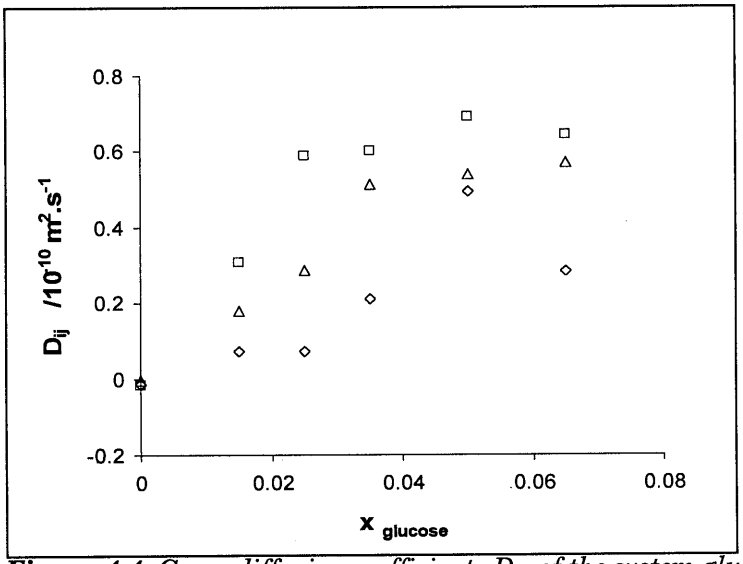

Figure 4.4. *Cross-diffusion coefficients D_{12} of the system glucose(1) + tracer(2) + water(0) at 25 °C and x_2 = 0: □, ethanol; ◊, methanol; Δ, acetone.*

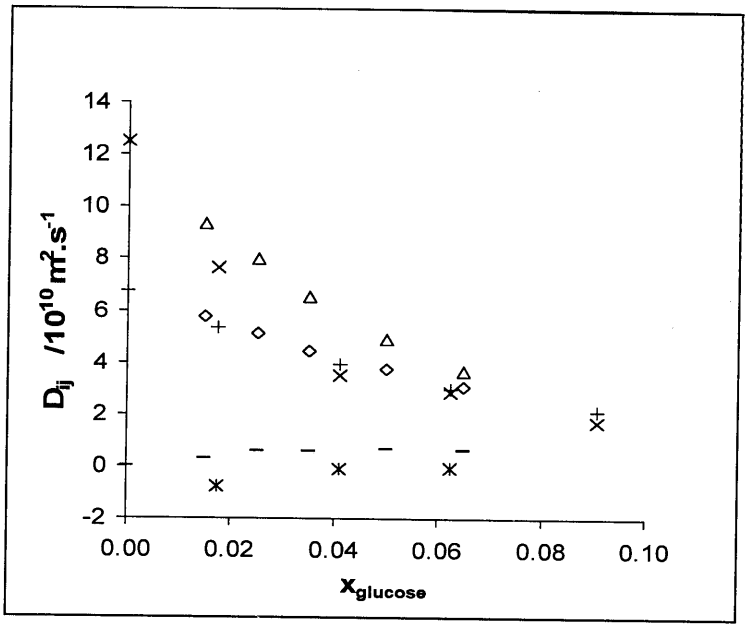

Figure 4.5. *Comparison of the experimental ternary diffusion coefficients of the system glucose(1) + ethanol(2) + water(0) with previous work at 25 °C and x_2 = 0: ◊, ternary D_{11} ; Δ, ternary D_{22} ; and -, ternary D_{12} , this work; +, ternary D_{11} ; ×, ternary D_{22} ; and ∗, ternary D_{12} , ref 1.*

diffusion coefficients decreased the precision. Furthermore, the cross-diffusion coefficient D^*_{12} was not set equal to 0. It is therefore understandable that comparison of the measured D_{12} with the converted D_{12} does not show a good agreement.

Conclusions

The Taylor dispersion method is a fast and convenient technique for measuring diffusion coefficients in liquid systems. In ternary systems with one component infinitely diluted, the precision of the method is dependent on the relative detector sensitivities of the components. Of the systems studied in this paper, the measured main-diffusion coefficients D_{11} and D_{22} are more precise than the measured cross-diffusion coefficient D_{12}.

References

[1] Chandrasekaran, S. K. and King, C. J., 1972, *AIChE J.*, **18**, 513.
[2] Leaist, D. G., 1991, *Ber. Bunsen-Ges. Phys. Chem.*, **95**, 117.
[3] Leaist, D. G., 1991, *J. Solution Chem.*, **20**, 175.
[4] Van de Ven - Lucassen, I. M. J. J., Kemmere, M. F., and Kerkhof, P. J. A. M., 1997, *J. Solution Chem.*, **26**, 1145. Chapter 3 in this thesis.
[5] Price, W. E., 1988, *J. Chem. Soc., Faraday Trans. I*, **84**, 2431.
[6] Alizadeh, A., Nieto de Castro, C. A., and Wakeham, W. A., 1980, *Int. J. Thermophys.*, **1**, 243.
[7] Leaist, D. G., Hao, L., and Ibrahimov, R., 1993, *J. Chem. Soc., Faraday Trans.*, **89**, 515.
[8] Leaist, D. G. and Hao, L., 1994, *J. Phys. Chem.*, **98**, 4702.
[9] Van de Ven - Lucassen, I. M. J. J., Kieviet, F. G., and Kerkhof, P. J. A. M., 1995, *J. Chem. Eng. Data*, **40**, 407. Chapter 2 in this thesis.
[10] Perry, R. H. and Chilton, C. H., 1969, *Chemical Engineers' Handbook,* 5th ed. (New York: McGraw-Hill Book).
[11] Vitagliano, V., Sartorio, R., Scala, S., and Spaduzzi, D., 1978, *J. Solution Chem.*, **7**, 605.
[12] Gladden, J. K. and Dole, M., 1953, *J. Am. Chem. Soc.*, **75**, 3900.
[13] Uedaira, H. and Uedaira, H., 1985, *J. Solution Chem.*, **14**, 27.
[14] Tyn, M. T. and Calus, W. F., 1975, *J. Chem. Eng. Data*, **20**, 310.
[15] Cerdeirina, C. A., Carballo, E., Tovar, C. A., and Romani, L., 1997, *J. Chem. Eng. Data*, **42**, 124.
[16] Taylor, J. B. and Rowlinson, J. S., 1955, *Trans. Faraday Soc.*, **51**, 1183.

CHAPTER 4

5. USING MOLECULAR DYNAMICS TO OBTAIN MAXWELL-STEFAN DIFFUSION COEFFICIENTS IN LIQUID SYSTEMS

Abstract*

Two methods are compared for the calculation of Maxwell-Stefan diffusion coefficients. The first method is a non-equilibrium molecular dynamics (NEMD) algorithm, in which the system is driven away from equilibrium and the system response is monitored. The second method is the equilibrium molecular dynamics (EMD) calculation of the appropriate Green-Kubo equation. Simulations were performed for systems of 250 and 300 Lennard-Jones particles at various densities and temperatures. The systems were divided into two or three components by attaching a colour label to the particles. Since a colour label plays no role in the dynamics, the Maxwell-Stefan diffusion coefficients of the binary and ternary systems are equal to the self-diffusion coefficient. In dense fluids, the system response to an external perturbation is not a first-order process, and the diffusion coefficients cannot be determined from the short-term response in the NEMD method. Only the long-term response can be used, after a steady state has been reached. In binary systems the Maxwell-Stefan diffusion coefficients, determined by the Green-Kubo (EMD) method, are more accurate than the NEMD coefficients. Since in the NEMD method only the long-term response can be used, the Green-Kubo method is also less time consuming and is therefore preferred for the calculation of the Maxwell-Stefan diffusion coefficients. In ternary systems the Green-Kubo method is tested for the 250 particles system. The Maxwell-Stefan diffusion coefficients agree well with the self-diffusion coefficient. For low mole fractions of the coloured components the diffusion coefficients were less accurate.

---

* The main part of this chapter has been published: Van de Ven - Lucassen, I. M. J. J., Vlugt, T. J. H., Van der Zanden, A. J. J., and Kerkhof, P. J. A. M., 1998, *Molec. Phys.*, **94**, 495.

Introduction

Multicomponent diffusion in liquids plays an important role in many chemical engineering processes like extraction and distillation. However, little is known about the concentration dependence of multicomponent diffusion coefficients [1]. The measurement of diffusion coefficients in liquid systems is difficult and time consuming [2, 3]. Therefore, it would be very interesting to predict multicomponent diffusion coefficients using a molecular simulation technique.

The transport coefficients in a system, simulated by molecular dynamics (MD), can be determined by two classes of methods. In the first class of equilibrium molecular dynamics (EMD) methods, the correlation function of fluctuating quantities in an equilibrium system is determined. The integrals of the correlation functions are related to the transport coefficients (e.g., diffusion coefficients) through the Green-Kubo formalism. EMD calculations were used by Schoen and Hoheisel [4] for the determination of the mutual diffusion coefficient in binary Lennard-Jones mixtures. In the second class of non-equilibrium molecular dynamics (NEMD) methods, the system is driven away from equilibrium and the system response is monitored. Diffusion can be simulated by applying an external acceleration to the individual particles in the system, as described by Berendsen [5]. However, no results of any NEMD diffusion studies using this method are available.

The purpose of this study is to compare the NEMD method, developed by Berendsen, with the EMD method, by performing simulations in Lennard-Jones mixtures at various temperatures and densities.

The Maxwell-Stefan approach for diffusion in liquids

A liquid mixture at temperature T and pressure p consists of n components with mole fractions x_1, x_2, ...x_n. When T and p are constant and when there are no external forces acting on the system, the molar fluxes $\mathbf{N}_1$,$\mathbf{N}_2$..$\mathbf{N}_n$ due to the gradient in the chemical potential μ_i of component i are given by

$$\sum_{\substack{j=1 \\ j\neq i}}^{n} \frac{x_i \mathbf{N}_j - x_j \mathbf{N}_i}{C_t D_{ij}} = \frac{x_i}{RT} \nabla_{T,p} \mu_i , \tag{5.1}$$

in which R is the gas constant, C_t the total molar concentration and D_{ij} the Maxwell-Stefan diffusion coefficient between components i and j. Because $D_{ij} = D_{ji}$ there are ½n(n-1) independent Maxwell-Stefan diffusion coefficients. The Maxwell-Stefan approach is preferred over Fick's law for describing diffusion under the influence of external body forces and in multicomponent systems [6]. An extensive description is given in [6, 7]. Using $\mathbf{N}_i = \mathbf{u}_i C_i$, in which $\mathbf{u}_i$ is the velocity and C_i the molar concentration of component i, equation 5.1 can be rewritten as

$$\nabla_{T,p} \mu_i = \sum_{\substack{j=1 \\ j\neq i}}^{n} \frac{RT}{D_{ij}} x_j \left(\mathbf{u}_j - \mathbf{u}_i \right). \tag{5.2}$$

Suppose one particle of component i is displaced Δx in the x-direction under constant temperature and pressure. The amount of work needed then is

$$\frac{F_{i,x}}{N_A} \Delta x = \frac{\mu_{i,x+\Delta x} - \mu_{i,x}}{N_A} , \tag{5.3}$$

in which $F_{i,x}$ is the molar force acting on component i in the x-direction and N_A is Avogadro's number. Combining equations 5.2 and 5.3 leads to the expression for the force acting on component i due to velocity differences with other components j

$$\mathbf{F}_i = \sum_{\substack{j=1 \\ j\neq i}}^{n} \frac{RT}{D_{ij}} x_j \left(\mathbf{u}_j - \mathbf{u}_i\right). \tag{5.4}$$

Equation 5.4 describes the mean force on component i, and is used as a basis for further derivations of the diffusion coefficients.

Calculating binary diffusion coefficients

For the determination of diffusion coefficients in a system two MD methods are described. The first is an NEMD method, in which the system is driven away from equilibrium and the system response is monitored. The second is a Green-Kubo method, in which the correlation function of fluctuating quantities in an equilibrium system is determined.

NEMD method

A non-equilibrium driving force for diffusion is the gradient in the chemical potential of the components (equation 5.1). In the NEMD method as developed by Berendsen [5] a gradient in chemical potential is simulated by imposing forces on both components in a given direction. Every MD timestep Δt the velocity of each particle of component i in the given direction is increased by $\mathbf{a}_i \Delta t$ in such a way that there is no net force acting on the system. This implies

$$M_1 x_1 \mathbf{a}_1 + M_2 x_2 \mathbf{a}_2 = \mathbf{0} \tag{5.5a}$$

and

$$M_1 x_1 \mathbf{u}_1 + M_2 x_2 \mathbf{u}_2 = \mathbf{0}, \tag{5.5b}$$

in which M is the molar mass. The system will respond to these imposed forces by

$$\frac{d\mathbf{u}_1}{dt} = \mathbf{a}_1 + \frac{RTx_2}{M_1 D_{12}}(\mathbf{u}_2 - \mathbf{u}_1)$$
$$\frac{d\mathbf{u}_2}{dt} = \mathbf{a}_2 + \frac{RTx_1}{M_2 D_{12}}(\mathbf{u}_1 - \mathbf{u}_2) \tag{5.6}$$

or

$$\frac{d(\mathbf{u}_1 - \mathbf{u}_2)}{dt} = (\mathbf{a}_1 - \mathbf{a}_2) - \frac{\mathbf{u}_1 - \mathbf{u}_2}{\tau_d}, \tag{5.7}$$

in which we have defined

$$\tau_d = \frac{M_1 M_2 D_{12}}{RT(M_1 x_1 + M_2 x_2)}. \tag{5.8}$$

With the initial condition $\mathbf{u}_1 = \mathbf{u}_2 = \mathbf{0}$ the solution of equation 5.7 is

$$\mathbf{u}_1(t) - \mathbf{u}_2(t) = \tau_d(\mathbf{a}_1 - \mathbf{a}_2)\left[1 - \exp\left(-\frac{t}{\tau_d}\right)\right]. \tag{5.9}$$

The stationary velocity of component 1 is equal to

$$\mathbf{u}_1(\infty) = \frac{\mathbf{a}_1 M_1 M_2 D_{12}}{RT(M_1 x_1 + M_2 x_2)}. \tag{5.10}$$

From equation 5.9 it follows that D_{12} can be calculated either from the short-term response by fitting equation 5.9 to the computed velocity differences for small t or from the long-term response by using equation 5.9 for $t \to \infty$ or equation 5.10 determining the slope of $\mathbf{u}_1(\infty)$ versus $\mathbf{a}_1$.

Green-Kubo method

The time correlation functions used in the Green-Kubo method are linked to the response to weak perturbations in the equilibrium system by linear response theory [8-10]. A very weak external

perturbation λB, applied at $t = 0$, changes the Hamiltonian H_0 of the system to $H = H_0 - \lambda B$, in which λ is the constant force of the perturbation and B the coupled system variable. The stationary response of a system variable $A(t)$ to this perturbation is then given by [10]

$$\langle A(\infty)\rangle - \langle A(0)\rangle = \frac{-\lambda}{k_B T}\int_0^\infty \left\langle B(0)\dot{A}(\tau)\right\rangle d\tau, \tag{5.11}$$

in which k_B is Boltzmann's constant. Using $\left\langle B(0)\dot{A}(\tau)\right\rangle = -\left\langle \dot{B}(0)A(\tau)\right\rangle$, equation 5.11 can be written as

$$\langle A(\infty)\rangle - \langle A(0)\rangle = \frac{\lambda}{k_B T}\int_0^\infty \left\langle \dot{B}(0)A(\tau)\right\rangle d\tau. \tag{5.12}$$

If we identify λ with $n_i M_i \mathbf{a}_i$, B with $\mathbf{r}_i$, and A with $\mathbf{u}_i$ then for very weak forces $n_i M_i \mathbf{a}_i$ on both components of a binary system, coupled to a mean displacement of the particles $\mathbf{r}_i$, the system variable $\mathbf{u}_1(\infty)$ is given by

$$\mathbf{u}_1(\infty) = \frac{\mathbf{a}_1 M_1 n_1}{3RT}\int_0^\infty \langle(\mathbf{u}_1(0) - \mathbf{u}_2(0))\bullet \mathbf{u}_1(t)\rangle dt, \tag{5.13}$$

in which n_1 is the number of particles of component 1. Using equation 5.5, the average velocity $\mathbf{u}_1$ of component 1 can be written as a function of the velocities, $\mathbf{v}_1^i$, of all particles of component 1

$$\langle(\mathbf{u}_1(0) - \mathbf{u}_2(0))\bullet \mathbf{u}_1(t)\rangle = \frac{1}{n_1^2}\left(1 + \frac{M_1 x_1}{M_2 x_2}\right)\left\langle \sum_{i=1}^{n_1}\mathbf{v}_1^i(0)\bullet\sum_{j=1}^{n_1}\mathbf{v}_1^j(t)\right\rangle. \tag{5.14}$$

Combining equations 5.10, 5.13 and 5.14 results in the equation for the binary Maxwell-Stefan diffusion coefficient

$$D_{12} = \frac{x_2}{3n_1}\left(\frac{M_1x_1 + M_2x_2}{M_2x_2}\right)^2 \int_0^\infty \left\langle \sum_{i=1}^{n_1} \mathbf{v}_1^i(0) \bullet \sum_{j=1}^{n_1} \mathbf{v}_1^j(t) \right\rangle dt \,. \tag{5.15}$$

Following Schoen & Hoheisel [4], equation 5.5 inserted into equation 5.15 gives

$$D_{12} = \frac{x_2}{3n_1n_2^2} \int_0^\infty \left\langle \left[n_2 \sum_{i=1}^{n_1} \mathbf{v}_1^i(0) - n_1 \sum_{j=1}^{n_2} \mathbf{v}_2^j(0) \right] \bullet \left[n_2 \sum_{k=1}^{n_1} \mathbf{v}_1^k(t) - n_1 \sum_{l=1}^{n_2} \mathbf{v}_2^l(t) \right] \right\rangle dt \tag{5.16}$$

A similar equation has been derived by Hansen and McDonald [11]. Neglecting the correlations between the velocities of two different particles at different times, equation 5.16 simplifies to the pure mutual diffusion coefficient, D_{12}^0:

$$D_{12}^0 = \frac{x_2}{3} \int_0^\infty \langle \mathbf{v}_1(0) \bullet \mathbf{v}_1(t) \rangle dt + \frac{x_1}{3} \int_0^\infty \langle \mathbf{v}_2(0) \bullet \mathbf{v}_2(t) \rangle dt \,. \tag{5.17}$$

This approximation is exact if one component is infinitely diluted or if component 1 and component 2 are identical and distinguished only by, for example, a colour label that plays no role in the dynamics. In the latter case the Maxwell-Stefan diffusion coefficient is equal to the self-diffusion coefficient.

$$D_{12} = D_{\text{self}} = \frac{1}{3} \int_0^\infty \langle \mathbf{v}(0) \bullet \mathbf{v}(t) \rangle dt \,. \tag{5.18}$$

Calculating ternary diffusion coefficients

Green-Kubo method

To derive the Green-Kubo equation for a ternary system, consider the case that

$$\lim_{t\to\infty} \mathbf{u}_1(t) = \lim_{t\to\infty} \mathbf{u}_2(t) = \mathbf{u}_1(\infty) \,. \tag{5.19}$$

With equations analogous to eqs 5.5 and 5.6 this leads to

$$\mathbf{a}_2 = \mathbf{a}_1 \frac{M_1 D_{31}}{M_2 D_{23}} \tag{5.20}$$

and

$$\mathbf{a}_3 = -\mathbf{a}_1 \frac{M_1}{M_3} \left(\frac{\mathrm{n}_1 + \mathrm{n}_2 \dfrac{D_{31}}{D_{23}}}{\mathrm{n}_3} \right). \tag{5.21}$$

The stationary velocity of component 1 is according to the linear response theory proportional to $\mathbf{a}_1$:

$$\mathbf{u}_1(\infty) = \frac{\mathbf{a}_1 M_1 \mathrm{n}_1}{3RT} Int_{131} + \frac{\mathbf{a}_1 M_1 \mathrm{n}_2 D_{31}}{3RTD_{23}} Int_{231} \ , \tag{5.22}$$

in which we have defined

$$Int_{\mathrm{ijk}} = \int_0^\infty \left\langle \left(\mathbf{u}_\mathrm{i}(0) - \mathbf{u}_\mathrm{j}(0) \right) \bullet \mathbf{u}_\mathrm{k}(t) \right\rangle dt \, . \tag{5.23}$$

This is also equal to

$$\mathbf{u}_1(\infty) = \frac{\mathbf{a}_1 M_1 M_3 D_{31}}{RT\left(M_1 x_1 + M_2 x_2 + M_3 x_3\right)} . \tag{5.24}$$

Combining equations 5.22 and 5.24 leads to an expression for D_{31}

$$\frac{D_{31}}{M_1 x_1 + M_2 x_2 + M_3 x_3} = \frac{\mathrm{n}_1}{3M_3} Int_{131} + \frac{\mathrm{n}_2 D_{31}}{3M_3 D_{23}} Int_{231} \, . \tag{5.25}$$

Similar equations for D_{12} and D_{23} can be obtained by assuming that the stationary velocities of two other components are equal. This leads to three independent equations with 3 unknowns D_{31}, D_{12} and D_{23}. The solution of these equations is given by

$$D_{ij} = \frac{n_i n_j M(Int_{iki} Int_{kjk} Int_{jij} + Int_{jki} Int_{ijk} Int_{kij})}{3n_i M_i Int_{iki} Int_{kjk} + 3n_j M_j Int_{jki} Int_{kij} - 3n_k M_k Int_{kjk} Int_{kij}}, \quad (5.26)$$

in which $M = M_i x_i + M_j x_j + M_k x_k$. Since $Int_{ijk}(i \neq j \neq k \neq i) = 0$, equation 5.26 simplifies to

$$D_{ij} = \frac{n_j M}{3M_i} Int_{jij}. \quad (5.27)$$

Simulations

To compare the NEMD method with the Green-Kubo method, simulations of a Lennard-Jones fluid were performed. The pair potential $U^{LJ}(r)$ of this model system is the truncated and shifted Lennard-Jones potential

$$U^{LJ}(r) = 4\varepsilon\left[\left(\frac{\sigma}{r}\right)^{12} - \left(\frac{\sigma}{r}\right)^{6}\right] \quad (5.28)$$

in which r is the particle-particle distance, ε the Lennard-Jones energy parameter and σ the Lennard-Jones size parameter. Using reduced units the reduced pair potential $U^{LJ*} \equiv U^{LJ}/\varepsilon$ is a dimensionless function of the reduced distance $r^* \equiv r/\sigma$. Other reduced quantities are the reduced time $t^* \equiv (t/\sigma)\cdot(\varepsilon/m)^{1/2}$, the reduced density $\rho^* \equiv \rho\cdot\sigma^3$, and the reduced temperature $T^* \equiv T\cdot k_B/\varepsilon$, in which m is the mass of the atoms in the system. In all simulations we will use reduced quantities and we, therefore, omit the superscripts *.

Systems of 250 and 300 particles with mass $m = 1$ were used in the simulations. Periodic boundary conditions were applied with a cut-off radius of the potential $R_{cut} = 2.5$ and a timestep $\Delta t = 0.001$. Starting with lattice configurations and random velocities, the total momenta of the systems were set to zero and the systems were equilibrated for 25 000 timesteps at $T = 0.728$ and $\rho = 0.8442$. During equilibration the temperature of the systems was scaled to the desired temperature after each timestep. The resulting velocities and

coordinates were used as a starting point for further work. Unless stated otherwise, the Berendsen thermostat was used with τ_T = 0.4 [12]. The coupling time constant for the temperature τ_T was determined by calculating the fluctuations in the kinetic, potential and total energy in molecular dynamics runs of 5000 timesteps.

Self-diffusion coefficients

MD simulations of multiples of 1000 timesteps (Δt = 0.001) were performed in both systems. Every 1000 timesteps a new starting value t = 0 was chosen and the velocity autocorrelation function vacf(t) $\equiv \langle \mathbf{v}(0) \cdot \mathbf{v}(t) \rangle$ was calculated. We denote such a row of vacf data as a set. Using equation 5.18, the self-diffusion coefficient D_{self} was determined by averaging over multiple vacf sets and integrating over (maximal) 1000 timesteps. For adequate integration times and a large number of vacf sets the self-diffusion coefficients became constant, as shown in figures 5.1 and 5.2. The accuracy of the self-diffusion coefficients was estimated by grouping the simulation data of 495 vacf sets into 5 blocks. From the standard deviation of the block averages the error in the diffusion coefficient was calculated [10]. Results are $D_{self,\ 250\ LJ} = 0.0315 \pm 0.0005$ and $D_{self,\ 300\ LJ} = 0.0327 \pm 0.0006$.

Maxwell-Stefan diffusion coefficients: Green-Kubo method

Each system was divided into two species or components by attaching a colour label to a mole fraction x_{colour} of the particles. So, the two species differ only by the colour label, which plays no role in the dynamics. The MS diffusion coefficients of the coloured systems were calculated as a function of the mole fraction coloured component. MD simulations of multiples of 5000 timesteps (Δt = 0.001) were performed for the systems of 250 and 300 LJ particles. Every 5 timesteps a new time origin was taken, resulting in 800 time origins per run of 5000 timesteps. During the simulation the multiple particle autocorrelation function $\sum \mathbf{v}_1^i(0) \bullet \sum \mathbf{v}_1^j(t)$ was calculated for 10 different values of the mole fraction coloured component x_1 simultaneously. The Maxwell-Stefan diffusion coefficients were determined by using equation 5.15 for several numbers of time origins and for various integration times. For a number of time origins more than 60 000, the MS diffusion coefficients became constant and

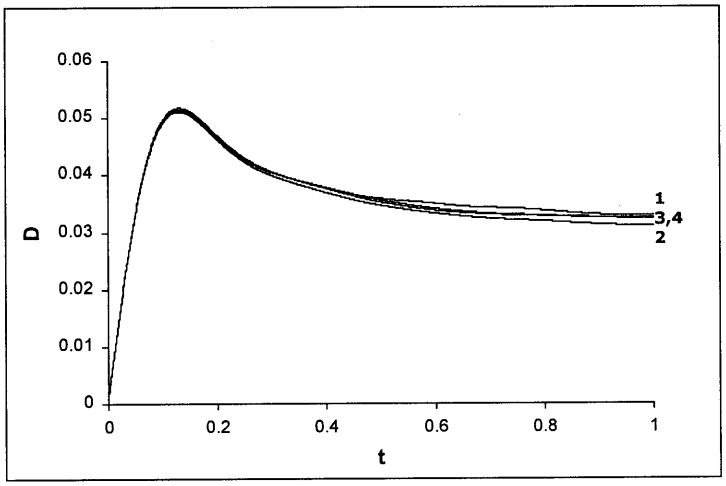

Figure 5.1. *Self-diffusion coefficient as a function of the integration time t:* 1, *99 vacf sets of 250 LJ particles;* 2, *495 vacf sets of 250 LJ particles;* 3, *99 vacf sets of 300 LJ particles; and* 4, *495 vacf sets of 300 LJ particles.*

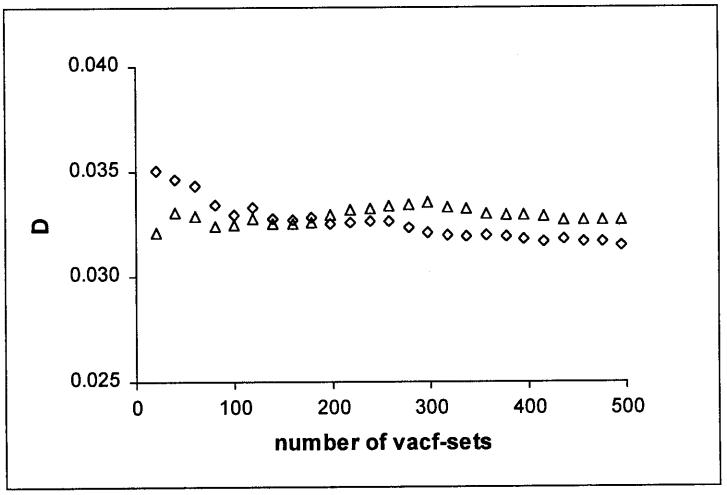

Figure 5.2. *Self-diffusion coefficient as a function of the number of averaging vacf sets:* Δ, *300 LJ particles; and* ◊, *250 LJ particles.*

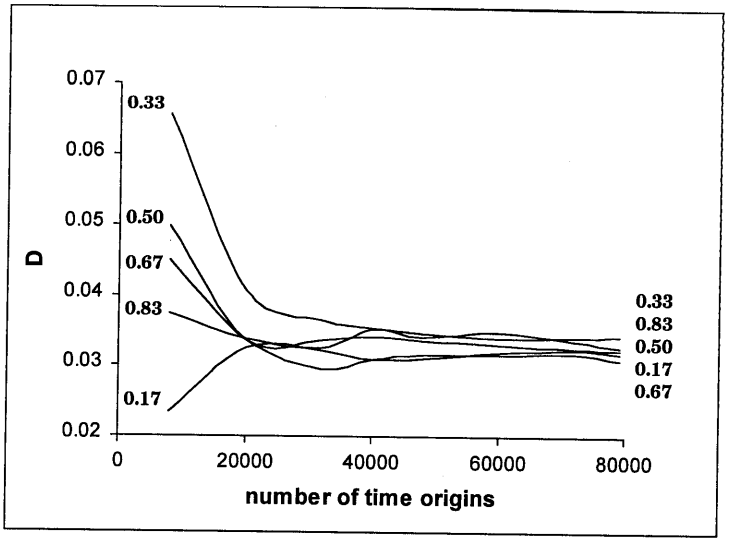

Figure 5.3. *Maxwell-Stefan diffusion coefficient as a function of the number of time origins for various mole fractions coloured component (300 LJ particles, $T = 0.728$, $\rho = 0.8442$).*

independent of the mole fraction coloured component, as shown in figure 5.3. Important to note is that for this system equation 5.15 is not the most efficient way of computing the diffusion coefficient (which is equation 5.18). However, here we are interested in comparing the NEMD method with EMD and for the more general case (for example, different masses) equation 5.15 must be used. The accuracy of the MS diffusion coefficients was estimated from the standard deviation of the averages of at least 5 consecutive simulations of 79 200 time origins, and an integration time $t = 1$. Calculations of the 250 and 300 particles systems did not differ significantly. The results of the 250 particles system are listed in table 5.1, and the differences between the values of the MS diffusion coefficients at various mole fractions are a measure for the accuracy of equation 5.15.

x_{colour}	D_{MS}
0.08	0.0329 ± 0.0006
0.16	0.0338 ± 0.0007
0.24	0.0349 ± 0.0007
0.32	0.0340 ± 0.0007
0.40	0.0350 ± 0.0009
0.48	0.0340 ± 0.0004
0.56	0.0346 ± 0.0009
0.64	0.034 ± 0.001
0.72	0.036 ± 0.002
0.80	0.035 ± 0.001

Table 5.1. *Maxwell-Stefan diffusion coefficient, calculated with equation 5.15 as a function of the mole fraction coloured component for an LJ fluid of 250 particles: $T = 0.728$, $\rho = 0.8442$.*

Maxwell-Stefan diffusion coefficients: NEMD method

NEMD simulations were performed in the 250 particles system at $x_{colour} = x_1 = 0.5$ and in the 300 particles system at $x_{colour} = x_1 = 0.417$. Constant accelerations $\mathbf{a}_1$ and $\mathbf{a}_2$, corresponding to equation 5.5, were applied to the particles of component 1 and component 2 during 1000 timesteps ($\Delta t = 0.001$). Starting from the same initial configuration, also an unperturbed simulation of 1000 timesteps was performed ($\mathbf{a}_1 = \mathbf{a}_2 = \mathbf{0}$). The average velocities of the component 1 and component 2 as functions of time were calculated by subtracting the perturbed and the unperturbed velocities [9, 13]. Subsequent simulations were started from the end configuration of the unperturbed simulation. Figure 5.4 shows an example of the calculated average velocities as functions of the simulation time. From $t = 0.2$ the velocities of the perturbed and unperturbed simulations started to be uncorrelated due to the Lyapunov instability [9], and resulting in strong fluctuations from $t = 0.8$. The calculation of the stationary velocity differences between component 1 and component 2 by averaging over $t = 0.4$ to $t = 0.8$ resulted in the smallest standard deviation. Figure 5.5 illustrates that the accuracy, estimated from the fluctuations in the velocity differences, was dependent on the number of starting configurations. The diffusion coefficients were calculated using the equation

$$D = T\frac{\mathbf{u}_1(\infty) - \mathbf{u}_2(\infty)}{\mathbf{a}_1 - \mathbf{a}_2}, \tag{5.29}$$

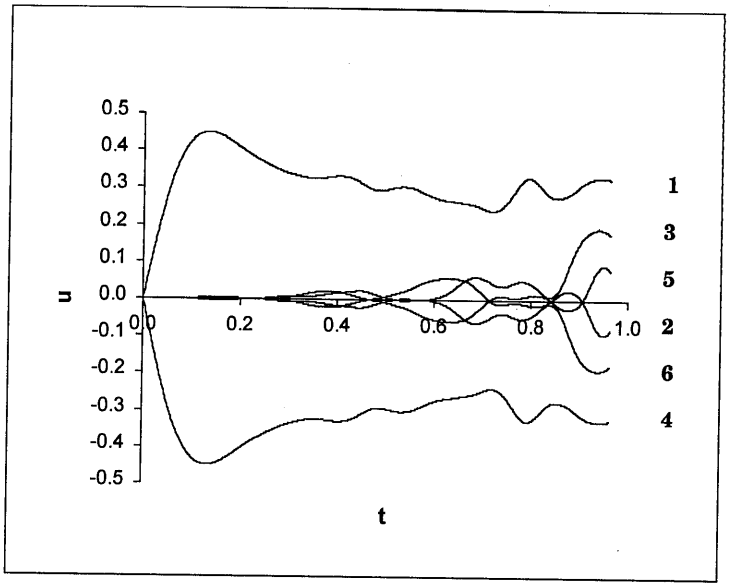

Figure 5.4. *Average velocities of the component 1 and component 2 as functions of the simulation time (250 LJ particles, $T = 0.728$, $\rho = 0.8442$, $x_1 = 0.5$, $\mathbf{a}_1 = 0.05$, 99 starting configurations):* 1, u_x *component 1;* 2, u_y *component 1;* 3, u_z *component 1;* 4, u_x *component 2;* 5, u_y *component 2; and* 6, u_z *component 2.*

which can be derived from equations 5.8 and 5.9 for $t \rightarrow \infty$. Results of the 250 LJ particles system did not differ significantly from the 300 particles system and are listed in table 5.2, which shows that the velocity differences $(\mathbf{u}_1(\infty) - \mathbf{u}_2(\infty))$, and consequently the diffusion coefficients, were independent on the acceleration $\mathbf{a}_1$. Calculation of the diffusion coefficient from the slope of $(\mathbf{u}_1(\infty) - \mathbf{u}_2(\infty))$ or $\mathbf{u}_1(\infty)$ versus $\mathbf{a}_1$ may increase the accuracy. Because the response of the velocity differences on the perturbation was non-exponential (figures 5.4 and 5.5), the method of calculating the diffusion coefficients from the short-time response (equation 5.9) could not be used. This is an important result of these simulations. The assumption by Berendsen, that the velocity difference responds with a first-order process [5], is not correct for dense fluids in general. So, in dense systems, the application of the NEMD method is restricted to the long-term response only, and one of the main advantages of this method, namely

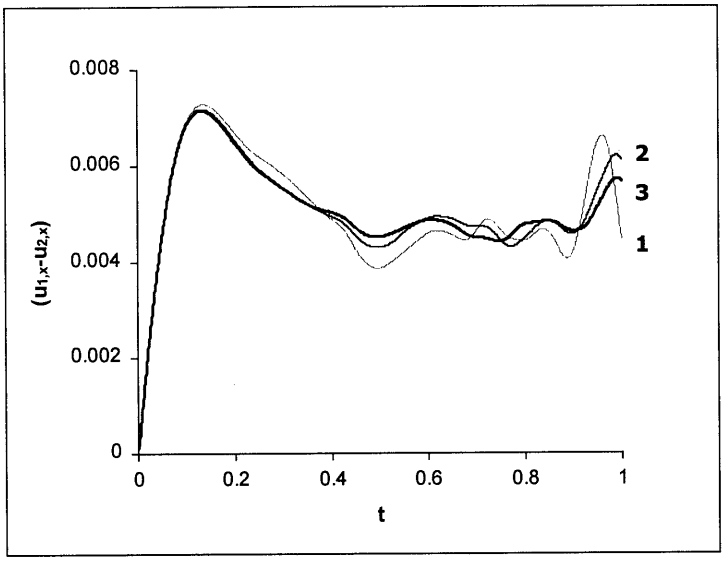

Figure 5.5. *Velocity differences between component 1 and component 2 as functions of the simulation time (250 LJ particles, T = 0.728, ρ = 0.8442, x_1 = 0.5, $\mathbf{a}_1$ = 0.05):* 1, *99 starting configurations;* 2, *297 starting configurations; and* 3, *495 starting configurations.*

Table 5.2. *Diffusion coefficient calculated from the stationary response in NEMD for LJ fluid of 250 particles: T = 0.728, ρ = 0.8442, x_1 = 0.5.*

	$\mathbf{u}_1(\infty) - \mathbf{u}_2(\infty)$		D_{MS}	
$\mathbf{a}_1$	99 starting configs	495 starting configs	99 starting configs	495 starting configs
0.01	0.00093 ± 0.00007	0.00003	0.034 ± 0.002	0.001
0.02	0.00186 ± 0.00013	0.00007	0.034 ± 0.002	0.001
0.03	0.0028 ± 0.0002	0.0001	0.034 ± 0.002	0.001
0.04	0.0037 ± 0.0003	0.0001	0.034 ± 0.002	0.001
0.05	0.0047 ± 0.0003	0.0002	0.034 ± 0.002	0.001
0.1	0.0096 ± 0.0006		0.035 ± 0.002	
0.2	0.019 ± 0.001		0.035 ± 0.002	
0.3	0.029 ± 0.002		0.035 ± 0.002	
0.4	0.038 ± 0.003		0.035 ± 0.003	
0.5	0.048 ± 0.004		0.035 ± 0.003	

the speed of the determination of the diffusion coefficients by using the short-term response, has disappeared.

The NEMD response was also tested in the 250 particles system with $x_{colour} = 0.5$ at $T = 1.5$ for various densities. Figure 5.6 shows that the short-time response of the velocity differences was dependent on the density of the system. So, diffusion coefficients of the systems at $T = 1.5$ were calculated from the stationary velocities by averaging over $t = 0.4$ to $t = 0.8$ (if $\rho = 0.5, 0.8$) or over $t = 1.1$ to $t = 1.5$ (if $\rho = 0.2$) and over 99 starting configurations. The accuracy depended on the density of the system and the averaging time interval, which is illustrated in figure 5.6. For low densities of the system the diffusion coefficient is higher and the time needed to attain stationary velocities increases (τ_D, defined in equation 5.8). For long simulation times, however, the fluctuations in the velocity differences become stronger due to the Lyapunov instability, and the accuracy of the determination of the stationary velocity differences decreases. The calculation of the self-diffusion coefficients (equation 5.18) of the 250 particles systems at $T = 1.5$ needed a longer integration time at lower densities (see later in figure 5.8), as expected because the velocity relaxation time $\tau_{relax} = D/T$ [8]. The integration time, needed in the calculation of the MS diffusion coefficients (equation 5.15) by the Green-Kubo method also was increased to (maximal) $t = 5$ for these systems. The results, listed in table 5.3, show that the NEMD diffusion coefficients deviated more from the self-diffusion coefficients and were less accurate, compared with the Green-Kubo values.

Comparison of the NEMD method with the Green-Kubo method for binary systems

The MS diffusion coefficients, determined by the Green-Kubo method, are more accurate than the NEMD coefficients and deviate less with the self-diffusion coefficients. Due to the strong fluctuations in the velocity differences of the NEMD method, several magnitudes of the disturbance $\mathbf{a}_i$ and many starting configurations were necessary to achieve a fair accuracy, and the CPU time increased strongly. Moreover, the choice of the time interval of averaging of the velocity differences strongly influenced the accuracy of the method (figure 5.6). The Green-Kubo method allows us to check the consistency of the simulation by calculating the diffusion coefficients as a function of the

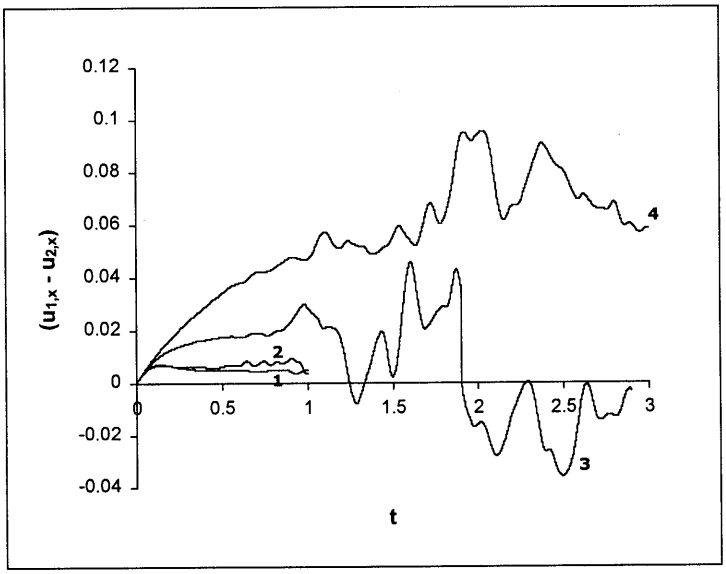

Figure 5.6. *Long-term response of the velocity differences between component 1 and component 2 as a function of the simulation time t (250 LJ particles, $x_1 = 0.5$, 99 starting configurations):* 1, $T = 0.728$, $\rho = 0.8442$; 2, $T = 1.5$, $\rho = 0.8$; 3, $T = 1.5$, $\rho = 0.5$; *and* 4, $T = 1.5$, $\rho = 0.2$.

Table 5.3. *Diffusion coefficients of an LJ Fluid: D_{self} is computed with equation 5.18, $D_{MS\text{-}NEMD}$ with equation 5.29, and $D_{MS\text{-}Green\text{-}Kubo}$ with equation 5.15.*

LJ part.	T	ρ	D_{self}	$D_{MS\text{-}NEMD}$	$D_{MS\text{-}Green\text{-}Kubo}$
300	0.728	0.844	0.0327 ± 0.0006	0.035 ± 0.003	0.0346 ± 0.0010
250	0.728	0.844	0.0315 ± 0.0005	0.034 ± 0.002	0.0340 ± 0.0004
250	1.5	0.8	0.106 ± 0.002	0.10 ± 0.01	0.102 ± 0.007
250	1.5	0.5	0.327 ± 0.004	0.27 ± 0.01	0.33 ± 0.01
250	1.5	0.2	1.029 ± 0.008	0.79 ± 0.04	1.03 ± 0.07

number of time origins (figure 5.3) and as a function of the integration time t (figure 5.7). To achieve the same accuracy in the diffusion coefficients, the number of timesteps needed in the Green-Kubo method could be less than in the NEMD method. An additional

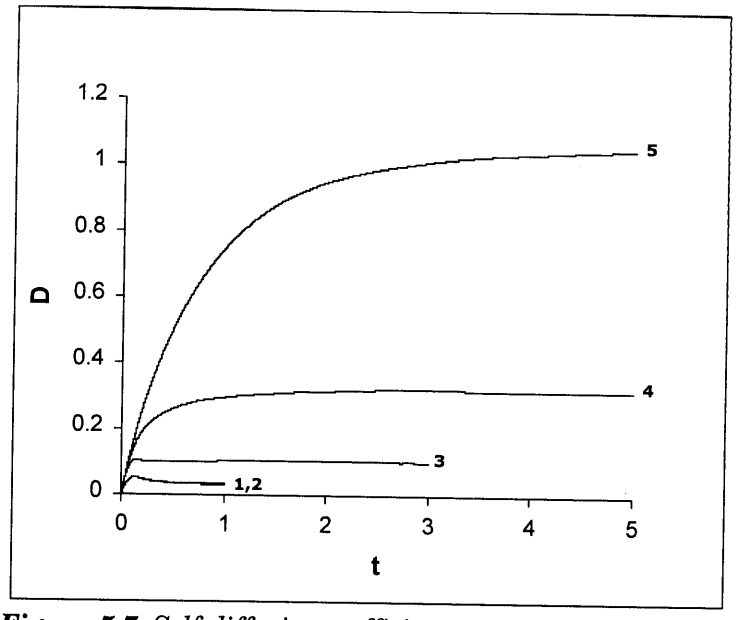

Figure 5.7. *Self-diffusion coefficient as a function of the integration time t:* 1, *300 LJ particles, T = 0.728, ρ = 0.8442;* 2, *250 LJ particles, T = 0.728, ρ = 0.8442;* 3, *250 LJ particles, T = 1.5, ρ = 0.8;* 4, *250 LJ particles, T = 1.5, ρ = 0.5; and* 5, *250 LJ particles, T = 1.5, ρ = 0.2.*

disadvantage of NEMD methods in general is the necessity of a completely new simulation for different transport properties. Therefore, the Green-Kubo method may be preferred for the simulation of diffusion in binary systems. This conclusion corresponds with the results of the MD simulations of the shear viscosity by Schoen and Hoheisel [14]. Since for the simulation in ternary systems, the velocity differences of the NEMD method were expected to be even more fluctuating, only the Green-Kubo method was tested in ternary systems.

Ternary systems

Simulations were performed for the system of 250 LJ particles at T = 0.728 and ρ = 0.8442 in the NVE ensemble. The system was divided into three species or components by attaching a colour label to the particles. Every 10 timesteps (Δt = 0.001) a new time origin was

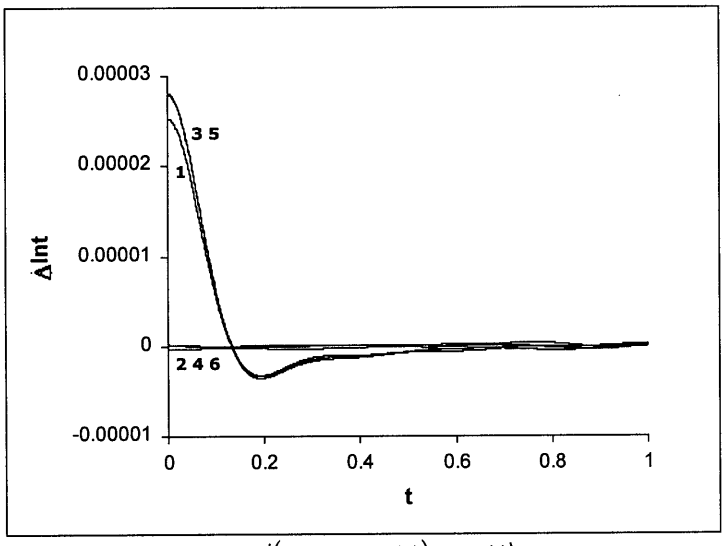

Figure 5.8. $\Delta Int_{ijk} = \left\langle \left(\mathbf{u}_i(0) - \mathbf{u}_j(0)\right) \bullet \mathbf{u}_k(t) \right\rangle$ *as a function of the integration time t (250 LJ particles, T = 0.728, ρ = 0.8442, x_1 = 0.36, x_2 = 0.32):* 1, ΔInt_{131}; 2, ΔInt_{231}; 3, ΔInt_{323}; 4, ΔInt_{321}; 5, ΔInt_{212}; *and* 6, ΔInt_{312}.

taken. The MS diffusion coefficients D_{ij} were calculated, using equations 5.26 and 5.27. The accuracy of the MS diffusion coefficients was estimated from the standard deviation of the averages of 5 consecutive simulations of 250 000 timesteps. Results are shown in table 5.4 and figures 5.8 and 5.9. Figure 5.8 shows that the $\Delta Int_{ijk}(i \neq j \neq k \neq i)$ were oscillating around zero, as expected. The amplitude of the oscillations decreased with increasing number of time origins. So, the $\Delta Int_{ijk}(i \neq j \neq k \neq i)$ can be used as a test of the consistency of the simulations. The values of the ternary diffusion coefficients agreed well with the self-diffusion coefficient. Equation 5.27 is exact and provided better results due to the neglect of the oscillating integrals $Int_{ijk}(i \neq j \neq k \neq i)$ (table 5.4 and figure 5.9). For low mole fractions of components i and j the diffusion coefficients were less accurate. More accurate results may be obtained by enlarging the ternary system size, the integration time of the velocity correlation functions or the number of time origins, c.q. the duration of the MD runs.

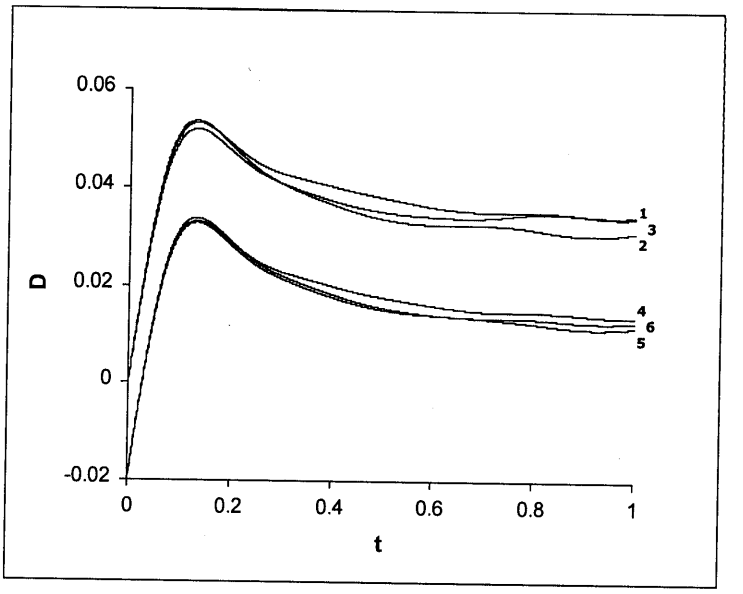

***Figure 5.9**. Ternary Maxwell-Stefan diffusion coefficients as a function of the integration time t (250 LJ particles, $T = 0.728$, $\rho = 0.8442$, $x_1 = 0.36$, $x_2 = 0.32$). For clarity, we have shifted the diffusion coefficients calculated by equation 5.27:* 1, D_{12}, *equation 5.26;* 2, D_{31}, *equation 5.26;* 3, D_{23}, *equation 5.26;* 4, $(D_{12} - 0.02)$, *equation 5.27;* 5, $(D_{31} - 0.02)$, *equation 5.27; and* 6, $(D_{23} - 0.02)$, *equation 5.27.*

Conclusion

Maxwell-Stefan diffusion coefficients in binary liquid systems can be determined by the Green-Kubo method as well as the NEMD method. In the NEMD method, the system is driven away from equilibrium by imposing an external force. If the system responds with a first-order process, the diffusion coefficients can be calculated from the short-term response ($t \rightarrow 0$). However, simulations with dense Lennard-Jones fluids showed that the response was not exponential. A non-exponential response was observed also for simulations with liquid methanol and liquid water. Since, in general, dense fluids do not respond with a first-order process to an external perturbation, the NEMD method, using the short-term response,

Table 5.4. *Ternary diffusion coefficients as a function of the mole fraction coloured component for an LJ fluid of 250 particles: $T = 0.728$, $\rho = 0.8442$.*

x_1	x_2		$D_{\text{MS, eq 5.26}}$	$D_{\text{MS, eq 5.27}}$
0.10	0.10	D_{12}	0.025 ± 0.021	0.033 ± 0.001
		D_{31}	0.033 ± 0.002	0.0324 ± 0.0009
		D_{23}	0.035 ± 0.002	0.035 ± 0.002
0.10	0.45	D_{12}	0.032 ± 0.006	0.032 ± 0.003
		D_{31}	0.035 ± 0.004	0.0326 ± 0.0007
		D_{23}	0.033 ± 0.001	0.033 ± 0.001
0.36	0.32	D_{12}	0.034 ± 0.001	0.0339 ± 0.0005
		D_{31}	0.031 ± 0.001	0.032 ± 0.001
		D_{23}	0.034 ± 0.004	0.033 ± 0.002
0.45	0.10	D_{12}	0.029 ± 0.003	0.034 ± 0.002
		D_{31}	0.031 ± 0.002	0.031 ± 0.002
		D_{23}	0.033 ± 0.005	0.033 ± 0.001
0.45	0.45	D_{12}	0.033 ± 0.002	0.032 ± 0.002
		D_{31}	0.035 ± 0.004	0.033 ± 0.002
		D_{23}	0.039 ± 0.008	0.034 ± 0.002
0.80	0.10	D_{12}	0.030 ± 0.002	0.031 ± 0.002
		D_{31}	0.032 ± 0.002	0.032 ± 0.002
		D_{23}	0.107 ± 0.052	0.036 ± 0.001

cannot be applied. Diffusion coefficients can be determined only from the long-term response after a steady state has been reached, and long simulations have to be performed. Using the long-term response, the NEMD method was even more time consuming than the Green-Kubo method, in which the diffusion coefficients are determined from the fluctuating quantities in the equilibrium system. Moreover, the diffusion coefficients, calculated by the Green-Kubo method, were more accurate than the NEMD coefficients, calculated from the steady state. Therefore, EMD (Green-Kubo) is preferred for the calculation of the Maxwell-Stefan diffusion coefficients.

In the ternary system the Maxwell-Stefan diffusion coefficients, calculated by equations 5.26 and 5.27, agreed well with the self-diffusion coefficient, calculated by equation 5.18. For low mole fractions of the coloured components i and j the diffusion coefficients were less accurate.

References

[1] Rutten, Ph. W. M., 1992, Ph. D. thesis, Delft University of Technology.

[2] Wakeham, W. A., Nagashima, A., and Sengers, J. V., 1991, *Measurement of the Transport Properties of Fluids, Experimental Thermodynamics Volume III* (Oxford: Blackwell) Chap. 9.

[3] Van de Ven – Lucassen, I. M. J. J., Kemmere, M. F., and Kerkhof, P. J. A. M., 1997, *J. Solution Chem.*, **26**, 1145. Chapter 4 in this thesis.

[4] Schoen, M., and Hoheisel, C., 1984, *Molec. Phys.*, **52**, 33.

[5] Berendsen, H. J. C., 1991, *Computer Simulation in Material Science* (Dordrecht: Kluwer) p. 139.

[6] Krishna, R., and Wesselingh, J. A., 1997, *Chem. Eng. Sci.*, **52**, 861.

[7] Taylor, R., and Krishna, R., 1993, *Multicomponent Mass Transfer* (New York: Wiley).

[8] Chandler, D., 1987, *Introduction to Modern Statistical Mechanics* (Oxford University Press) Chap. 8.

[9] Evans, D. J., and Morriss, G. P., 1990, *Statistical Mechanics of Non-Equilibrium Fluids* (San Diego: Academic Press) p. 192.

[10] Frenkel, D. and Smit, B., 1996, *Understanding Molecular Simulation* (San Diego: Academic Press) App. D; App. A.

[11] Hansen, J. P., and McDonald, I. R., 1986, *Theory of Simple Liquids*, 2nd Edn. (London: Academic Press) Chap. 8.

[12] Berendsen, H. J. C., Postma, J. P. M., Van Gunsteren, W. F., Dinola, A., and Haak, J. R., 1984, *J. Chem. Phys.*, **81**, 3684.

[13] Ciccotti, G., Jacucci, G., and McDonald, I. R., 1979, *J. Statist. Phys.*, **21**, 1

[14] Schoen, M., and Hoheisel, C., 1985, *Molec. Phys.*, **56**, 653.

6. MOLECULAR DYNAMICS SIMULATION OF THE MAXWELL-STEFAN DIFFUSION COEFFICIENTS IN LENNARD-JONES LIQUID MIXTURES

Abstract*

Maxwell-Stefan (MS) diffusion coefficients in multicomponent liquids have been determined by the equilibrium molecular dynamics calculation of the appropriate Green-Kubo equation. Simulations were performed for systems of 300 LJ particles at various compositions. The unary system was divided into three components by attaching a colour label to the particles, which plays no role in the dynamics. The binary system argon + krypton was divided into three species by attaching a colour label to the particles of argon. The ternary system consisted of argon, krypton and neon. The results of the calculation of the MS diffusion coefficients in the unary and binary systems agreed well with the literature values. The MS diffusion coefficients of the unary system did not differ significantly from the self-diffusion coefficient. The MS diffusion coefficients of the ternary system behaved as expected from other physical properties.

---

* The main part of this chapter has been accepted for publication: Van de Ven – Lucassen, I. M. J. J., Otten, A. M. V. J., Vlugt, T. J. H., and Kerkhof, P. J. A. M., 1999, *Molecular Simulation*.

Introduction

Multicomponent diffusion in liquid systems plays an important role in chemical engineering and knowledge of diffusion coefficients is required, for example, for the design of process equipment. However, it is very time consuming and difficult to measure diffusion coefficients in multicomponent systems [1, 2]. Simulation techniques like molecular dynamics provide an attractive alternative to determine the diffusion coefficients.

For the calculation of the diffusion coefficients in a binary or ternary mixture of Lennard-Jones particles equilibrium molecular dynamics methods have been developed, in which the correlation function of fluctuating quantities is determined [3-6]. The integrals of the correlation functions are related to the diffusion coefficients through the Green-Kubo formalism. In ref [6] we have shown that this so-called Green-Kubo method is preferred above a non-equilibrium method, in which the system is driven away from equilibrium and the system response is monitored. The Green-Kubo method was tested by performing simulations in coloured Lennard-Jones mixtures: the particles in the binary and ternary system had identical LJ potential parameters and differed only by a colour label, which plays no role in the dynamics [6]. The purpose of the work presented here is to use the Green-Kubo method by performing simulations in binary and ternary Lennard-Jones mixtures, in which the particles have different LJ potential parameters and different masses.

Theory

Molecular diffusion in multicomponent systems can be described by the Maxwell-Stefan approach. When temperature T and pressure p are constant, and when there are no external forces acting on the system, the molar fluxes $\mathbf{N}_i$, $\mathbf{N}_j$ of components i, j due to the gradient in the chemical potential μ_i of component i are given by

$$\sum_{\substack{j=1 \\ j\neq i}}^{n} \frac{x_i \mathbf{N}_j - x_j \mathbf{N}_i}{C_t D_{ij}} = \frac{x_i}{RT} \nabla_{T,p} \mu_i , \tag{6.1}$$

in which R is the gas constant, x_i the mole fraction of component i and C_t the total molar concentration. D_{ij} is the Maxwell-Stefan diffusion coefficient between components i and j. Because $D_{ij} = D_{ji}$, there are n(n-1)/2 independent Maxwell-Stefan diffusion coefficients. An extensive description of the Maxwell-Stefan approach is given in [7].

Maxwell-Stefan diffusion coefficients can be calculated using an equilibrium molecular dynamics (EMD) method based on the Green-Kubo formalism. This Green-Kubo method uses the time correlation functions of fluctuating quantities in an equilibrium system; these time correlation functions are linked to the response to weak perturbations in the equilibrium system by linear response theory [8-10]. The Maxwell-Stefan diffusion coefficient D_{12} of a binary system is then given by

$$D_{12} = \frac{x_2}{3n_1} \left(\frac{M_1 x_1 + M_2 x_2}{M_2 x_2} \right)^2 \int_0^\infty \left\langle \sum_{i=1}^{n_1} \mathbf{v}_1^i(0) \bullet \sum_{j=1}^{n_1} \mathbf{v}_1^j(t) \right\rangle dt , \tag{6.2}$$

in which t is the simulation time, M_i is the molar mass of component i, n_1 the number of particles of component 1, and $\mathbf{v}_1^i$ the velocity of particle i of component 1.

Calculation of the self-diffusion coefficient D_i of component i can be performed simultaneously, using

$$D_i = \frac{1}{3}\int_0^\infty \langle \mathbf{v}_i(0) \bullet \mathbf{v}_i(t) \rangle dt \,. \tag{6.3}$$

The derivation of equations 6.2 and 6.3 has been given in [6].

Calculating ternary diffusion coefficients

Diffusion in a ternary system can be described by the independent Maxwell-Stefan diffusion coefficients D_{12}, D_{31} and D_{23}. For the calculation of these ternary diffusion coefficients the following equation has been derived [6]

$$D_{ij} = \frac{n_i n_j M(Int_{iki} Int_{kjk} Int_{jij} + Int_{jki} Int_{ijk} Int_{kij})}{3n_i M_i Int_{iki} Int_{kjk} + 3n_j M_j Int_{jki} Int_{kij} - 3n_k M_k Int_{kjk} Int_{kij}}, \tag{6.4}$$

in which $M = M_i x_i + M_j x_j + M_k x_k$ and Int_{ijk} has been defined by

$$Int_{ijk} = \int_0^\infty \langle (\mathbf{u}_i(0) - \mathbf{u}_j(0)) \bullet \mathbf{u}_k(t) \rangle dt \,, \tag{6.5}$$

with $\mathbf{u}_i$ is the velocity of component i.
Since $Int_{ijk}(i \neq j \neq k \neq i) = 0$, equation 6.4 simplifies to

$$D_{ij} = \frac{n_j M}{3M_i} Int_{jij} \,. \tag{6.6}$$

Simulations

To investigate the Green-Kubo method, simulations of a Lennard-Jones fluid were performed. We used the truncated and shifted potential

$$U^{tr-sh}(r) = \begin{cases} U^{LJ}(r) - U^{LJ}(R_{cut}) & r \leq R_{cut} \\ 0 & r > R_{cut} \end{cases} . \tag{6.7}$$

$U^{LJ}(r)$ is the Lennard-Jones potential

$$U^{LJ}(r) = 4\varepsilon\left[\left(\frac{\sigma}{r}\right)^{12} - \left(\frac{\sigma}{r}\right)^{6}\right], \tag{6.8}$$

in which r is the particle-particle distance, ε the Lennard-Jones energy parameter and σ the Lennard-Jones size parameter. The cross interaction parameters were obtained from the Lorentz-Berthelot rules $\varepsilon_{12} = (\varepsilon_{11}\cdot\varepsilon_{22})^{1/2}$ and $\sigma_{12} = (\sigma_{11} + \sigma_{22})/2$. Using reduced units the reduced pair potential $U^{LJ*} \equiv U^{LJ}/\varepsilon$ is a dimensionless function of the reduced distance $r^* \equiv r/\sigma$. Other reduced quantities are the reduced time $t^* \equiv (t/\sigma)\cdot(\varepsilon/m)^{1/2}$, the reduced density $\rho^* \equiv \rho\cdot\sigma^3$, the reduced pressure $p^* \equiv p\cdot\sigma^3/\varepsilon$, and the reduced temperature $T^* \equiv T\cdot k_B/\varepsilon$, in which m is the mass of the atoms in the system, and k_B is Boltzmann's constant. In all simulations we will use reduced quantities and we, therefore, omit the superscripts *.

Systems of 300 particles were used in the simulations. Periodic boundary conditions were applied with a cut-off radius of the potential R_{cut} = 2.5 and a timestep Δt = 0.001. Starting with lattice configurations and random velocities, the total momenta of the systems were set to zero, and the systems were equilibrated for 25 000 timesteps at the desired temperature and density. During equilibration the temperature of the systems was scaled to the desired temperature after each timestep. The resulting velocities and coordinates were used as a starting point for further simulations.

Simulations in a unary Lennard-Jones system

Simulations were performed on a system of 300 identical Lennard-Jones particles at T = 0.728 and ρ = 0.8442 in the NVE-ensemble. The system was divided into three species or components by attaching a colour label to a mole fraction x_i of the particles. So, the three species differ only by the colour label, which plays no role in the dynamics. MD simulations of multiples of 25 000 timesteps (Δt = 0.001) were performed and every 10 timesteps a new time origin was taken for the calculation of the multiple particle autocorrelation function $\sum \mathbf{v}_1^i(0) \bullet \sum \mathbf{v}_1^j(t)$ of eq 6.2, resulting in 2350 time origins per run of 25 000 time steps.

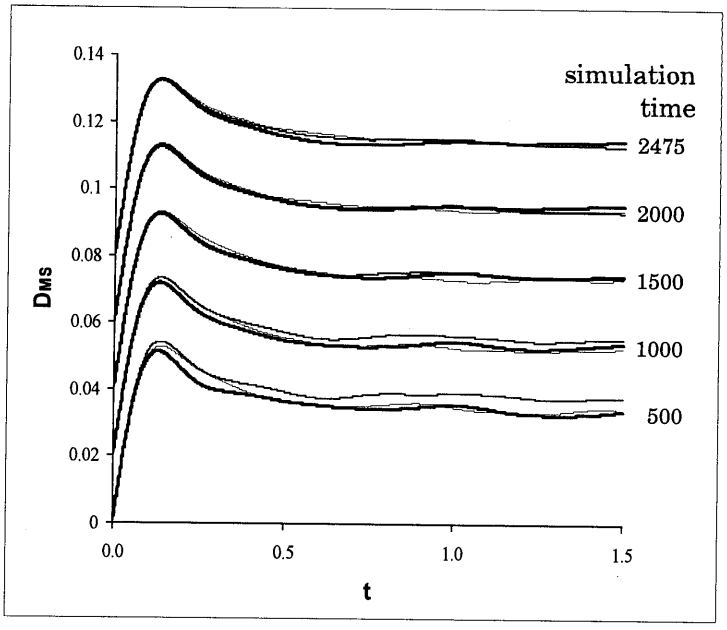

***Figure 6.1**. Maxwell-Stefan diffusion coefficients as a function of the integration time for various simulation times (300 LJ particles, T = 0.728, ρ = 0.884, x_1 = 0.5, x_2 = 0.25, x_3 = 0.25). For clarity, we have shifted the diffusion coefficients with +0.02 subsequently: ——, D_{12}; ——, D_{31}; ——, D_{23}.*

The MS diffusion coefficients were calculated using equation 6.6 for several numbers of time origins and for various integration times (maximal 1500 timesteps). The accuracy of the MS diffusion coefficients in this unary system, as well as in the following binary and ternary systems, was estimated from the standard deviation of the averages of at least 5 consecutive simulations of 250 000 timesteps. The MS diffusion coefficients became constant for integration times > 1.0 (1000 timesteps). This was independent of the simulation time, as illustrated in figure 6.1. For all mole fractions the accuracy of the calculation was not improved significantly, if the simulation time was extended longer than 1250 (figure 6.2).

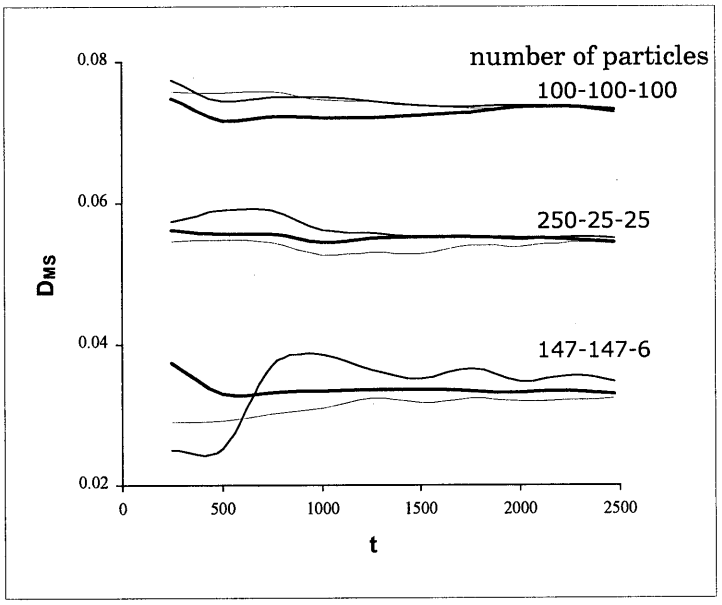

Figure 6.2. *Maxwell-Stefan diffusion coefficients as a function of the simulation time for various numbers of particles (300 LJ particles, T = 0.728, ρ = 0.884, integration time = 1.0). For clarity, we have shifted the diffusion coefficients with +0.02 subsequently:* ——— , D_{12} ; ——— , D_{31} ; ——— , D_{23} .

The consistency of the calculations was also tested using the integrals Int_{ijk} of equation 6.5 [6]. Figure 6.3 shows that the $\Delta Int_{ijk} = \left\langle \left(\mathbf{u}_i(0) - \mathbf{u}_j(0)\right) \bullet \mathbf{u}_k(t) \right\rangle$ (i ≠ j ≠ k ≠ i) were oscillating around zero, as expected. The amplitude of the oscillations decreased with increasing number of time origins (simulation time) and became constant for a simulation time longer than 1250, as illustrated in figure 6.4.

The results of the simulations with a simulation time of 1250 and an integration time of 1.0 are listed in table 6.1. The differences between the values of the MS diffusion coefficients at various mole fractions are a measure for the accuracy of equation 6.6 and of the calculations. The results of the simulations of the 300 particles system agree very well with the simulations of the 250 particles system given by [6], as expected.

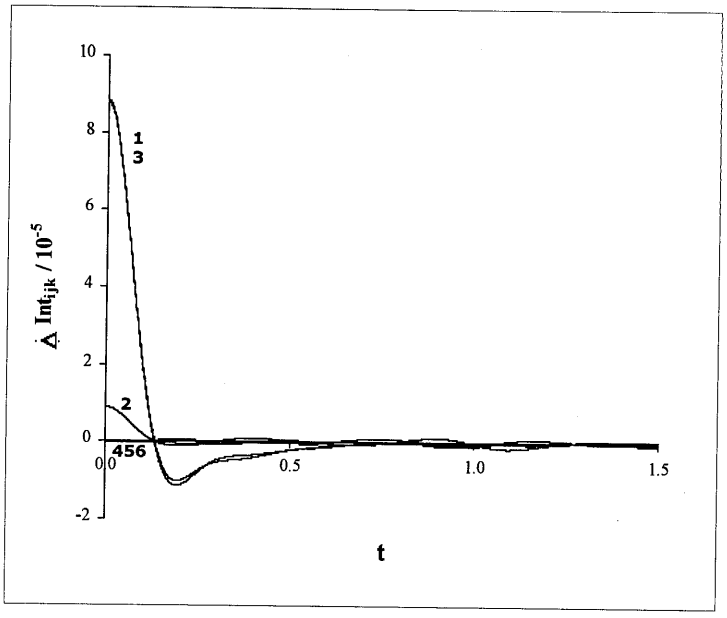

Figure 6.3. $\Delta Int_{ijk} = \left\langle \left(\mathbf{u}_i(0) - \mathbf{u}_j(0)\right) \bullet \mathbf{u}_k(t) \right\rangle$ *as a function of the integration time t (300 LJ particles, T = 0.728, ρ = 0.884, x_1 = 0.5, x_2 = 0.25, x_3 = 0.25, simulation time = 1250):* 1, ΔInt_{212} *;* 2, ΔInt_{131} *;* 3, ΔInt_{323} *;* 4, ΔInt_{231} *;* 5, ΔInt_{321} *; and* 6, ΔInt_{312} *.*

Table 6.1. *Ternary diffusion coefficients as a function of the mole fraction coloured component for a unary LJ fluid of 300 particles: T = 0.728, ρ = 0.884, simulation time = 1250, integration time = 1.0.*

x_1	x_2	x_3	D_{12}	D_{31}	D_{23}
0.067	0.467	0.467	0.034 ± 0.003	0.032 ± 0.001	0.033 ± 0.002
0.250	0.250	0.500	0.032 ± 0.002	0.034 ± 0.001	0.033 ± 0.002
0.250	0.500	0.250	0.031 ± 0.001	0.0348 ± 0.0007	0.034 ± 0.001
0.333	0.333	0.333	0.032 ± 0.001	0.034 ± 0.001	0.034 ± 0.001
0.467	0.067	0.467	0.0308 ± 0.0007	0.033 ± 0.002	0.031 ± 0.003
0.467	0.467	0.067	0.031 ± 0.001	0.033 ± 0.004	0.0325 ± 0.0009
0.490	0.490	0.020	0.034 ± 0.001	0.036 ± 0.007	0.032 ± 0.002
0.500	0.250	0.250	0.031 ± 0.001	0.034 ± 0.001	0.033 ± 0.002
0.833	0.083	0.083	0.035 ± 0.001	0.036 ± 0.002	0.033 ± 0.001
0.933	0.033	0.033	0.033 ± 0.002	0.033 ± 0.001	0.032 ± 0.002
0.980	0.010	0.010	0.031 ± 0.001	0.035 ± 0.002	0.034 ± 0.001

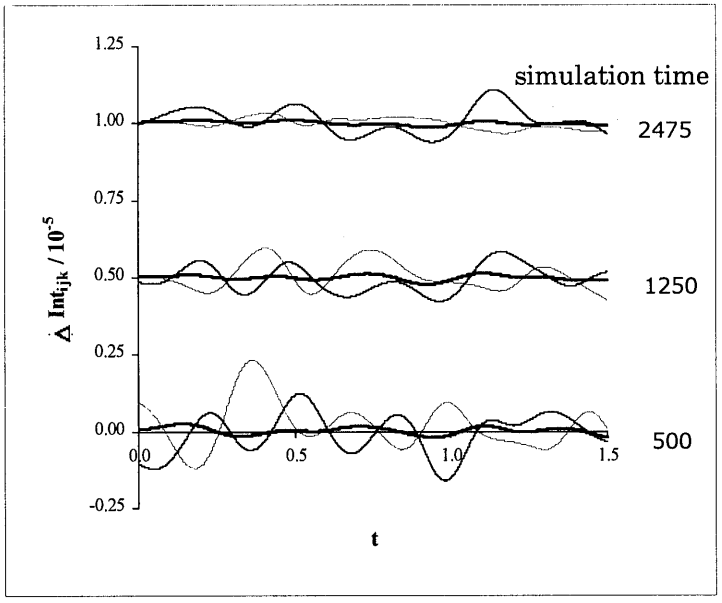

Figure 6.4. $\Delta Int_{ijk} = \left\langle \left(\mathbf{u}_i(0) - \mathbf{u}_j(0)\right) \bullet \mathbf{u}_k(t) \right\rangle$ *as a function of the integration time t for various simulation times (300 LJ particles, T = 0.728, ρ = 0.884, x_1 = 0.5, x_2 = 0.25, x_3 = 0.25). For clarity, we have shifted the ΔInt_{ijk} with +0.5* subsequently): ▬▬, ΔInt_{231}; ——, ΔInt_{321}; *and* ——, ΔInt_{312}.

Naghizadeh and Rice [11] derived a corresponding state relationship for the self-diffusion coefficients of liquid argon, krypton, and xenon:

$$\log D = 0.05 + 0.07p - \frac{1}{T}(1.04 + 0.1p), \tag{6.9}$$

in which p is the reduced pressure, T is the reduced temperature and D is the reduced self-diffusion coefficient. The LJ energy parameter ε = $1.71.10^{-21}$ J and the LJ size parameter σ = $3.418.10^{-10}$ m of argon used by Nagazideh and Rice [11] differed from the parameters used in our study (table 6.2). The reduced temperature T = 0.728 and the reduced pressure p = 0.98 of our simulations were therefore recalculated into T = 0.702 and p = 0.95 for use in equation 6.9. The

self-diffusion coefficient calculated using equation 6.9, D = 0.032, agrees very well with the results of our simulations.

Table 6.2. *Lennard-Jones parameters and molecular mass*

	Substance		
	Ar	Kr	Ne
ε (10^{-21} J)	1.65	2.30	0.19
σ (10^{-10} m)	3.41	3.64	2.75
m (10^{-26} kg)	6.64	13.92	3.36

Simulations in a binary Lennard-Jones system

Simulations were performed for binary systems of 300 LJ particles at T = 0.8 and ρ = 0.7901 in the NVE ensemble. All reduced units are constructed using the parameters of argon atoms. The first component argon with a mole fraction (x_1+x_2) was divided into two species by attaching a colour label to a mole fraction x_1 of the particles. The mole fraction of the second component was x_3. For this second component we used the Lennard-Jones parameters describing krypton. The potential parameters used are given in table 6.2. MD simulations of multiples of 25 000 timesteps (Δt = 0.001) were performed and every 10 timesteps a new time origin was taken. The MS diffusion coefficients were calculated, using equation 6.6 for several numbers of time origins and for various integration times (maximal 1500 timesteps). The MS diffusion coefficients became constant for integration times > 1.0, independent of the simulation time and the mole fractions. The amplitude of the oscillations of ΔInt_{ijk}(i ≠ j ≠ k ≠ i) decreased with an increasing number of time origins and became constant for a simulation time > 1750, if the number of the particles of one component was very low. For higher numbers of the particles a simulation time > 1250 was sufficient.

The results of the simulations with an integration time of 1.0 are listed in table 6.3. The values of the MS diffusion coefficients D_{31} and D_{23} were identical within the simulation error for each system, as expected, since the particles with a mole fraction x_1 and x_2 differed only by colour. Moreover, the MS diffusion coefficients were independent of the mole fraction coloured component for all

Table 6.3. *Ternary diffusion coefficients as a function of the mole fraction for a binary LJ fluid Ar(1,2) + Kr(3) of 300 particles: T = 0.8, ρ = 0.7901, integration time = 1.0.*

sim. time	x_1	x_2	x_3	D_{12}	D_{31}	D_{23}
2475	0.10	0.40	0.50	0.035 ± 0.001	0.0185 ± 0.0003	0.0211 ± 0.0007
2475	0.25	0.25	0.50	0.037 ± 0.002	0.0194 ± 0.0008	0.022 ± 0.001
2475	0.33	0.17	0.50	0.038 ± 0.002	0.0202 ± 0.0008	0.022 ± 0.001
2475	0.49	0.01	0.50	0.038 ± 0.001	0.0212 ± 0.0007	0.018 ± 0.003
1250	0.33	0.33	0.33	0.042 ± 0.003	0.025 ± 0.001	0.030 ± 0.001
1250	0.10	0.40	0.50	0.034 ± 0.004	0.0187 ± 0.0005	0.020 ± 0.001
1250	0.25	0.25	0.50	0.035 ± 0.003	0.0183 ± 0.0008	0.020 ± 0.001
1250	0.33	0.17	0.50	0.036 ± 0.002	0.0195 ± 0.0009	0.0194 ± 0.0008
1250	0.49	0.01	0.50	0.039 ± 0.002	0.020 ± 0.001	0.024 ± 0.007
1250	0.17	0.17	0.67	0.031 ± 0.002	0.0156 ± 0.0008	0.017 ± 0.001

calculations with x_3 = 0.5. The values of the MS diffusion coefficients increased with an increasing mole fraction of argon (x_1+x_2).

For comparison with the literature values the calculated MS diffusion coefficients had to be converted to Fick diffusion coefficients. For a ternary system the Fick diffusivities and the MS diffusivities are related by [7, 12]

$$\left[D^{\mathrm{f}}\right] = [B]^{-1}[\Gamma], \tag{6.10}$$

in which $[D^{\mathrm{f}}]$ is the 2×2 matrix of the Fick diffusivities and $[\Gamma]$ is the 2×2 matrix of the thermodynamic factors. The elements of the 2×2 matrix $[B]$ are equal to

$$B_{\mathrm{ii}} = \frac{x_{\mathrm{i}}}{D_{\mathrm{in}}} + \sum_{\substack{\mathrm{k=1} \\ \mathrm{k\neq i}}}^{\mathrm{n}} \frac{x_{\mathrm{k}}}{D_{\mathrm{ik}}}, \quad \mathrm{i, j = 1,2; n = 3} \tag{6.11}$$

and

$$B_{\mathrm{ij,i\neq j}} = -x_{\mathrm{i}}\left(\frac{1}{D_{\mathrm{ij}}} - \frac{1}{D_{\mathrm{in}}}\right), \quad \mathrm{i, j = 1,2; n = 3,} \tag{6.12}$$

in which D_{ij} are the MS diffusivities. In an ideal mixture the matrix of the thermodynamic factors [Γ] is equal to [I], the identity matrix. For the coloured binary mixture with composition $x_1 = x_2 = 0.25$ and $x_3 = 0.5$ the values of the MS diffusivities were calculated to be $D_{12} = 0.037$ and $D_{31} = D_{23} = 0.020$. The Fick diffusivities $D_{11} = D_{22}$ can then be calculated from equation 6.10, assuming an ideal mixture: $D^f_{11} = D^f_{22} = 0.023$, or in real units $D^{fr}_{11} = D^{fr}_{22} = 1.26.10^{-9}$ m^2.s^{-1} at 99 K. Schoen and Hoheisel [3] computed the following binary diffusion coefficients: $D^{fr}_{12} = 2.78.10^{-9}$ m^2.s^{-1} at 116 K, and $D^{fr}_{12} = 2.05.10^{-9}$ m^2.s^{-1} at 109 K for equimolar mixtures with comparable potential parameters and masses. Assuming an exponential relation $D = A \cdot \exp(-B/T)$ between the diffusion coefficient D and the temperature T [11], the values of Schoen and Hoheisel [3] would result in $D^{fr}_{12} = 1.23.10^{-9}$ m^2.s^{-1} at 99 K. This value is in very good agreement with our simulations. Lee [13] performed MD simulations for an equimolar mixture of argon and krypton at 608 K, 266 K, and 117 K. An exponential extrapolation of his results to 99 K would lead to a value of D^{fr}_{12} between 5.10^{-10} m^2.s^{-1} and 2.10^{-9} m^2.s^{-1}; this extrapolation is very inaccurate but covering our simulations.

Simulations in a ternary Lennard-Jones system

Simulations were performed for ternary systems of 300 particles at $T = 0.8$ and $\rho = 0.7901$ in the NVE ensemble. All reduced units are constructed using the parameters of argon atoms. Each system was a liquid mixture of argon, krypton, and neon. The LJ potential parameters used are given in table 6.2. MD simulations of multiples of 25 000 timesteps ($\Delta t = 0.001$) were performed and every 10 timesteps a new time origin was taken. The MS diffusion coefficients were calculated using equation 6.6 for various simulation times (maximal 2 500 000 timesteps) and for various integration times (maximal 1500 timesteps). A simulation time of 2475 was sufficient for the MS diffusion coefficients to become constant. At this simulation time the values of the MS diffusion coefficients were independent of the integration time t for $t > 1.0$. The results of the simulations with a simulation time of 2475 and an integration time of 1.0 are given in table 6.4 and figure 6.5.

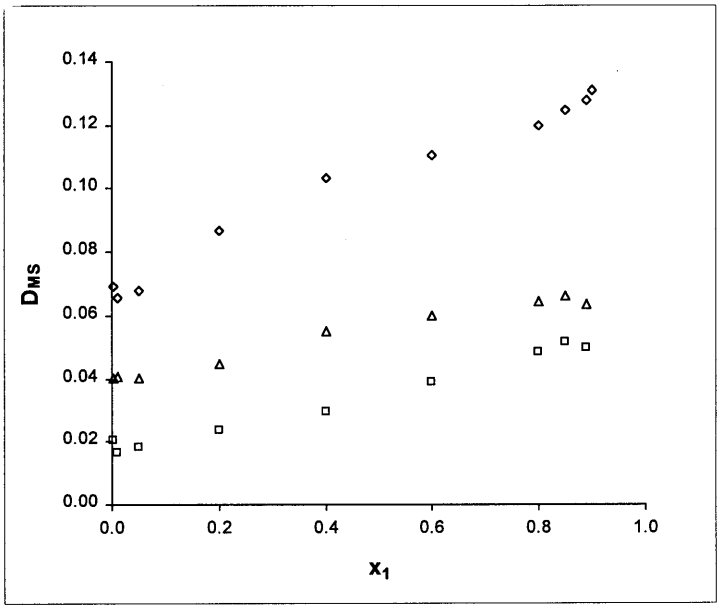

Figure 6.5. *Maxwell-Stefan diffusion coefficients of the ternary system Ar(1) + Kr(2) + Ne(3) as a function of the mole fraction Ar (300 LJ particles, T = 0.8, ρ = 0.7901, integration time = 1.0, x_3 = 0.1): □, D_{12}; ◊, D_{31}; Δ, D_{23}.*

Table 6.4. *Ternary diffusion coefficients as a function of the mole fraction for a ternary LJ mixture Ar(1) + Kr(2) + Ne(3) of 300 particles: T = 0.8, ρ = 0.7901, simulation time = 2475, integration time = 1.0.*

x_1	x_2	x_3	p	D_{12}	D_{31}	D_{23}
0.003	0.897	0.10	1.72	0.020 ± 0.002	0.069 ± 0.002	0.0401 ± 0.0009
0.01	0.89	0.10	1.69	0.016 ± 0.003	0.066 ± 0.004	0.041 ± 0.002
0.05	0.85	0.10	1.58	0.0182 ± 0.0003	0.068 ± 0.003	0.040 ± 0.002
0.20	0.70	0.10	1.14	0.0235 ± 0.0005	0.087 ± 0.006	0.0446 ± 0.0007
0.40	0.50	0.10	0.82	0.030 ± 0.001	0.103 ± 0.007	0.055 ± 0.002
0.60	0.30	0.10	0.60	0.039 ± 0.001	0.110 ± 0.008	0.060 ± 0.002
0.80	0.10	0.10	0.50	0.0481 ± 0.0009	0.120 ± 0.007	0.0645 ± 0.0007
0.85	0.05	0.10	0.48	0.0514 ± 0.0008	0.125 ± 0.002	0.066 ± 0.002
0.89	0.01	0.10	0.48	0.050 ± 0.001	0.128 ± 0.003	0.064 ± 0.004
0.90	0.00	0.10	0.47		0.131 ± 0.003	

The values of the MS diffusion coefficients increase with an increasing mole fraction x_1. An increase of approximately 15% from x_1 = 0 to x_1 = 0.9 might be explained by the decrease of the pressure values of the simulated systems from 1.7 to 0.47 [11]. The MS diffusion coefficient between argon and neon (D_{31}) is higher than the MS diffusion coefficient between krypton and neon (D_{23}), which is in his turn higher than the MS diffusion coefficient between argon and krypton (D_{12}). This is in accordance with our expectations, since the MS diffusion coefficients are inversely proportional to the frictional coefficients between the particles [7], and these frictional coefficients will increase with increasing masses of the components.

Conclusion

Maxwell-Stefan diffusion coefficients in unary, binary and ternary systems of LJ particles can be determined by the Green-Kubo method. For all systems the MS diffusion coefficients became constant for integration times > 1.0. The simulation times required were dependent on the number of different components in the systems, and increased from 1250 for a unary system, and 1750 for a binary system to 2475 for a ternary system. The Maxwell-Stefan diffusion coefficients calculated by equation 6.6 agreed well with the literature values available, or were in accordance with the behaviour as expected from other physical properties.

References

[1] Wakeham, W. A., Nagashima, A., and Sengers, J. V., 1991, *Measurement of the Transport Properties of Fluids, Experimental Thermodynamics*, Vol III (Oxford: Blackwell).

[2] Van de Ven - Lucassen, I. M. J. J., Kemmere, M. F., and Kerkhof, P. J. A. M., 1997, *J. Solution Chem.*, **26**, 1145. Chapter 3 in this thesis.

[3] Schoen, M., and Hoheisel, C., 1984, *Molec. Phys.*, **52**, 33.

[4] Schoen, M., and Hoheisel, C., 1984, *Molec. Phys.*, **52**, 1029.

[5] Hansen, J. P., and McDonald, I. R., 1986, *Theory of Simple Liquids*, 2nd Edn. (London: Academic Press) Chap. 8.

[6] Van de Ven - Lucassen, I. M. J. J., Vlugt, T. J. H., Van der Zanden, A. J. J., and Kerkhof, P. J. A. M., 1998, *Molec. Phys.*, **94**, 495. Chapter 5 in this thesis.

[7] Taylor, R., and Krishna, R., 1993, *Multicomponent Mass Transfer*, (New York: Wiley).

[8] Chandler, D., 1987, *Introduction to Modern Statistical Mechanics* (Oxford University Press) Chap. 8.

[9] Evans, D. J., and Morriss, G. P., 1990, *Statistical Mechanics of Non-Equilibrium Fluids* (San Diego: Academic Press).

[10] Frenkel, D., and Smit, B., 1996, *Understanding Molecular Simulation* (San Diego: Academic Press).

[11] Naghizadeh, J., and Rice, S. A., 1962, *J. Chem. Phys.*, **36**, 2710.

[12] Krishna, R., and Wesselingh, J. A., 1997, *Chem. Eng. Sci.*, **52**, 861.

[13] Lee, J. C., 1997, *Physica A*, **247**, 140.

7. MOLECULAR DYNAMICS SIMULATION OF SELF-DIFFUSION AND MAXWELL-STEFAN DIFFUSION COEFFICIENTS IN LIQUID MIXTURES OF METHANOL AND WATER

Abstract*

Self-diffusion coefficients and Maxwell-Stefan diffusion coefficients in liquids have been determined by the equilibrium molecular dynamics calculation of the appropriate Green-Kubo equation. Simulations of water, methanol and mixtures of water and methanol have been carried out to calculate the diffusion coefficients at 300 K. In order to study the influence of the force field on the calculated self-diffusion coefficients of the pure liquids, two different force fields for each component have been used. The Van Leeuwen/Smit force field calculated the self-diffusion of methanol accurately. The SPC/E force field gave the best, but moderate, results for water. In mixtures of water and methanol the self-diffusion coefficients of both components were more accurate at high mole fractions of methanol. This can be explained by the better performance of the methanol force field. The Maxwell-Stefan diffusion coefficients in the mixtures of methanol and water agreed fairly well with the experimental values. More accurate results can be obtained by using optimised parameters in the water force field, and by enlarging the integration time and the duration of the simulation runs.

* The main part of this chapter has been submitted for publication: Van de Ven – Lucassen, I. M. J. J., Vlugt, T. J. H., Van der Zanden, A. J. J., and Kerkhof, P. J. A. M.

Introduction

Diffusion in liquid systems plays an important role in chemical engineering and knowledge of diffusion coefficients is required, for example, for the design of process equipment. However, in particular for mixtures it is very time consuming and difficult to measure diffusion coefficients [1, 2]. Hence, theoretical models for the estimation of the diffusion coefficients in any given system may be an attractive alternative. Simulation techniques like molecular dynamics provide a convenient method to determine the diffusion coefficients only from parameters describing the inter- and intramolecular interactions of the components of the fluid mixture.

The purpose of this study is to compute the diffusion coefficients in a methanol + water mixture. Simulations are performed on pure water, pure methanol, and on liquid mixtures of methanol + water over the entire concentration range. The results of the MD simulations are compared with experimental values from the literature.

Theory

Molecular diffusion in a binary system can be described by Fick's first law:

$$\mathbf{J}_1 = -C_t D_{12}^f \nabla x_1 , \tag{7.1}$$

in which $\mathbf{J}_1$ is the diffusion flux of component 1, C_t the total molar concentration and ∇x_1 the mole fraction gradient of component 1. D^f_{12} is the Fick diffusion coefficient. For component 2 an analogous relation can be written

$$\mathbf{J}_2 = -C_t D_{21}^f \nabla x_2 . \tag{7.2}$$

Because $\mathbf{J}_1 + \mathbf{J}_2 = 0$ and $x_1 + x_2 = 1$, it can be derived that $D^f_{12} = D^f_{21}$, i.e. only one Fick diffusion coefficient describes diffusion in a binary system. Computations of diffusion coefficients from measurements are mostly performed using Fick's description of diffusion [1].

Another method for describing molecular diffusion is the Maxwell-Stefan approach. When temperature T and pressure p are constant, and when there are no external forces acting on the system, the molar fluxes $\mathbf{N}_i$, $\mathbf{N}_j$ of components i, j due to the gradient in the chemical potential μ_i of component i are given by

$$\sum_{\substack{j=1 \\ j\neq i}}^{n} \frac{x_i \mathbf{N}_j - x_j \mathbf{N}_i}{C_t D_{ij}} = \frac{x_i}{RT} \nabla_{T,p} \mu_i , \tag{7.3}$$

in which R is the gas constant. D_{ij} is the Maxwell-Stefan diffusion coefficient between components i and j. Because $D_{ij} = D_{ji}$, there is also only one Maxwell-Stefan diffusion coefficient describing diffusion in a binary system. The Maxwell-Stefan approach is preferred over Fick's law for describing diffusion under influence of external forces and in multicomponent systems [3].

For a binary system the Fick diffusivity D^f_{12} and the Maxwell-Stefan diffusivity D_{12} are related by

$$D_{12}^{f} = D_{12} \cdot \Gamma \,, \tag{7.4}$$

in which Γ is the thermodynamic factor:

$$\Gamma = 1 + x_1 \frac{\partial \ln \gamma_1}{\partial x_1}, \tag{7.5}$$

with γ_1 is the activity coefficient of component 1. An extensive description of both methods has been given in [4].

For the calculation of Maxwell-Stefan diffusion coefficients in a binary or ternary mixture of Lennard-Jones particles an equilibrium molecular dynamics method was developed, in which the correlation function of fluctuating quantities is determined [5-8]. The integrals of the correlation functions are related to the diffusion coefficients through the Green-Kubo formalism. This so-called Green-Kubo method is preferred above a non-equilibrium method, in which the system is driven away from equilibrium and the system response is monitored [8].

The Green-Kubo method links the time correlation functions of the fluctuating quantities in an equilibrium system to the response to weak perturbations in the equilibrium system by linear response theory [9-11]. The Maxwell-Stefan diffusion coefficient D_{12} is then given by

$$D_{12} = \frac{x_2}{3n_1}\left(\frac{M_1 x_1 + M_2 x_2}{M_2 x_2}\right)^2 \int_0^\infty \left\langle \sum_{i=1}^{n_1} \mathbf{v}_1^i(0) \bullet \sum_{j=1}^{n_1} \mathbf{v}_1^j(t) \right\rangle dt \tag{7.6}$$

in which t is the simulation time, M_i is the molar mass of component i, n_1 the number of particles of component 1, and $\mathbf{v}_1^i$ the velocity of particle i of component 1. Calculation of the self-diffusion coefficient D_i of component i can be performed simultaneously, using

$$D_i = \frac{1}{3}\int_0^\infty \langle \mathbf{v}_i(0) \bullet \mathbf{v}_i(t) \rangle dt \,. \tag{7.7}$$

The derivation of equations 7.6 and 7.7 has been given in [8].

Details of the simulations

Simulations of methanol, water, and mixtures of methanol + water were carried out using the GROMOS (GRoningen MOlecular Simulation) computer package with the standard GROMOS force field [Appendix, 12, 13]. The choice of the parameter set for the GROMOS force field influences the results of the simulations. In the literature various parameter sets are described for water [14-18] and for methanol [16-21]. Those parameter values were developed to reproduce the thermodynamic properties (e.g. density, energy, heat of vaporization), the structural properties, and sometimes the dynamic properties (self-diffusion coefficient) of the fluid as accurately as possible. In the simulations of this work the simple point charge (SPC) parameters and the extended SPC (SPC/E) parameters were used for the water particles. The SPC parameter set was optimised to predict the density and vaporization energy of water; the SPC/E model is a reparametrization of the SPC model to obtain the correct density and potential energy [13, 14]. For the methanol particles the standard GROMOS parameters were used as well as the parameters derived by Van Leeuwen and Smit [13, 21]. The available parameter sets for methanol, for example the GROMOS set, were optimised to predict the liquid properties at ambient temperature and pressure; only the Van Leeuwen/Smit parameter set was optimised to describe liquid coexistence densities at two temperatures and predicts the vapor-liquid curve with much higher accuracy [21]. See table 7.1. Note that the model of Van Leeuwen and Smit uses an Ewald summation technique for handling the long-range dipolar interactions. The GROMOS package applies a spherical cut-off, which will influence the performance of the Van Leeuwen/Smit parameter set.

Unless stated otherwise, the simulations were performed on a cubic periodic system, using a timestep of 0.002 ps and a cut-off radius R_{cut} = 0.9 nm. After an initial energy minimisation, the system was coupled to a bath of constant temperature (300 K) with a coupling time constant τ_T = 0.4 ps and equilibrated for 25 000 timesteps; a constant volume was maintained by using a coupling time constant for pressure $\tau_p = \infty$ [22]. All bond lengths were kept fixed using the SHAKE procedure with a relative tolerance of 0.0001. The pair list was updated every 5 steps. The resulting velocities and coordinates were used as a starting point for further work.

***Table 7.1**. Force field parameters*

	water			methanol	
	SPC	SPC/E		GROMOS	v.Leeuwen/ Smit
$r_{O\text{-}HW1}$	0.100000	0.100000	$r_{OMet\text{-}HMet}$	0.100000	0.100000
$r_{O\text{-}HW2}$	0.100000	0.100000	$r_{OMet\text{-}CMet}$	0.143000	0.143000
$r_{HW1\text{-}HW2}$	0.163299	0.163299	$r_{CMet\text{-}HMet}$	0.198842	0.198842
q_{OW}	-0.820	-0.8476	q_{OMet}	-0.574	-0.700
q_{HW}	0.410	0.4238	q_{HMet}	0.398	0.435
			q_{CMet}	0.176	0.265
$C^{1/2}{}_6$(OW)	0.05116	0.05116	$C^{1/2}{}_6$(OMet)	0.04756	0.04717
$C^{1/2}{}_6$(HW)	0.0	0.0	$C^{1/2}{}_6$(HMet)	0.0	0.0
			$C^{1/2}{}_6$(CMet)	0.09421	0.09783
$C^{1/2}{}_{12}$(OW)	$1.623.10^{-3}$	$1.623.10^{-3}$	$C^{1/2}{}_{12}$(OMet)	$1.227.10^{-3}$	$1.3121.10^{-3}$
$C^{1/2}{}_{12}$(HW)	0.0	0.0	$C^{1/2}{}_{12}$(HMet)	0.0	0.0
			$C^{1/2}{}_{12}$(CMet)	$4.5665.10^{-3}$	$5.117.10^{-3}$
R_{cut}	0.9	0.8	R_{cut}	0.9	0.9

r, R in nm; q in e; $C^{1/2}{}_6$ in $(kJ.mol^{-1}.nm^6)^{1/2}$; $C^{1/2}{}_{12}$ in $(kJ.mol^{-1}.nm^{12})^{1/2}$
$C_6 = 4.\varepsilon.\sigma^6$; $C_{12} = 4.\varepsilon.\sigma^{12}$

Simulations of liquid water and liquid methanol

To compare the SPC force field with the SPC/E force field in water, and the GROMOS force field with the Van Leeuwen/Smit force field in methanol, MD simulations were performed on two pure liquid systems of each force field with a box length of approximately 2.5 nm and 3.0 nm respectively. See table 7.2. In each system the self-diffusion coefficients and the Maxwell-Stefan diffusion coefficients using the Green-Kubo method were calculated.

Self-diffusion coefficients

MD simulations of multiples of 1000 timesteps were carried out on all systems. Every 1000 timesteps a new starting value $t = 0$ was chosen and the velocity autocorrelation function $vacf(t) \equiv \langle \mathbf{v}(0) \cdot \mathbf{v}(t) \rangle$ was calculated. Such a row of vacf data was denoted as a vacf set. The

Table 7.2. *Self-diffusion coefficients of water and methanol, calculated with equation 7.7*

System	par. set	$N_{part.}$	bl*	D_{water}*	$D_{methanol}$*
1	SPC	509	2.50	4.9 ± 0.2	
2	SPC	898	3.02	4.7 ± 0.1	
3	SPC/E	519	2.50	3.1 ± 0.2	
4	SPC/E	889	3.00	3.45 ± 0.09	
5	meth-GR*	240	2.54		4.3 ± 0.1
6	meth-GR*	415	3.05		4.3 ± 0.1
7	meth-VL/S*	240	2.54		2.5 ± 0.1
8	meth-VL/S*	415	3.05		2.4 ± 0.1
Mills (at 25 °C: 2.299) [23]				2.41	
Hurle and Woolf [26]					2.5

* bl = box length in nm; D in 10^{-9} $m^2.s^{-1}$; GR, GROMOS force field; VL/S, Van Leeuwen/Smit force field

self-diffusion coefficient was determined by averaging over multiple vacf sets and integrating over 1000 timesteps (2 ps), using equation 7.7. The accuracy of the self-diffusion coefficients was estimated by grouping the simulation data of 99 vacf sets into 5 - 10 blocks. From the standard deviation of the block averages the error in the diffusion coefficient was calculated [11]. Results are listed in table 7.2.

Maxwell-Stefan diffusion coefficients

To calculate the Maxwell-Stefan diffusion coefficients of a unary system, each system was divided into two species or components by attaching a colour label to a mole fraction x_{colour} of the particles. The two species differ only by the colour label, which plays no role in the dynamics. MD simulations of 260 000 – 346 500 timesteps were performed on the systems 1, 3 and 5 - 8. Every 10 timesteps a new time origin was taken. During the simulation the multiple particle autocorrelation function $\sum \mathbf{v}_1^i(0) \bullet \sum \mathbf{v}_1^j(t)$ was calculated for 10 different values of the mole fraction coloured component x_1 simultaneously. The Maxwell-Stefan diffusion coefficients were determined as a function of the mole fraction coloured component by integrating over 1000 timesteps (2 ps), using equation 7.6. The

accuracy of the Maxwell-Stefan diffusion coefficients was estimated by grouping the simulation data into 6 – 8 blocks; from the standard deviation of the block averages the error in the diffusion coefficients was calculated. Results are listed in table 7.3.

Comparison of the force fields

Tables 7.2 and 7.3 show a better performance of the SPC/E parameter set in water. The self-diffusion coefficient of the SPC/E model is closer to the experimental value of Mills [23, 24] than the SPC value, with comparable standard deviations. Simulations of Berendsen et al [14] also showed an improvement of the value of the self-diffusion coefficient from $4.3.10^{-9}$ $m^2.s^{-1}$ using the SPC parameters to $2.5.10^{-9}$ $m^2.s^{-1}$ using the SPC/E parameters; the SPC/E value was even within simulation error of the experimental value. However, Caldwell & Kollman [17] could not obtain this value in non-additive MD simulations using their polarizable model with the SPC/E parameters, and calculated a self-diffusion coefficient of $3.1.10^{-9}$ $m^2.s^{-1}$. The simulations of Berendsen et al as well as the simulations of Caldwell & Kollman were performed on a cubic box of 216 particles. An influence of the system size on the calculation of the self-diffusion coefficient might explain the differences between the results of the simulations of both Berendsen et al and Caldwell & Kollman and the results of our simulations given in table 7.2 [25]. Since the SPC/E model agreed best with the experimental data, we decided to use this model for further work.

Tables 7.2 and 7.3 show a good performance of the Van Leeuwen/Smit parameter set in methanol. The self-diffusion coefficient is in good agreement with the value $2.50.10^{-9}$ $m^2.s^{-1}$ from the literature [26]. The Van Leeuwen/Smit parameter set also performs better than the polarizable model of Caldwell & Kollman, which gives a value of $2.65.10^{-9}$ $m^2.s^{-1}$ [17], and than the refinements of Jorgensen (parameter sets J1 and J2), and Haughney (parameter sets H1 and H2) of the three-site united-atom approach for the intermolecular potential of Jorgensen tested by Haughney et al [20]. Casulleras and Guardia used the J2 model for their simulations of liquid methanol at 298 K, in which they studied the effect of the system size on the transport properties and the structure of liquid methanol [25].

***Table 7.3**. Maxwell-Stefan diffusion coefficients, calculated with equation 7.6, as a function of the mole fraction coloured component for pure liquids*

Water

system 1 (SPC, 509 part.)		system 3 (SPC/E, 519 part.)	
x_{colour}	D_{MS}*	x_{colour}	D_{MS}*
0.098	4.6 ± 0.2	0.096	3.5 ± 0.3
0.196	4.3 ± 0.3	0.193	3.6 ± 0.3
0.295	4.8 ± 0.3	0.289	3.4 ± 0.3
0.393	4.9 ± 0.3	0.385	3.5 ± 0.2
0.491	5.1 ± 0.3	0.482	3.6 ± 0.2
0.589	4.7 ± 0.4	0.578	4.1 ± 0.3
0.688	4.9 ± 0.5	0.674	3.9 ± 0.3
0.786	4.7 ± 0.4	0.771	3.4 ± 0.2
0.884	5.6 ± 0.3	0.867	3.3 ± 0.2
0.982	5.2 ± 0.4	0.963	3.8 ± 0.2

Methanol

system 5 (meth-GR, 240 part.)		system 6 (meth-GR, 415 part.)	
x_{colour}	D_{MS}*	x_{colour}	D_{MS}*
0.083	4.3 ± 0.2	0.096	4.4 ± 0.3
0.167	4.6 ± 0.5	0.193	4.5 ± 0.6
0.250	4.0 ± 0.4	0.289	4.2 ± 0.4
0.333	3.9 ± 0.3	0.386	4.1 ± 0.4
0.417	4.1 ± 0.5	0.482	4.2 ± 0.5
0.500	4.3 ± 0.4	0.578	4.7 ± 0.4
0.583	4.2 ± 0.4	0.675	4.6 ± 0.3
0.667	4.0 ± 0.6	0.771	4.8 ± 0.4
0.750	4.1 ± 0.5	0.867	4.5 ± 0.3
0.833	4.6 ± 0.2	0.964	4.4 ± 0.2

system 7 (meth-VL/S, 240 part.)		system 8 (meth-VL/S, 415 part.)	
x_{colour}	D_{MS}*	x_{colour}	D_{MS}*
0.083	2.5 ± 0.3	0.096	2.7 ± 0.5
0.167	2.7 ± 0.2	0.193	3.1 ± 0.7
0.250	3.0 ± 0.2	0.289	3.6 ± 1.0
0.333	2.8 ± 0.1	0.386	2.9 ± 0.6
0.417	2.5 ± 0.2	0.482	2.6 ± 0.7
0.500	2.6 ± 0.3	0.578	3.3 ± 0.7
0.583	2.6 ± 0.2	0.675	3.1 ± 0.8
0.667	2.7 ± 0.2	0.771	3.3 ± 0.8
0.750	2.6 ± 0.2	0.867	3.1 ± 0.6
0.833	2.5 ± 0.2	0.964	2.5 ± 0.4

* D_{MS} in 10^{-9} $m^2.s^{-1}$

The self-diffusion coefficient D_m of methanol increased from D_m = $2.23.10^{-9}$ $m^2.s^{-1}$ to D_m = $2.59.10^{-9}$ $m^2.s^{-1}$ with increasing number of particles N from N = 125 to N = 512. The Van Leeuwen/Smit model was constant within the simulation error (table 7.2). Therefore, for further work the Van Leeuwen/Smit parameter set was used for methanol.

The Maxwell-Stefan diffusion coefficients in the pure liquids, shown in table 7.3, agree fairly well with the self-diffusion coefficients, shown in table 7.2, but are less accurate. This is in accordance with the results of the simulations performed for Lennard-Jones systems by Van de Ven – Lucassen et al [8]. Increasing the integration time and the simulation time might improve the accuracy of the Maxwell-Stefan diffusion coefficients.

Simulations of mixtures of water and methanol

Simulations were performed on 10 systems of methanol + water particles at 300 K and 1 atm. (table 7.4). In the systems with a mole fraction of methanol x_m lower than 0.5, methanol was treated as a solute in the solvent water; at higher mole fractions (x_m > 0.5) water was a solute in the solvent methanol. After energy minimisation, the systems were equilibrated for 25 000 timesteps. MD simulations of multiples of 5000 timesteps were performed, resulting in 495 000 timesteps. During the simulation every 5 timesteps a new time origin was taken and the multiple particle autocorrelation function $\sum \mathbf{v}_1^i(0) \bullet \sum \mathbf{v}_1^j(t)$ was calculated. The Maxwell-Stefan diffusion coefficients were determined by using equation 7.6 for integration times of 1000 and 1500 timesteps (2 and 3 ps), resulting in 800 and 700 time origins used per run of 5000 timesteps. Simultaneously, every 1000 timesteps a new time origin was taken to calculate the velocity autocorrelation functions $vacf_i(t) \equiv \langle \mathbf{v}_i(0) \cdot \mathbf{v}_i(t) \rangle$ (i = 1, 2), resulting in 5 $vacf_i$ sets (i = 1, 2) per run of 5000 timesteps. The self-diffusion coefficients of methanol and water were determined by using equation 7.7, and integrating over 1000 timesteps (2 ps). The accuracy of the diffusion coefficients was estimated from the standard deviation of the block averages, into which the simulation data were grouped (at least 5 blocks).

***Table 7.4**. Self-diffusion coefficients of methanol and water in methanol + water mixtures, calculated with equation 7.7*

$N_{methanol}$	N_{water}	ρ*	bl*	$x_{methanol}$	$D_{methanol}$*	D_{water}*
80	744	977	3.006	0.097	1.69 ± 0.11	2.55 ± 0.07
150	596	955	3.001	0.201	1.58 ± 0.05	1.96 ± 0.05
200	499	937	3.011	0.286	1.41 ± 0.03	1.80 ± 0.03
250	385	914	3.006	0.394	1.28 ± 0.04	1.75 ± 0.04
275	339	903	3.016	0.448	1.38 ± 0.03	1.58 ± 0.03
283	250	885	2.942	0.531	1.37 ± 0.07	1.58 ± 0.09
298	210	874	2.937	0.587	1.37 ± 0.05	1.58 ± 0.09
336	150	852	2.972	0.691	1.46 ± 0.04	1.59 ± 0.08
361	100	832	2.988	0.783	1.68 ± 0.03	1.63 ± 0.09
393	50	810	3.024	0.887	1.98 ± 0.06	1.50 ± 0.11

* ρ = density in kg.m^{-3}; bl = box length in nm; D in 10^{-9} m^2.s^{-1}

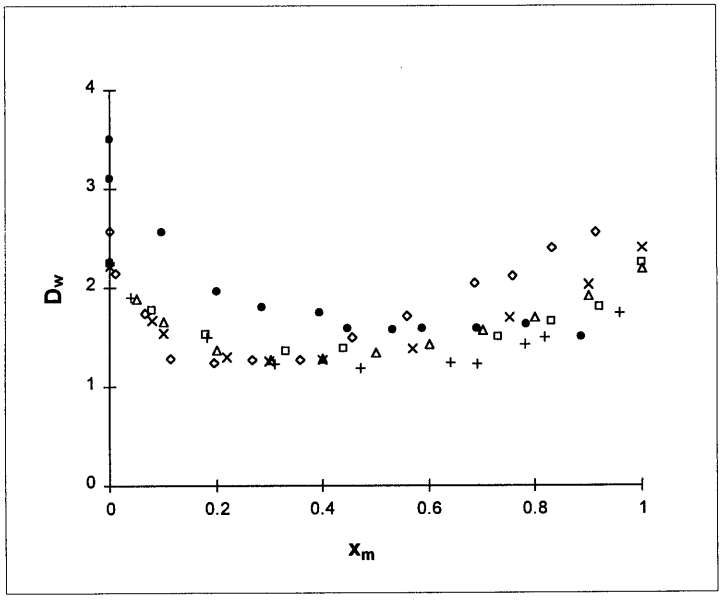

***Figure 7.1**. Self-diffusion coefficient of water (10^{-9} m^2.s^{-1}) as a function of the mole fraction methanol x_m: •, calculated in the simulation at 300 K; □, ref 27, as estimated from the graph published; ×, ref 28, as estimated from the graph published; Δ, ref 29; +, ref 30; ◊, ref 31.*

Self-diffusion coefficients

The self-diffusion coefficients were calculated by averaging over 495 000 simulation steps (495 $vacf_i$ sets) as well as by averaging over 395 000 simulation steps (395 $vacf_i$ sets), using the first 100 000 steps for further equilibration of the system. There was no significant difference between the values of the calculated self-diffusion coefficients. Results of the calculation over 495 $vacf_i$ sets are given in table 7.4. In figures 7.1 and 7.2 the calculated self-diffusion coefficients (300 K) are compared with values at 25 °C, obtained from the literature. The self-diffusion coefficients of water and methanol, as given by Kida and Uedaira [27], were measured at 32 °C. To compare these values with the other values from the literature, the self-diffusion coefficients of water were multiplied by a factor $2.299 \cdot 10^{-9}$ / $2.733 \cdot 10^{-9}$ (equal to $D_{water,25°C}$ / $D_{water,32°C}$), and the self-diffusion coefficients of methanol were multiplied by $2.50 \cdot 10^{-9}$ / $2.75 \cdot 10^{-9}$ (equal to $D_{methanol,25°C}$ / $D_{methanol,32°C}$).

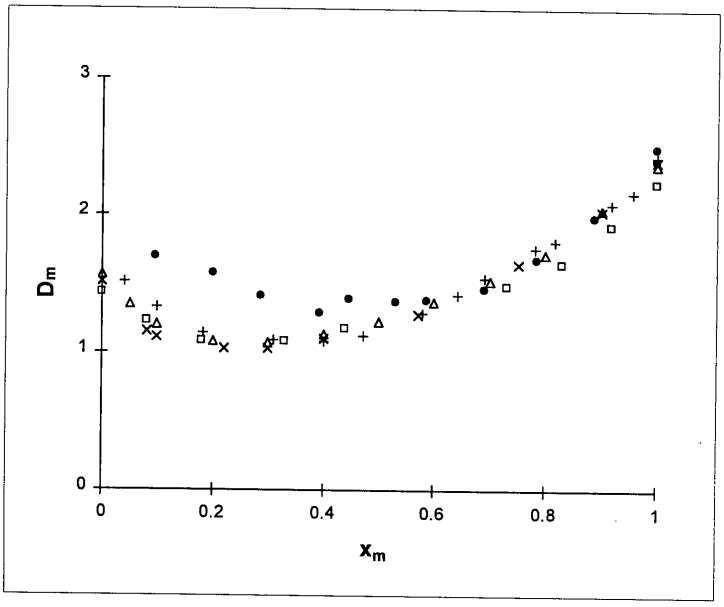

Figure 7.2. *Self-diffusion coefficient of methanol (10^{-9} $m^2.s^{-1}$) as a function of the mole fraction methanol x_m: •, calculated in the simulation at 300 K; □, ref 27, as estimated from the graph published; ×, ref 28, as estimated from the graph published; Δ, ref 29; +, ref 30.*

Figure 7.1 shows a better agreement of the calculated self-diffusion coefficients of water with the literature values at high mole fractions of methanol; at low mole fractions of methanol the self-diffusion coefficient of water was high. The calculated self-diffusion coefficient of methanol agrees very well at high mole fractions of methanol, as shown in figure 7.2; at low mole fractions the self-diffusion coefficient of methanol is high, too. The larger deviations of the self-diffusion coefficients at low values of the mole fraction methanol might be explained by the use of the force fields chosen. The SPC/E force field of water gives a much higher value of the self-diffusion coefficient in pure water; the Van Leeuwen/Smit force field of methanol calculates the self-diffusion coefficient of methanol more accurate. At low mole fractions of methanol the influence of the SPC/E force field on the calculation of the diffusion coefficients might be larger, and the accuracy of the calculations might be smaller.

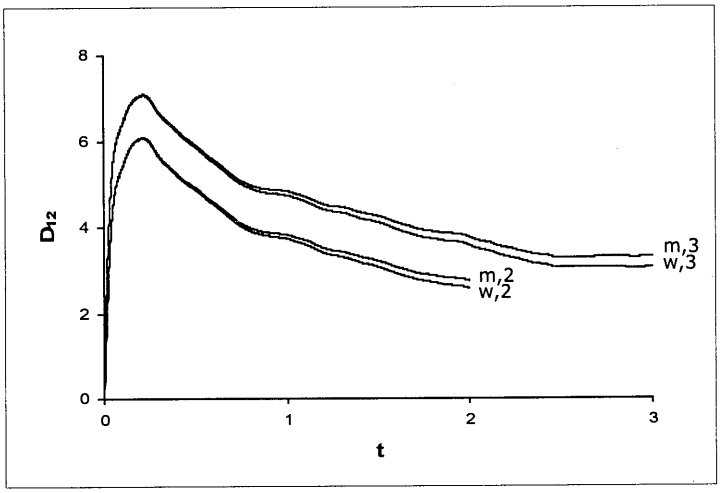

Figure 7.3. *Maxwell-Stefan diffusion coefficient (10^{-9} $m^2.s^{-1}$) as a function of the integration time t (ps): —* m,2, *equation 7.6 for the methanol particles, integration time is 2 ps; —* w,2, *equation 7.6 for the water particles, integration time is 2 ps; —* m,3, *equation 7.6 for the methanol particles, integration time is 3 ps; —* w,3, *equation 7.6 for the water particles, integration time is 3 ps.*

Table 7.5. *Maxwell-Stefan diffusion coefficients in methanol + water mixtures, calculated with equation 7.6*

$x_{methanol}$	$D_{12,m,495,2}$*	$D_{12,w,495,2}$*	$D_{12,m,395,2}$*	$D_{12,w,395,2}$*
0.097	2.2 ± 0.4	2.2 ± 0.4	1.8 ± 0.2	1.8 ± 0.2
0.201	2.0 ± 0.5	2.0 ± 0.4	1.7 ± 0.3	1.7 ± 0.2
0.286	1.9 ± 0.2	1.9 ± 0.2	1.7 ± 0.1	1.7 ± 0.1
0.394	2.1 ± 0.3	2.1 ± 0.3	1.8 ± 0.2	1.8 ± 0.2
0.448	1.8 ± 0.3	1.7 ± 0.3	1.5 ± 0.1	1.4 ± 0.1
0.531	2.3 ± 0.6	2.2 ± 0.6	1.7 ± 0.1	1.7 ± 0.1
0.587	2.2 ± 0.4	2.1 ± 0.4	1.9 ± 0.2	1.8 ± 0.2
0.691	2.9 ± 0.5	2.9 ± 0.5	2.5 ± 0.4	2.4 ± 0.3
0.783	2.7 ± 0.6	2.6 ± 0.6	2.2 ± 0.4	2.1 ± 0.4
0.887	3.5 ± 1.5	3.2 ± 1.5	2.1 ± 0.2	1.7 ± 0.2
$x_{methanol}$	$D_{12,m,495,3}$*	$D_{12,w,495,3}$*	$D_{12,m,395,3}$*	$D_{12,w,395,3}$*
0.097	2.4 ± 0.4	2.4 ± 0.4	2.0 ± 0.2	2.1 ± 0.3
0.201	1.5 ± 0.2	1.5 ± 0.1	1.5 ± 0.1	1.6 ± 0.1
0.286	1.8 ± 0.4	1.8 ± 0.3	1.6 ± 0.2	1.5 ± 0.2
0.394	1.8 ± 0.4	1.8 ± 0.4	1.5 ± 0.3	1.5 ± 0.3
0.448	1.8 ± 0.2	1.7 ± 0.1	1.6 ± 0.1	1.5 ± 0.1
0.531	1.9 ± 0.5	1.7 ± 0.4	1.4 ± 0.2	1.4 ± 0.1
0.587	1.8 ± 0.2	1.7 ± 0.1	1.7 ± 0.1	1.6 ± 0.1
0.691	2.7 ± 0.7	2.5 ± 0.6	2.2 ± 0.6	2.0 ± 0.5
0.783	2.3 ± 0.4	2.1 ± 0.3	2.0 ± 0.2	1.8 ± 0.2
0.887	3.1 ± 1.4	2.6 ± 1.3	1.8 ± 0.2	1.3 ± 0.2

* D in 10^{-9} $m^2.s^{-1}$; $D_{12,m,495,2}$: calculated with equation 7.6 for methanol, averaged over 495 000 steps, and integrated over 2 ps

Mutual diffusion coefficients

The mutual Maxwell-Stefan diffusion coefficients D_{12} were determined by using equation 7.6 for the time origins obtained in a simulation of 495 000 timesteps as well as for the time origins obtained in a simulation of 395 000 timesteps, using the first 100 000 steps for further equilibration of the system. The integration times were 1000 and 1500 timesteps (2 and 3 ps), and D_{12} was calculated both for the methanol particles ($D_{12,m}$) and the water particles ($D_{12,w}$). Results are listed in table 7.5. The difference between the values of $D_{12,m}$ and $D_{12,w}$ can be a measure for the accuracy of the simulation. In general, results were more accurate if the equilibration of the systems was increased with 100 000 timesteps. Figure 7.3 shows that an

integration time of 2 ps was not always sufficient for the diffusion coefficient to become constant. The fluctuations in the calculated diffusion coefficients for long integration times will decrease, and the accuracy will increase, with an increasing number of time origins or simulation steps. For comparison with the literature values we used the average values of $D_{12,m}$ and $D_{12,w}$ obtained after further equilibration and by integrating over 3 ps. Since the diffusion coefficients given in the literature were Fick diffusion coefficients, they were divided by the thermodynamic factor Γ to obtain the Maxwell-Stefan diffusion coefficients (equation 7.4). The values of Γ used were given by Mills et al [33].

The simulated diffusion coefficients agreed fairly well with the literature values, as shown in figure 7.4. The deviations were mainly caused by the short integration times of the multiple particle autocorrelation functions and the low number of simulation steps, resulting in a low number of time origins (figure 7.3). The same procedure has been performed for the values of Γ given by Hall et al [34]; no significant difference could be observed.

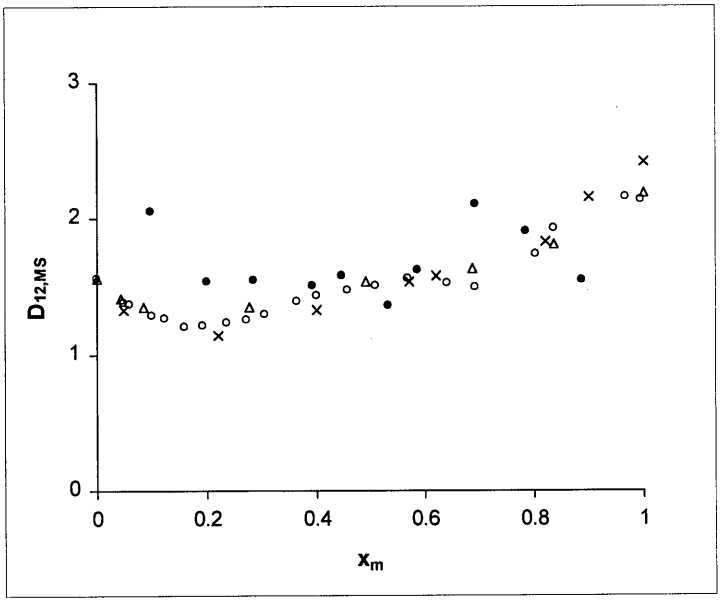

Figure 7.4. *Mutual Maxwell-Stefan diffusion coefficient (10^{-9} $m^2.s^{-1}$) as a function of the mole fraction methanol x_m: •, calculated in the simulation at 300 K; ○, ref 32; ×, ref 28, as estimated from the graph published; Δ, ref 29.*

Conclusions

The self-diffusion and mutual Maxwell-Stefan diffusion coefficients in a binary system can be determined by the Green-Kubo method. The accuracy of the method is dependent on the parameters of the force field used in the molecular dynamics simulation. The force field of the methanol particles gives better results in the calculation of the self-diffusion coefficient of pure methanol than the force field of the water particles in the calculation of the pure water self-diffusion coefficient. In mixtures of water and methanol the self-diffusion coefficients of methanol and water are more accurate at high mole fractions of methanol, which can be explained by the greater influence of the methanol force field. The results of the simulations of the mutual Maxwell-Stefan diffusion coefficients agree fairly well with the experimental values, given in the literature. More accurate results can be obtained by using optimised parameters in the water force field, and by enlarging the system size, the integration time or the number of time origins, c.q. the duration of the MD runs.

References

[1] Wakeham, W. A., Nagashima, A., and Sengers, J. V., 1991, *Measurement of the Transport Properties of Fluids, Experimental Thermodynamics*, Vol III (Oxford: Blackwell).

[2] Van de Ven - Lucassen, I. M. J. J., Kemmere, M. F., and Kerkhof, P. J. A. M., 1997, *J. Solution Chem.*, **26**, 1145. Chapter 3 in this thesis.

[3] Krishna, R., and Wesselingh, J. A., 1997, *Chem. Eng. Sci.*, **52**, 861.

[4] Taylor, R., and Krishna, R., 1993, *Multicomponent Mass Transfer*, (New York: Wiley).

[5] Schoen, M., and Hoheisel, C., 1984, *Molec. Phys.*, **52**, 33.

[6] Schoen, M., and Hoheisel, C., 1984, *Molec. Phys.*, **52**, 1029.

[7] Hansen, J. P., and McDonald, I. R., 1986, *Theory of Simple Liquids*, 2nd Edn. (London: Academic Press) Chap. 8.

[8] Van de Ven - Lucassen, I. M. J. J., Vlugt, T. J. H., Van der Zanden, A. J. J., and P.J.A.M. Kerkhof, P. J. A. M., 1998, *Molec. Phys.*, **94**, 495. Chapter 5 in this thesis.

[9] Chandler, D., 1987, *Introduction to Modern Statistical Mechanics* (Oxford University Press) Chap. 8.
[10] Evans, D. J., and Morriss, G. P., 1990, *Statistical Mechanics of Non-Equilibrium Fluids* (San Diego: Academic Press).
[11] Frenkel, D., and Smit, B., 1996, *Understanding Molecular Simulation* (San Diego: Academic Press).
[12] Van Gunsteren, W. F., and Berendsen, H. J. C., 1987/1996, *GROMOS, Groningen Molecular Simulation computer package*, (University of Groningen, and ETH Zürich).
[13] W.F. van Gunsteren, W. F., Billeter, S. R., Eising, A. A., Hünenberger, P. H., Krüger, P., Mark, A. E., Scott, W. R. P., and Tironi, I. G., 1996, *Biomolecular Simulation: The GROMOS96 Manual and User Guide* (Zürich: vdf Hochschulverlag AG an der ETH Zürich and BIOMOS b.v.).
[14] Berendsen, H. J. C., Grigera, J. R., and Straatsma, T. P., 1987, *J. Phys. Chem.*, **91**, 6269.
[15] Tanaka, H., Walsh, J., and Gubbins, K. E., 1992, *Molec. Phys.*, **76**, 1221.
[16] Mezei, M., 1992, *Molecular Simulation*, **9**, 257.
[17] Caldwell, J. W., and Kollman, P. A., 1995, *J. Phys. Chem.*, **99**, 6208.
[18] Jorgensen, W. L., and Madura, J. D., 1983, *J. Am. Chem. Soc.*, **105**, 1407.
[19] Jorgensen, W. L., 1986, *J. Phys. Chem.*, **90**, 1276.
[20] Haughney, M., Ferrario, M., and McDonald, I. R., 1987, *J. Phys. Chem.*, **91**, 4934.
[21] Van Leeuwen, M. E., and Smit, B., 1995, *J. Chem. Phys.*, **99**, 1831.
[22] Berendsen, H. J. C., Postma, J. P. M., Van Gunsteren, W. F., Dinola, A., and Haak, J. R., 1984, *J. Chem. Phys.*, **81**, 3684.
[23] Mills, R., 1973, *J. Phys. Chem.*, **77**, 685 (1973)
[24] Harris, K. R., and Newitt, P. J., 1997, *J. Chem. Eng. Data*, **42**, 346.
[25] Casulleras, J., and Guardia, E., 1992, *Molecular Simulation*, **8**, 273.
[26] Hurle, R. L., and Woolfe, L. A., 1980, *Aust. J. Chem.*, **33**, 1947.
[27] Kida, J., and Uedaira, H., 1977, *J. Magn. Resonance*, **27**, 253.
[28] Hertz, H. G., and Leiter, H., 1982, *Zeitschrift Phys. Chem. Neue Folge.*, **133**, 45.

[29] Derlacki, Z. J., Easteal, A. J., Edge, A. V. J., and Woolf, L. A., 1985, *J. Phys. Chem.*, **89**, 5318.

[30] Reimschüssel, W., and Hawlicka, E., 1982, *Radiochimica Acta*, **31**, 157.

[31] Erdey-Grúz, T., Inzelt, Gy., and Fodor-Csanyi, P., 1973, *Acta Chim. Ac. Sci. Hung.*, **77**(2), 173.

[32] Van de Ven - Lucassen, I. M. J. J., Kieviet, F. G. and Kerkhof, P. J. A. M., 1995, *J. Chem. Eng. Data*, **40**, 407. Chapter 2 in this thesis.

[33] Mills, R., Malhotra, R., Woolf, L. A., and Miller, D. G., 1994, *J. Chem. Eng. Data*, **39**, 929.

[34] Hall, D. J., Mash, C. J., and Pemberton, R. C., 1979, *NPL Report Chem 95*.

APPENDIX

The GROMOS force field

The Gromos force field or interaction function has the following form

$$V^{\text{phys}}(\boldsymbol{r};s) = V^{\text{bon}}(\boldsymbol{r};s) + V^{\text{nonb}}(\boldsymbol{r};s), \tag{A.1}$$

in which the term V^{bon} describes the interaction between covalently bonded atoms and V^{nonb} the non-bonded (van der Waals and electrostatic) interaction. The interaction between covalently bonded atoms is described by four terms: a bond-streching term, a bond-angle term, a (harmonic) improper dihedral-angle bending term, and a (trigonometric) dihedral-angle torsion term. The non-bonded interaction is described by

$$V^{\text{nonb}}(\boldsymbol{r};s) = \sum_{\substack{\text{nonbonded}\\ \text{pairs (i,j)}}} \left[\frac{C_{12}(\text{i,j})}{\left(r_{\text{ij}}^{4\text{D}}\right)^6} - C_6(\text{i,j}) \right] \frac{1}{\left(r_{\text{ij}}^{4\text{D}}\right)^6} + \\ + \sum_{\substack{\text{nonbonded}\\ \text{pairs (i,j)}}} \frac{q_{\text{i}} q_{\text{j}}}{4\pi\varepsilon_0\varepsilon_1} \left[\frac{1}{r_{\text{ij}}^{4\text{D}}} - \frac{\frac{1}{2}C_{\text{rf}}\left(r_{\text{ij}}^{3\text{D}}\right)^2}{R_{\text{rf}}^3} - \frac{1-\frac{1}{2}C_{\text{rf}}}{R_{\text{rf}}} \right] \tag{A.2}$$

The first term in equation A.2 represents the non-bonded van der Waals interaction. The Gromos van der Waals parameters for an atom pair (i,j) are derived from single atom van der Waals parameters using the relations

$$C_6(\text{i,j}) = C_6^{\frac{1}{2}}(\text{i,i}) \cdot C_6^{\frac{1}{2}}(\text{j,j}) \tag{A.3}$$

and

$$C_{12}(\text{i,j}) = C_{12}^{\frac{1}{2}}(\text{i,i}) \cdot C_{12}^{\frac{1}{2}}(\text{j,j}). \tag{A.4}$$

C_6 and C_{12} are a function of the Lennard-Jones energy- and size parameters.

The second term in equation A.2 represents the electrostatic interaction. R_{rf} is the cut-off radius of the reaction field force. The reaction field force coefficient C_{rf} depends on the relative dielectric permittivity and an inverse Debye screening length.

The values of all parameters can be found in the interaction function parameter files of the GROMOS package.

An extensive description of the GROMOS force field is given in: W.F. van Gunsteren, W. F., Billeter, S. R., Eising, A. A., Hünenberger, P. H., Krüger, P., Mark, A. E., Scott, W. R. P., and Tironi, I. G., 1996, *Biomolecular Simulation: The GROMOS96 Manual and User Guide* (Zürich: vdf Hochschulverlag AG an der ETH Zürich and BIOMOS b.v.).

8. DISCUSSION AND CONCLUSION

The Taylor dispersion method is used to measure diffusion coefficients in aqueous non-electrolyte solutions. This method is fast and convenient for binary liquid mixtures. After preparation of the solvents and the injection solutions the measurements are performed fully automated, and the data gathered during the experiments are processed fast and easily. In order to obtain a high accuracy, it is necessary to work very precisely and in accordance with the experimental conditions, as described in chapter 2. The concentration of the injection solutions and the flow velocity of the carrier stream have to be within certain constraints. Furthermore, adsorption of one component at the wall of the diffusing tube can cause tailing in the measured dispersion profiles, resulting in an asymmetric peak. This has to be avoided.

The extension of the Taylor dispersion method to measure diffusion coefficients in ternary liquid mixtures is not simple. Compared with the binary measurements, the calculation of the diffusion coefficients from the measured dispersion profiles is much more complicated, and the accuracy is influenced more by the carefulness of the experimental work. In the experiments there are strong constraints to the concentrations of the injection solutions and the flow velocity, and adsorption has to be avoided. Furthermore, in ternary mixtures also the ratio of the injected amounts and the relative detector sensitivity for the components are very important. An unfavourable relative sensitivity of the detector can hinder the measurement of accurate dispersion profiles. In that case the calculation of accurate diffusion coefficients from the dispersion profiles is not possible. This problem cannot always be solved by the use of a detector of a different type or by the use of two different detectors simultaneously. Another experimental technique has to be chosen then.

EMD methods as well as NEMD methods have been investigated to simulate diffusion in liquids. Simulations of binary coloured

systems of Lennard-Jones particles show that for dense systems the Green-Kubo (GK) method (an EMD method) performs better than the method developed by Berendsen (an NEMD method). The GK method is less time-consuming and the calculations are more accurate. Because of these results, only the GK method has been extended for simulations on ternary systems. This extended GK method performs well determining the diffusion coefficients of the ternary coloured systems, and of binary and ternary systems of Lennard-Jones particles, which differ by the values of the mass- and Lennard-Jones parameters.

For the simulation of diffusion in methanol + water mixtures a more complex force field than the Lennard-Jones potential is required. The results of the simulations depend on the values of the parameter sets used. For instance, the Van Leeuwen/Smit parameter set for methanol performs much better than the other parameter sets used in the simulations of the self-diffusion coefficients in pure water and pure methanol. Only the Van Leeuwen/Smit parameter set was obtained from vapour-liquid equilibrium simulations; the other parameter sets were developed from density-, hydrogen bond strength-, or energy calculations. The simulations of the self-diffusion coefficients in the methanol + water mixtures, using the most suitable and available parameter sets for each component, show more accurate results for higher concentrations of methanol. Thus, it would be interesting to develop a parameter set for water, analogous to the Van Leeuwen/Smit set for methanol, and to investigate the performance of this parameter set simulating diffusion in pure water and in the water + methanol liquid mixture. If the diffusion coefficients can be calculated more accurately using the "Van Leeuwen/Smit" parameter sets for both methanol and water, it is worthwhile to examine other liquids and liquid mixtures in the same manner. If the parameter sets obtained from phase equilibrium calculations perform well on simulating diffusion for various binary mixtures, then a "general" procedure might be developed for calculating accurate diffusion coefficients, using these parameter sets. Next, diffusion simulations in ternary mixtures of complex molecules can be investigated.

The MD simulations of the methanol + water mixtures show the possibility of predicting the diffusion coefficients provided that the force fields and the simulation procedures (system size, simulation

time) are optimised. The calculated diffusion coefficients are Maxwell-Stefan coefficients. For comparison with the measurements, which provide Fick coefficients, the thermodynamic correction factors are necessary. These thermodynamic factors can be obtained from the literature, measurements, or, also, from computer simulations.

List of symbols

$\mathbf{a}_i$	acceleration of component i	($m.s^{-2}$)
a	drift parameter	(U)
b	drift parameter	($U.s^{-1}$)
C_i	radially-averaged concentration of component i at time t relative to the background concentration	($mol.m^{-3}$)
C_t	total molar concentration	($mol.m^{-3}$)
d	internal diameter of the diffusion tube (= *i.d.*)	(m)
d_b	internal diameter of the water bath	(m)
d_c	internal diameter of the tubing coil	(m)
De	Dean number	(-)
D	self-diffusion coefficient	($m^2.s^{-1}$) or (-)
D_{eff}	effective diffusion coefficient	($m^2.s^{-1}$) or (-)
D_{12}	binary molecular diffusion coefficient	($m^2.s^{-1}$)
D_{ii}	main-diffusion coefficient	($m^2.s^{-1}$) or (-)
$D_{ij,\ i\neq j}$	cross-diffusion coefficient	($m^2.s^{-1}$) or (-)
$\mathbf{F}$	molar force	($J.mol^{-1}.m^{-1}$)
g	gravity constant	($m.s^{-2}$)
Gr	Grashof number	(-)
$\mathbf{J}_i$	diffusion flux of component i	($mol.m^{-2}.s^{-1}$)
k	dispersion coefficient	($m^2.s^{-1}$)
k_B	Boltzmann's constant	($J.K^{-1}$)
L	diffusion tube length	(m)
m	atom mass	(kg) or (-)
M	molar mass	($kg.mol^{-1}$)
M_i	number of moles of component i in the injected pulse in excess of those in the same volume of the carrier stream	(mol)
n	number of components	(-)
n_i	number of particles of component i	(-)
N_A	Avogadro's number	(mol^{-1})
$\mathbf{N}_i$	molar flux of component i	($mol.m^{-2}.s^{-1}$)
p	pressure	($N.m^{-2}$) or (-)
$\mathbf{r}$	mean displacement of the particles	(m) or (-)

r	particle-particle distance	(m) or (-)
R	gas constant	($j.mol^{-1}.K^{-1}$)
R	internal radius of the diffusion tube	(m)
R_c	radius of the tubing coil	(m)
R_{cut}	cut-off radius	(m) or (-)
s	detector signal	(U)
Sc	Schmidt number	(-)
T	temperature	(K) or (-)
t	time	(s) or (-)
$\bar{t}$	first moment	(s)
$\mathbf{u}_i$	velocity of component i	($m.s^{-1}$)
U	linear velocity averaged over the cross section	($m.s^{-1}$)
U^{LJ}	Lennard-Jones pair potential	(J) or (-)
$\mathbf{v}_1^i$	velocity of particle i of component 1	($m.s^{-1}$)
$\overline{V}_i$	partial molar volume of component i	($m^3.mol^{-1}$)
$V_i c_i$	number of moles of component i in the injected pulse in excess of those in the same volume of the carrier stream	(mol)
w	detector sensitivity	($U.m^3.mol^{-1}$)
x	mole fraction	(-)
y	discrete detector signal	(U)
α	constant	(-)
γ	activity coefficient	(-)
Γ_{ij}	thermodynamic mole fraction-based matrix	(-)
δ_{ij}	Kronecker delta	(-)
ε	detector signal noise	(U)
ε	Lennard-Jones energy parameter	(J)
μ	molar chemical potential	($J.mol^{-1}$)
ν	kinematic viscosity	($m^2.s^{-1}$)
η	viscosity	($N.s.m^{-2}$)
ρ	density	($kg.m^{-3}$) or (-)
ρ	particle density	(m^{-3}) or (-)
σ	Lennard-Jones size parameter	(m)
σ^2	second moment	(s^2)
τ	mean residence time	(s)
τ	coupling time constant	(s) or (-)

subscripts

0	solvent
b	background (carrier stream)
c	molar concentration-based
i	component i
p	pressure
s	solvent-fixed
T	temperature
MS	Maxwell-Stefan
RI	refractive index detector
UV	ultraviolet-visible detector

superscripts

f	Fick
i	particle number
j	particle number
LJ	Lennard-Jones
r	real units
*	reduced units

DANKWOORD

Aan het einde van dit proefschrift wil ik mijn eerste promotor, Piet Kerkhof, bedanken voor de geboden mogelijkheid, het in mij gestelde vertrouwen en de grote mate van vrijheid bij het doen van het onderzoek. Mijn tweede promotor, Berend Smit, bedank ik voor de waardevolle adviezen bij de moleculaire simulaties, en co-promotor Ton van der Zanden voor de begeleiding tijdens het onderzoek.

Marius Vorstman toonde altijd belangstelling en zorgde voor een prettige werksfeer op de kamer; zijn opmerkingen waren erg waardevol.

De afstudeerders Frank Kieviet, Maartje Kemmere en Gert-Jan Nollen leverden een zeer belangrijke bijdrage aan de metingen, en Thijs Vlugt en Anita Otten aan de moleculaire simulaties.

Philip Rutten, Henk Claessens en Ton Staring gaven advies en technische ondersteuning bij de apparatuur en Gerben Mooiweer bij de gegevensverwerking van de metingen. Prof. Berendsen en zijn medewerkers van de vakgroep Biofysische Chemie van de R.U. Groningen adviseerden bij de aanpak van de simulaties. Gert-Jan Visser van het Rekencentrum maakte het gebruik van het GROMOS simulatie programma mogelijk.

Ook Jan Coumans, Anniek van Bemmelen, de technici, de magazijnmedewerkers en anderen van de vakgroep Chemische Proceskunde droegen bij aan de totstandkoming van dit proefschrift.

Tenslotte wil ik familie, vrienden en kennissen bedanken voor de belangstelling in de afgelopen jaren. Maar het belangrijkst waren en zijn natuurlijk Alex, Stephanie en Annick.

CURRICULUM VITAE

Irma van de Ven - Lucassen werd op 3 mei 1953 geboren te Margraten. In mei 1970 behaalde zij het gymnasium-β diploma aan het Sophianum te Vaals. Aansluitend studeerde zij Scheikundige Technologie aan de toenmalige Technische Hogeschool Eindhoven. Zij ontving in 1974 de Unilever Chemie prijs. Het afstudeerwerk werd verricht bij Prof.ir. M. Tels in de vakgroep Fysische Technologie. In januari 1976 behaalde zij cum laude het ingenieursdiploma. Vervolgens was zij werkzaam als wetenschappelijk medewerker aan het Natuurkundig Laboratorium van de NV Philips te Eindhoven, als docente scheikunde, natuurkunde en informatica aan diverse scholen voor voortgezet en hoger onderwijs, en als wetenschappelijk onderzoeker aan de faculteit Scheikundige Technologie van de Technische Universiteit Eindhoven.

Het in dit proefschrift beschreven onderzoek werd van februari 1991 tot januari 1999 uitgevoerd in het Laboratorium voor Scheidingsprocessen en Transportverschijnselen van Prof.dr.ir. P.J.A.M. Kerkhof.

Stellingen

behorende bij het proefschrift van Irma van de Ven – Lucassen

1. Dichtheidsmetingen met behulp van de Taylor dispersie methode, zoals voorgesteld door Matthews en Akgerman, zijn alleen zinvol als nevenproduct van de metingen van de diffusiecoëfficiënt.
   M.A. Matthews and A. Akgerman, 1987, Int. J. Thermophysics, 8, 363.

2. Vereenvoudiging van de practische uitvoering van de metingen van de diffusiecoëfficiënt ten gevolge van de vergaande automatisering leidt niet tot een vermindering van het theoretisch inzicht, dat nodig is voor een juiste interpretatie van de verkregen data.
   Dit proefschrift, hoofdstuk 2 en 3.
   W. Loh, C.A. Tonegutti, and P.L.O. Volpe, 1993, J. Chem. Soc. Faraday Trans., 89(1), 113.

3. Ten gevolge van de ontwikkelingen in de computertechnologie hoeft de simulatieduur geen rol meer te spelen bij de keuze voor een NEMD- of een EMD-algoritme.
   Methods in Molecular Simulation, CCCP5 Spring School, University of Bristol, 1997.

4. Zolang diffusie in vloeistoffen onvoldoende begrepen wordt op moleculaire schaal, zullen er steeds weer nieuwe en 'betere', (semi)empirische relaties voor het voorspellen van de diffusiecoëfficiënt afgeleid worden.
   P.T. Cummings and D.J. Evans, 1992, Ind. Eng. Chem. Res., 31, 1237.

5. Omdat voor goede resultaten bij de natuurwetenschappen niet alleen practisch en logisch denken nodig is, maar ook creatief en fantasierijk, dienen de expressievakken in het voortgezet onderwijs gehandhaafd te blijven. Dit wordt ondermeer geïllustreerd door het feit dat het principe voor het mobiele telefoonverkeer uitgevonden is door een filmster en een componist.
   H. Kramers-Pals, 1999, NVOX, 24, 51.
   http://www.ncafe.com/chris/pat2/patstart.html.
   http://www.microtimes.com/166/coverstory166.html.

6. Mensen die wel ingewikkelde muziekpartituren kunnen lezen, maar beweren geen aanleg te hebben voor wiskunde, hebben waarschijnlijk last van wiskundevrees en onvoldoende motiverend onderwijs.

   Sheila Tobias, 1993, Overcoming Math Anxiety. Revised and expanded (New York: Norton).
   Keith Devlin, 1997, Mathematics. The Science of patterns (New York: The Scientific American Library).

7. Velen zijn nog steeds doof voor de waarschuwingen van Rachel Carson, want ze lijken een 'Silent Spring' niet erg te vinden.

   Rachel Carson, 1962, Silent Spring (Boston: Houghton Mifflin Company).
   Centrale Raad voor het Bedrijfsleven, 07.05.1998, Advies betreffende het opnemen van lindaan en dichloorvos op de lijst van actieve stoffen van bestrijdingsmiddelen die onderworpen zijn aan de milieutaks (Brussel).
   A.W. Galston, 1994, Life processes of plants (New York: The Scientific American Library).
   A.P. Dobson, 1995, Conservation and biodiversity (New York: The Scientific American Library).

8. In een samenleving, die zich modern en democratisch noemt, dient de toelatingsprocedure voor nieuwe medicijnen onafhankelijk te zijn van de samenstelling en de behoeften van de toelatingscommissie.

   K. Itoi, 1999, The great Viagra emergency, Newsweek, CXXXIII, 39.
   H. Buurma, L.T.W. de Jong-van den Berg en H.G.M. Leufkens, 1996, Het geneesmiddel (Utrecht: Bunge).

9. Een patiëntenbijsluiter, waarin een groot aantal bijwerkingen, waarschuwingen en voorzorgen opgenoemd wordt, roept – zo hij al wordt gelezen - de vraag op of er ook nog genezende werking is.

10. Het rigoureus boycotten van buitenlandse woorden leidt niet automatisch tot een verrijking van de Nederlandse taal.

11. Bij de aanduiding 'het millenniumprobleem' staat de komma één plaats verkeerd.